

REPORT DOCUMENTATION PAGE

Form Approved
OMB No. 0704-01881a. REPORT SECURITY CLASSIFICATION
UNCLASSIFIED

1b. RESTRICTIVE MARKINGS

NONE

3. DISTRIBUTION/AVAILABILITY OF REPORT
APPROVED FOR PUBLIC RELEASE;
DISTRIBUTION UNLIMITED.

AD-A220 913

(S)

5. MONITORING ORGANIZATION REPORT NUMBER(S)
AFIT/CI/CIA-90-006D6a. NAME OF PERFORMING ORGANIZATION
AFIT STUDENT AT
Univ of Washington6b. OFFICE SYMBOL
(If applicable)7a. NAME OF MONITORING ORGANIZATION
AFIT/CIA

6c. ADDRESS (City, State, and ZIP Code)

7b. ADDRESS (City, State, and ZIP Code)

Wright-Patterson AFB OH 45433-6583

8a. NAME OF FUNDING/SPONSORING
ORGANIZATION8b. OFFICE SYMBOL
(If applicable)

9. PROCUREMENT INSTRUMENT IDENTIFICATION NUMBER

8c. ADDRESS (City, State, and ZIP Code)

10. SOURCE OF FUNDING NUMBERS

PROGRAM
ELEMENT NO.PROJECT
NO.TASK
NO.WORK UNIT
ACCESSION NO.

11. TITLE (Include Security Classification) (UNCLASSIFIED)

Use of Ab Initio Theory in Studying Various Chemical Systems

12. PERSONAL AUTHOR(S)

Michael B. Coolidge

13a. TYPE OF REPORT

THESIS/DISSERTATION

13b. TIME COVERED

FROM _____ TO _____

14. DATE OF REPORT (Year, Month, Day)

1990

15. PAGE COUNT

130

16. SUPPLEMENTARY NOTATION

APPROVED FOR PUBLIC RELEASE IAW AFR 190-1
ERNEST A. HAYGOOD, 1st Lt, USAF
Executive Officer, Civilian Institution Programs

17. COSATI CODES

18. SUBJECT TERMS (Continue on reverse if necessary and identify by block number)

FIELD

GROUP

SUB-GROUP

19. ABSTRACT (Continue on reverse if necessary and identify by block number)

DTIC
ELECTE
APR 25 1990
B D

90 04 23 067

20. DISTRIBUTION/AVAILABILITY OF ABSTRACT

☒ UNCLASSIFIED/UNLIMITED ☐ SAME AS RPT. ☐ DTIC USERS

21. ABSTRACT SECURITY CLASSIFICATION

UNCLASSIFIED

22a. NAME OF RESPONSIBLE INDIVIDUAL

ERNEST A. HAYGOOD, 1st Lt, USAF

22b. TELEPHONE (Include Area Code)

(513) 255-2259

22c. OFFICE SYMBOL

AFIT/CI

Abstract (147 Pages)

Use of Ab Initio Theory in Studying Various Chemical Systems

by Michael B. Coolidge

Captain, USAF

Ph.D. Chemistry, 1990

University of Washington

Chairperson of the Supervisory Committee: Professor Weston Thatcher Borden
Department of Chemistry

Using ab initio calculations to supplement existing experimental data, a variety of chemical phenomena have been investigated. These include: the effects of substituents on altering carbon-hydrogen and silicon-hydrogen bond strengths, the mode by which the empty orbital on boron alters the properties of an adjacent phosphorous atom, and the effect of substituents on the singlet-triplet energy gap in a non-Kekulé molecule. It has been found that substituents can alter the strength of carbon-hydrogen and silicon-hydrogen bonds through both π delocalization and σ electron donation/withdrawal. The prediction has been made that two BH_2 groups cooperate and hence increase the calculated π bond strength in diborylphosphine. Last, that the strength of the carbonyl bond has been shown to be largely responsible for reducing the singlet-triplet energy gap in oxyallyl to near degeneracy and in causing dimethyloxyallyl to have a predicted singlet electronic ground state.

Use of Ab Initio Theory in Studying Various Chemical Systems

by

Michael B. Coolidge

A dissertation submitted in partial fulfillment
of the requirements for the degree of

Doctor of Philosophy

University of Washington

1990

Approved by Walter T. Borden
(Chairperson of Supervisory Committee)

Program Authorized
to Offer Degree Chemistry

Date 5 Mar 1990

Accession For	
NTIS GRA&I	<input checked="checked" type="checkbox"/>
DTIC TAB	<input type="checkbox"/>
Unannounced	<input type="checkbox"/>
Justification	
By	
Distribution/	
Availability Codes	
Dist	Avail and/or Special
A-1	

Doctoral Dissertation

In presenting this dissertation in partial fulfillment of the requirements for the Doctoral degree at the University of Washington. I agree that the Library shall make its copies freely for inspection. I further agree that extensive copying of this dissertation is allowed only for scholarly purposes, consistent with "fair use" as prescribed in the U.S. Copyright Law. Request for copying or reproduction of this dissertation may be referred to University Microfilms, 300 North Zeeb Road, Ann Arbor, Michigan 48106, to whom the author has granted "the right to reproduce and sell (a) copies of the manuscript in microform and/or (b) printed copies of the manuscript made from microform."

Signature

Michael B. Bolick

Date

5 Mar 1990

University of Washington

Abstract

Use of Ab Initio Theory in Studying Various Chemical Systems

by Michael B. Coolidge

Chairperson of the Supervisory Committee: Professor Weston Thatcher Borden
Department of Chemistry

Using ab initio calculations to supplement existing experimental data, a variety of chemical phenomena have been investigated. These include: the effects of substituents on altering carbon-hydrogen and silicon-hydrogen bond strengths, the mode by which the empty orbital on boron alters the properties of an adjacent phosphorous atom, and the effect of substituents on the singlet-triplet energy gap in a non-Kekulé molecule. It has been found that substituents can alter the strength of carbon-hydrogen and silicon-hydrogen bonds through both π delocalization and σ electron donation/withdrawal. The prediction has been made that two BH_2 groups cooperate and hence increase the calculated π bond strength in diborylphosphine. Last, that the strength of the carbonyl bond has been shown to be largely responsible for reducing the singlet-triplet energy gap in oxyallyl to near degeneracy and in causing dimethyloxyallyl to have a predicted singlet electronic ground state.

Table of Contents

List of Figures	v
List of Tables	vi

Chapter 1 Introduction 1

Section 1-1 Introduction	1
Section 1-2 Overview of ab initio Theory	2
Section 1-2-1 The Time Independent Schrödinger Equation	2
Section 1-2-2 Potential Energy Surfaces	4
Section 1-2-3 Expressing the Wave Function as Molecular Orbitals	5
Section 1-2-4 Hartree-Fock Theory	7
Section 1-2-5 Closed Shell Systems	11
Section 1-2-6 Open Shell Systems	11
Section 1-3 Beyond a Single-Determinant Wave Function Solution	12
Section 1-3-1 The Different Levels of CI Calculations Possible	15
Section 1-3-2 Møller-Plesset Perturbation Theory	17
Section 1-3-3 Multi-Configuration SCF Theory	18
Section 1-4 Basis Sets	19
Section 1-5 Isodesmic Reactions	22
Chapter 1 Notes	25

Chapter 2 Substituent Effects on Carbon-Hydrogen versus Silicon-Hydrogen Bond Strengths. 28

Section 2-1 Carbon-Hydrogen versus Silicon-Hydrogen Bond Strengths	28
Section 2-2 Theoretical Methodology	29
Section 2-3 First Row Substituents	31
Section 2-3-1 Substituents with Empty p Orbitals	31
Section 2-3-2 Substituents with Lone Pairs	34

Section 2-3-3 Methyl and Silyl as Substituents	39
Section 2-3-4 Origin of the σ Electronegativity Effect	41
Section 2-3-5 First-row Substituents Containing π Bonds	42
Section 2-4 Second Row π Donor Substituents	43
Section 2-5 Vinylic Substituents Containing Silicon	46
Section 2-5-1 Computational Methodology Used	47
Section 2-5-2 Effects of Vinyl Substituents Containing Silicon on BDEs	48
Section 2-5-3 Calculation of Allylic Resonance Energies	51
Section 2-5-3-1 Unsymmetrical Allylic Radicals	52
Section 2-5-3-2 Symmetrical Allylic Radicals	52
Section 2-5-4 Effects of Vinyl Substituents at Unconjugated Geometries	54
Section 2-6 Conclusions	58
Chapter 2 Notes	59
 Chapter 3 Pyramidalization of Phosphorus in Borylphosphines	 61
Section 3-1 Chemical Background	61
Section 3-1-1 Phosphorus versus Nitrogen	61
Section 3-1-2 Competition for Electron Density	61
Section 3-1-3 Experimental Examples of Electron Delocalization from Phosphorus	63
Section 3-2 Theoretical Methodology	64
Section 3-3 Results	70
Section 3-3-1 Monoboryl Phosphine	70
Section 3-3-2 Diboryl Phosphine	71
Section 3-3-3 Triboryl Phosphine	73
Section 3-4 Competition versus Cooperation	75
Section 3-4-1 The H_2PBH_2 Potential Surface	77

Section 3-4-2 The $\text{HP}(\text{BH}_2)_2$ Potential Surface	78
Section 3-4-3 Concluding Remarks on the $\text{H}_{3-n}\text{P}(\text{BH}_2)_n$ Molecules	81
Section 3-5 Ring Systems Containing P-B π Bonds	82
Chapter 3 Notes	85
 Chapter 4 Study of Oxyallyl and Dimethyl Oxyallyl	 88
Section 4-1 Introduction	88
Section 4-1-2 Prior Work on Oxyallyl	89
Section 4-2 Computational Methodology	91
Section 4-2-1 CI Configuration Selection	93
Section 4-3 Results	95
Section 4-3-1 Oxyallyl	95
Section 4-3-2 Dimethyloxyallyl	100
Section 4-4 Conclusion	101
Chapter 4 Notes	102
 Bibliography	 105
Appendix 1 Geometries and Energies of Carbon Centered Radicals	117
Appendix 2 Geometries and Energies of Silicon Centered Radicals	120
Appendix 3 Geometries and Energies of Selected Closed-Shell Carbon Molecules	123
Appendix 4 Geometries and Energies of Selected Closed-Shell Silicon Molecules	124
Appendix 5 Geometries and Energies of Saturated Allylic Systems	125
Appendix 6 Geometries and Energies of Allylic Radicals	126
Appendix 7 Geometries and Energies of Twisted Allylic Systems	127
Appendix 8 Geometry Information for H_2PBH_2	128
Appendix 9 Geometry Information for $\text{HP}(\text{BH}_2)_2$	129
Appendix 10 Geometry Information for $\text{P}(\text{BH}_2)_3$	130

List of Figures

3-1	H_2PBH_2 geometries	65
3-2	$HP(BH_2)_2$ geometries	66
3-3	$P(BH_2)_3$ geometries	68
3-4	$P_2B_2H_4$ and $P_3B_3H_6$ geometries	69
3-5	Separation of the Total Energy into Planarization Energy and Conjugation Energy	76
3-6	One dimensional H_2PBH_2 potential energy surface in ϕ	78
3-7	One dimensional $HP(BH_2)_2$ potential energy surface in ϕ	79
4-1	Structure of TMM, oxyallyl and dimethyloxyallyl	89
4-2	Geometric data for oxyallyl	92

List of Tables

2-1	Experimental data for bond dissociation energies	28
2-2	Effect of substituents with empty p orbitals on BDEs	32
2-3	Effect of substituents with lone pairs on BDEs	35
2-4	Effect of methyl and silyl substituents on BDEs	40
2-5	Effect of first row substituents containing π bonds on BDEs	43
2-6	Comparison of effects of second and first row substituents on BDEs	44
2-7	Effects of vinyl derivative substituents on BDEs	48
2-8	Allylic Resonance Energies	51
2-9	σ Effects of vinyl analogous substituents on BDEs	55
3-1	Relative energies for H_2PBH_2	70
3-2	Relative energies for $HP(BH_2)_2$	72
3-3	Relative energies for $P(BH_2)_3$	74
3-4	Barrier to rotation of one BH_2 group out of conjugation in $H_{3-n}P(BH_2)_n$	75
3-5	Relative energies for $P_2B_2H_4$ and $P_3B_3H_6$	83
4-1	Number of spin adapted configurations in CI calculations	93
4-2	Energies of 1A_1 states of oxyallyl and dimethyloxyallyl	94
4-3	Results of MCSCF and contracted CI calculations on oxyallyl	96
4-4	Predicted ΔE_{S-T} for oxyallyl and dimethyloxyallyl	97
4-5	$P-\pi$ orbital total electron population analysis	99

ACKNOWLEDGMENTS

Of all the people I wish to thank, the first must be my parents, Ken and Mariette Coolidge. One of the marvelous jobs involved in parenting is to teach and encourage children to dream. This represents the fulfillment of such a dream.

Some dreams, in order to be attained, need assistance. This dream reaching fruition is due largely to the tutelage of Professor Weston T. Borden. With his guidance, I was able to bring about this body of work. However, this does not represent the end of a dream, merely a chance to dream again. Thank you for your constant demand of perfection.

Others have encourage me along the way. David Hrovat was always there to offer technical guidance and listen to my ideas. Paul and Beth Schomber helped me forget the woes of the past week. My extended family offered constant encouragement. There are many others who each contributed in their own way, to them all, I offer my thanks.

Those I wish to extend my deepest gratitude to are my wife and children. They have supported me throughout providing me every opportunity to do research. I cannot repay them for all the time I have spent away from home. The only thing I can give in return is to encourage them all to dream.

To my children,
may you always dream.

Chapter 1 Introduction

Section 1-1 Introduction

During the 1980's, advances in computer hardware and software have made it possible to perform ab initio calculations on medium sized molecules at levels of sophistication that are capable of yielding chemically useful and reliable results.¹ Indeed, ab initio calculations offer a probe into molecular behavior that may not be easily accessible with experimental techniques. Ab initio calculations may be regarded as another tool, equal to experiment, to gain further insight into chemical systems.

Using ab initio calculations to supplement existing experimental data, I have investigated a variety of chemical phenomena. These include: the effects of substituents on altering carbon-hydrogen and silicon-hydrogen bond strengths, the mode by which the empty orbital on boron alters the physical properties of an adjacent phosphorous atom, and the effect of substituents on the singlet-triplet energy gap in a non-Kekulé molecule.

Each of these topics is covered separately in the following chapters; but first, a brief discussion of ab initio theory is presented, in order to familiarize the reader with the computational methodology that has been used.

Section 1-2 Overview of Ab Initio Theory

Quantum chemistry is comparatively young, having its origins in the mid-1920's with the introduction of Schrödinger's equation. This equation describes the behavior of particles, such as electrons and nuclei, which comprise atoms and molecules. Thus, at least in principle, the physical solutions of the Schrödinger equation should allow the prediction of physical properties and chemical reactions of atoms and molecules. First, however, methods had to be found to obtain a mathematical solution to the time independent Schrödinger equation.

Section 1-2-1 The Time Independent Schrödinger Equation

The time independent Schrödinger equation is:

$$\hat{H} \Psi = E \Psi \quad (1)$$

where \hat{H} is the Hamiltonian, an operator, which defines the allowed wave functions, Ψ , and associated energy levels, E , for a particular system. The Hamiltonian is comprised of two distinct terms, one describing the potential energy of the system, \hat{V} , and another for the kinetic energy of the system, \hat{T} .

$$\hat{H} = \hat{V} + \hat{T} \quad (2)$$

$$\hat{V} = \sum_i \sum_{j < i}^{\text{all particles}} \left(\frac{e_i e_j}{r_{ij}} \right) \quad (3)$$

$$\hat{T} = -\frac{\hbar^2}{2} \sum_i^{\text{all particles}} \frac{1}{m_i} \left(\frac{\partial^2}{\partial x_i^2} + \frac{\partial^2}{\partial y_i^2} + \frac{\partial^2}{\partial z_i^2} \right) \quad (4)$$

Where e_i is the charge of each particle, m_i is its mass, and \hbar is Planck's constant divided by 2π .

Since the mass of an electron is about one thousandth that of a proton, the electrons should be able to adjust their motion rapidly to adjust to any changes in position of the nuclei. Hence, separating the motion of the electrons from that of the nuclei is possible and makes solving the Schrödinger equation much easier. This separation of motion is referred to as the Born-Oppenheimer approximation.²

This approximation allows transformation of the Schrödinger equation to:

$$\hat{H}^{elec}(\mathbf{r}, \mathbf{R}) \Psi^{elec}(\mathbf{r}) = E^{elec}(\mathbf{R}) \Psi^{elec}(\mathbf{r}) \quad (5)$$

where the electronic Hamiltonian depends on both the positions of the electrons (\mathbf{r}) and the nuclei (\mathbf{R}), but operates only on the wave function for the electrons. For a particular set of \mathbf{R} , the electronic wave function is an explicit function only of the positions, \mathbf{r} , of the electrons. Solutions of equation (5) thus give the electronic wave functions and associated energies at a given set of values of \mathbf{R} . Nuclear motion can be determined by solutions of a nuclear Schrödinger equation in which the nuclei move in an effective potential, which is provided by the electrons and is equal to $E^{elec}(\mathbf{R})$.

Section 1-2-2 Potential Energy Surfaces

The electronic wave function of most interest is usually the lowest energy solution of equation (5), and this wave function is called the ground state wave function.

The variations with \mathbf{R} of the energy, $E^{\text{elec}}(\mathbf{R})$, including the nuclear repulsion energy, for the ground state wave function gives the ground state potential energy surface. Stationary points on this surface represent points that have zero first derivatives of the energy with respect to all nuclear motions. Hence, at stationary points the nuclei have no net force exerting on them.

If a stationary point is an energy minimum, all the second derivatives of the energy at this point are positive. Such a point may only be a local minimum.³ The global minimum -- the minimum with the lowest energy on a surface -- is commonly referred to by chemists as the equilibrium geometry.

Another type of stationary point of interest on the potential surface is a transition state. Transition states are saddle points, i.e. they are stationary points at which the energy is a maximum for one direction of nuclear motion.⁴ Mathematically, the matrix of second derivatives of the potential surface -- the Hessian matrix -- has exactly one negative eigenvalue. Transition states are the highest energy point along the lowest energy pathway connecting two minima.

Section 1-2-3 Expressing the Wave Function as Molecular Orbitals

For one-electron atoms or molecules, exact solutions to equation (5) can be obtained in closed form. For many-electron (> 1) systems, this is not possible and the first step in solving equation (5) is determining an appropriate representation of the electronic wave function. If electrons are assumed to behave as independent particles, each electron's spatial wave function motion is described with its own orbital, ψ . The square modulus, $|\psi|^2$, represents the probability distribution of the position of an electron in ψ spatially.

In addition to a spatial wave function, each electron also has a spin wave function with a spin quantum number of $\pm \frac{1}{2}$. The two possible spin wave functions are usually referred to as α , and β . As a result, the space-spin orbital for a single electron is either $\psi^\alpha(x,y,z)$ or $\psi^\beta(x,y,z)$. These space-spin wave functions are sometimes abbreviated as $\chi_n(i)$ where i identifies which electron occupies this space-spin orbital, χ_n .

If electrons are approximated to behave as independent particles, one might be tempted to write the overall wave function, Ψ , as a simple product of the individual space-spin orbitals:

$$\Psi = \chi_1(1) \chi_2(2) \cdots \chi_n(n) \quad (6)$$

However, since electrons are indistinguishable, fermion particles, if any two electrons are transposed, the sign of the wave function must change. Hence, the wave function must be antisymmetrized. This is most easily accomplished by writing the wave

$$\Psi = \begin{vmatrix} \chi_1(1) & \chi_2(1) & \cdots & \chi_n(1) \\ \chi_1(2) & \chi_2(2) & \cdots & \chi_n(2) \\ \vdots & \vdots & \ddots & \vdots \\ \chi_1(n) & \chi_2(n) & \cdots & \chi_n(n) \end{vmatrix} \quad (7)$$

function as a Slater determinant, as expressed in equation (7). Since a determinant goes to zero if any two columns are the same, it is clear that each electron must have a unique χ_n . This gives rise to the Pauli exclusion principle⁵ which states that two electrons cannot have the same spin and space wave functions.

Writing Ψ as a determinant is rather cumbersome. Ψ can be expressed more conveniently in Dirac notation as either a bra or a ket, using the space-spin functions found on the principle diagonal of the Slater determinant. Thus, in this shorthand designation, Ψ , written as a ket, can be abbreviated

$$\Psi = | \chi_1(1) \chi_2(2) \cdots \chi_n(n) \rangle \quad (8)$$

Next to be determined is an appropriate mathematical expression for the spatial part, ψ , of each χ in Ψ . If Ψ were the wave function for a single atom, atomic orbitals, ϕ , such as Slater-type atomic orbitals,⁶ would be appropriate for ψ . For molecules comprised of many atoms, an approximate method is to describe each molecular orbital (MO), ψ_n , as a linear combination of atomic orbitals (LCAO).⁷ Mathematically,

$$\psi_n = \sum_i c_{ni} \phi_i \quad (9)$$

where each ψ_n has its own unique and orthogonal set of c_{ni} , but all ψ_n are formed from the same atomic orbitals ϕ_i . Hence, for a given geometry, any two unique MOs will differ only by the coefficients representing the contributions of each atomic orbital.

Section 1-2-4 Hartree-Fock Theory

The electronic wave function of interest most often is the ground state wave function. One way to find the lowest energy wave function is by application of the variation principle.⁸ Assuming that Ψ has the form in (7), the spatial parts, ψ , of Ψ are varied, subject to the constraint that the ψ remain orthogonal and normalized.

$$\int \psi_i^* \psi_j d\tau = \delta_{ij} \quad (10)$$

This gives rise to the Hartree-Fock equations^{8,9} for finding the optimal ψ_i to use in the wave function, Ψ , for the ground state,

$$\hat{F}\psi_i = \epsilon_i \psi_i \quad (11)$$

where \hat{F} is called the Fock operator and ϵ_i is the energy of orbital, ψ_i .

Although the Fock operator is a one-electron operator, it includes the effect of Coulomb repulsion between electrons by containing terms for the effective field felt by each electron. Thus, in order to compute \hat{F} , one must already know Ψ . In practice, this involves using successive approximations -- guessing Ψ , using this guess

to compute \hat{F} , finding a new set of orbitals, ψ , with which to construct Ψ , recomputing \hat{F} , and continuing on until the process converges to a self-consistent solution. Thus, Hartree-Fock (HF) theory is sometimes also called Self-Consistent Field (SCF) theory.

If the LCAO approximation in equation (9) is made, the energy, E , must be minimized with respect to variations in the coefficients c_{ni} . The coefficients of the atomic orbitals in the LCAO-MOs must again satisfy the orthonormalization conditions,

$$\int \psi_i \psi_j d\tau = \sum_{n=1}^N \sum_{m=1}^N c_{ni}^* S_{nm} c_{mj} = \delta_{ij} \quad (12)$$

where S_{nm} is the overlap matrix between atomic orbitals, whose elements are defined by

$$S_{nm} = \int \phi_n^*(1) \phi_m(1) d\tau \quad (13)$$

The LCAO approximation leads to the Roothaan-Hall equation

$$\sum_{m=1}^N (\hat{F}_{nm} - \epsilon_i \hat{S}_{nm}) c_{mi} = 0 \quad n=1,2,\dots,N \quad (14)$$

for finding the coefficients in the MO's ψ_i , that minimize the total energy. In the above equation, ϵ_i is again the one-electron energy of LCAO-MO ψ_i ; and F_{nm} is called the Fock matrix, whose elements are defined by

$$F_{nm} - H_{nm}^{core} + \sum_{\lambda=1}^N \sum_{\sigma=1}^N P_{\lambda\sigma} \left[\langle nm | \lambda \sigma \rangle - \frac{1}{2} \langle n \lambda | m \sigma \rangle \right] \quad (15)$$

The first term found in equation (15) is given by

$$H_{nm}^{core} = \int \phi_n^*(1) \hat{H}^{core}(1) \phi_m(1) dx_1 dy_1 dz_1 \quad (16)$$

where $H^{core}(1)$ is comprised of those terms in the Hamiltonian that operate on one electron at time, kinetic energy and nuclear-electron attraction.

$$\hat{H}^{core}(1) = -\frac{\hbar^2}{2m_i} \left(\frac{\partial^2}{\partial x_1^2} + \frac{\partial^2}{\partial y_1^2} + \frac{\partial^2}{\partial z_1^2} \right) - \sum_{A=1}^M \frac{Z_A}{r_{1A}} \quad (17)$$

Thus, the first term in equation (15) gives the kinetic energy of and the nuclear attraction energy experienced by the electron in the region where ϕ_n and ϕ_m overlap. The second term in equation (15) represents the average Coulombic repulsion experienced by an electron in this region, where

$$\langle nm | \lambda \sigma \rangle = \int \int \phi_n^*(1) \phi_m(1) \left(\frac{e^2}{r_{12}} \right) \phi_\lambda^*(2) \phi_\sigma(2) dx_1 dy_1 dz_1 dx_2 dy_2 dz_2 \quad (18)$$

is the classic Coulomb repulsion energy, and the third term,

$$\langle n \lambda | m \sigma \rangle = \int \int \phi_n^*(1) \phi_\lambda(1) \left(\frac{e^2}{r_{12}} \right) \phi_m^*(2) \phi_\sigma(2) dx_1 dy_1 dz_1 dx_2 dy_2 dz_2 \quad (19)$$

is a correction that comes from antisymmetrization of the electronic wave function (Pauli exclusion principle) and from the fact that electrons do not repel themselves. Finally,

$$P_{nm} = 2 \sum_{i=1}^{occ} c_{ni}^* c_{mi} \quad (20)$$

is the bond order between atomic orbitals ϕ_n and ϕ_m .

The total energy, E , of a system can be calculated, using components of the Roothaan-Hall equations, by adding the nuclear repulsion energy to the purely electronic energy.

$$E = \frac{1}{2} \sum_{n=1}^N \sum_{m=1}^N P_{nm} (F_{nm} + H_{nm}^{core}) + \sum_{A=1}^M \sum_{B=1}^{A-1} \frac{Z_A Z_B}{R_{AB}} \quad (21)$$

As with the Hartree-Fock equation, the main difficulty in solving the Roothaan-Hall equation (14) is that the Fock matrix is dependent on Ψ , through the dependence of F_{nm} on the bond order, P_{nm} , in equation (15). Therefore, solving equation (14) is an iterative process. A guess is made for Ψ , which is then used to calculate P_{nm} , which is required to compute each element, F_{nm} , of the Fock matrix. Then solving equation (14) for c_{ni} gives a better guess for P_{nm} which is then used in turn to determine a new Fock matrix. This cycle is repeated until self-consistency is reached.

Section 1-2-5 Closed Shell Systems

In general, closed shell systems are easier to calculate than open shell systems. With a closed shell system, two electrons occupy each MO; so there is no need to differentiate the orbitals occupied by the α spin electrons from those occupied by the β spin electrons. The two sets of MOs can have the same spatial functional form; hence, only one set of coefficients for the atomic orbitals is needed in order to completely specify the wave function for each pair of electrons. This method is designated Restricted Hartree-Fock (RHF) since the orbitals for electrons of opposite spin are restricted to be the same.

Section 1-2-6 Open Shell Systems

Some features of open-shell molecules cannot be adequately described using a RHF wave function.¹⁰ According to the Pauli exclusion principle, two electrons of the same spin cannot be in the same region of space at the same time; hence, electrons of the same spin are always correlated in an antisymmetrized wave function. However, the same is not true of electrons of opposite spin. Since an open-shell system has one or more singly occupied orbitals, the forces acting on each α spin electron are usually different from those acting on each β spin electron. As a result, the optimal MOs containing the α spin electrons are not necessarily spatially identical to those containing the β spin electrons. If the molecular orbitals for electrons of opposite spin are not restricted to be identical, a self-consistent field calculation is referred to as unrestricted Hartree-Fock (UHF).

Section 1.3 Beyond a Single-Determinant Wave Function Solution

Approximate solution, via Hartree-Fock theory, of the time independent Schrödinger equation using a single-determinant wave function is sufficient to describe many molecular systems.¹ However, Hartree-Fock theory does not provide a correct treatment of electron correlation. Electrons of the same spin are partially correlated via antisymmetrization; but electrons of opposite spin are not correlated at all with a RHF wave function. When electron correlation is important, a single-determinant wave function does not provide even a qualitatively adequate description of the wave function; and multiple-determinantal wave functions are required.¹

Correlation of the electrons serves to reduce the probability of two electrons simultaneously occupying the same region; and, thus, correlation reduces the Coulomb repulsion energy. The need for including electron correlation becomes apparent from consideration of the dissociation of H_2 to form two neutral hydrogen atoms. The Hartree-Fock solution of the wave function at any separation is given by

$$\Psi = |\sigma^{\alpha}(1) \sigma^{\beta}(2) \rangle \quad (22)$$

where, in LCAO-MO approximation

$$\sigma = \frac{1}{\sqrt{2 + 2S}} (\phi_A + \phi_B) \quad (23)$$

The spatial portion of this wave function can be expanded to give

$$\Psi = \frac{1}{2+2S} [\phi_A(1)\phi_B(2) + \phi_B(1)\phi_A(2) + \phi_A(1)\phi_A(2) + \phi_B(1)\phi_B(2)] \quad (24)$$

This predicts that at any internuclear separation of atoms A and B, the electrons will be localized to separate hydrogen atoms only half the time; the other half, they will both be on the same hydrogen. However, at infinite separation of A and B, the electrons should always be on different nuclei. This requires that the wave function at infinite separation be

$$\Psi_{\infty} = \frac{1}{\sqrt{2}} [\phi_A(1)\phi_B(2) + \phi_B(1)\phi_A(2)] \quad (25)$$

which cannot be written as a single determinant using the molecular orbitals from the Hartree-Fock wave function.

In order to obtain (25), a second determinant containing the σ anti-bonding orbitals must be included. A wave function, general enough to give equation (25) at large internuclear distances, can be written, using the Hartree-Fock orbitals as

$$\Psi = c_1 |\sigma^a(1) \sigma^b(2)\rangle - c_2 |\sigma^{*a}(1) \sigma^{*b}(2)\rangle \quad (26)$$

where

$$\sigma^* = \frac{1}{\sqrt{2-2S}} (\phi_A - \phi_B) \quad (27)$$

since Ψ of equation (26) can be expanded to

$$\Psi = c_C [\phi_A(1)\phi_B(2) + \phi_B(1)\phi_A(2)] + c_I [\phi_A(1)\phi_A(2) + \phi_B(1)\phi_B(2)] \quad (28)$$

where the coefficient, $c_C \approx c_1 + c_2$, of the covalent terms and that, $c_I \approx c_1 - c_2$, of the ionic terms are no longer restricted to contribute equally.

The most straightforward way of correlating the motions of many-electrons is to obtain variationally a multiple-determinant wave function, formed as a linear combination of Slater determinants, which are each comprised of orbitals obtained from Hartree-Fock theory. This treatment is called configuration interaction (CI). Alternately, instead of finding the wave function and its energy variationally, perturbation theory can be applied. A third approach is to start with a multiple-determinant wave function and simultaneously optimize both the mixing coefficients of the determinants and the orbitals in them. This approach is called Multi-Configuration Self-Consistent Field (MCSCF).

The main premise behind most CI and perturbation calculations is that the Hartree-Fock wave function is a reasonable approximation to the actual wave function. Therefore, it is reasonable to write

$$E(\text{exact}) = E(\text{Hartree-Fock}) + E(\text{correlation}) \quad (29)$$

where $E(\text{exact})$ is the lowest possible energy one can obtain from a given set of atomic orbitals after completely accounting for electron correlation. Ideally, this energy contribution, $E(\text{correlation})$, is small and, hence, as discussed later, may even be calculated from perturbation theory.

The electronic configurations whose mixing with the ground state wave function will lower the overall energy are those of the same spin multiplicity and overall symmetry as this wave function. These configurations are generated by exciting one or more electrons from the ground state HF orbitals to higher, unoccupied, virtual orbitals. Starting from HF orbitals, Brillouin's theorem guarantees that only doubly excited configurations mix directly with the HF configuration.¹¹ The coefficients of each excited configuration can either be calculated variationally or obtained from perturbation theory.

Section 1-3-1 The Different Levels of CI Calculations Possible

In a CI calculation, one must determine the interaction energy of each configuration with all the others, store the resulting matrix, and obtain the lowest

eigenvalue and eigenvector. Since, the number of configurations grows very rapidly with the number of electrons and orbitals, one does not always have enough disk space to store all the CI matrix elements or have enough CPU time available to be able to calculate them or to extract the CI energy of the lowest state. As a result, one is often forced to preselect the configurations that are expected to contribute the most and to consider only those. This may be done either by limiting the number of electrons excited simultaneously from the ground state HF wave function or by reducing the number of orbitals from which or into which excitations are permitted. The limitations imposed are then included when referring to the type of calculation performed.

FULL-CI considers all possible excitations from the HF wave function. A FULL-CI energy represents the lowest energy one can attain with a given set of orbitals. More often, one must restrict the excitations to just singles, doubles, triples, etc., or combinations of these. The shorthand technique for specifying which were considered is to use the capital letter of each allowed. Therefore, a CI-SDQ considers all possible single, double, and quadruple excitations from the HF configuration.

Sometimes, symmetry can be used to reduce the number of orbitals that are treated in a CI calculation. For example, in an unsaturated molecule, one might only consider excitations between orbitals of π symmetry. These orbital restrictions are once again included when referring to the calculations. For instance, σ -S, π -SD CI

specifies only single excitations from molecular orbitals of σ symmetry and single and double excitations from molecular orbitals of π symmetry.

Section 1-3-2 Møller-Plesset Perturbation Theory

A non-variational approach to electron correlation is through the perturbative technique developed by Møller and Plesset.¹² They express the effect of including electron correlation as a perturbation to the Hamiltonian derived under Hartree-Fock theory, \hat{H}_{HF} . Hence, if the real hamiltonian is \hat{H}_0 , and the perturbative hamiltonian is \hat{H} , with a weight of λ , then they are related by the following equation

$$\hat{H}_0 = \hat{H}_{HF} + \lambda \hat{H} \quad (30)$$

Under Rayleigh-Schrödinger perturbation theory, the wave function then becomes

$$\Psi_0 = \Psi_{HF}^{(0)} + \lambda \Psi^{(1)} + \lambda^2 \Psi^{(2)} + \dots \quad (31)$$

and the resultant energy is¹³

$$E_0 = E_{HF}^{(0)} + \lambda E^{(1)} + \lambda^2 E^{(2)} + \dots \quad (32)$$

where $\Psi^{(i)}$ is called the i^{th} order correction to the HF wave function, $E^{(i)}$ is the i^{th} order correction to the HF energy, and Ψ_0 and E_0 are, respectively, the true wave function and the exact energy.

An important practical consideration is how many terms are included in approximating E_0 . For example, an MP2 calculation includes up to the second order term in the Møller-Plesset perturbation energy. For higher levels, such as fourth order, not all of the lower order terms are always considered. For instance, the difference between MP4SDQ and MP4SDTQ is that, in the former, triple excitations are not included, so that expansion is actually a truncated or partial fourth-order level of perturbation theory.

Perturbative techniques for electron correlation provide results that are size-consistent¹⁴, whereas CI techniques less than full do not. Perhaps of even greater practical importance, perturbation theory requires substantially less CPU time¹⁵ and disk space than do CI techniques that include the same levels of excitation. However, the drawback to perturbation theory is that molecules which are not well represented by a single Slater determinant are poorly described, since the perturbation theory expansion is slow to converge.

Section 1-3-3 Multi-Configuration SCF Theory.

Especially when attempting to calculate diradical species, expressing a singlet wave function with a single determinant is grossly inadequate. In such cases, a multi-configuration wave function must be used as a zeroth order approximation. The exact number of configurations required to describe accurately the wave function for a molecule may vary from state to state and also for a given state, with changes in geometry.

In cases where a single-determinantal SCF wave function is inadequate, it is usually best to obtain a multi-configuration (MC) wave function by performing an MCSCF calculation. An MCSCF wave function has the same form as a CI wave function, but in a MCSCF calculation, both the orbitals and the mixing coefficients are simultaneously optimized. Consequently, for the same set of configurations, a MCSCF calculation provides a variationally better wave function. However, CI calculations are usually capable of handling many more configurations than MCSCF calculations.

MCSCF calculations are capable of providing a good zeroth-order wave function; but, for all but atoms and very small molecules, not a completely correlated one. Of course, additional electron correlation can be added to improve an MCSCF wave function, just as correlation can be added to improve a RHF or UHF wave function. In the event that additional correlation is added, excitations from all the configurations used in the MCSCF wave function are usually included.

Section 1-4 Basis Sets

Of equal or greater importance to the adequate inclusion of electron correlation is the adequate description of the orbitals used in the Slater determinants that comprise SCF, MCSCF and CI wave functions. If MOs are written as LCAOs, the quality of the MOs depends on the quality of the functions used to represent the atomic orbitals. These functions are called the basis set.

A type of orbital used frequently in atomic calculations is a Slater type orbitals. These orbitals have the functional form:

$$\phi = Y_{\ell m}(\theta, \omega) * f(R, \ell) * e^{-\zeta R} \quad (33)$$

where $Y_{\ell m}(\theta, \omega)$ is the angular portion of the wave function, $f(R, \ell)$ is the radial harmonic portion, and R is the radial distance from atomic center.

The drawback of Slater type orbitals for molecular calculations is that multiplying two or more Slater orbitals on different centers, gives integrals that are difficult to evaluate. Almost all calculations today are done using basis sets composed of several gaussian type functions in place of the exponential part of Slater type orbitals. Mathematically,

$$e^{-\zeta R} \sim \sum_{i=1}^J a_i e^{-(b_i R^2)} \quad (34)$$

where a_i and b_i are constants that can be varied to give the closest fit to a Slater orbital or that can be optimized for calculation on molecules.

The advantage of replacing one Slater orbital with several gaussians is that integrals over gaussians can be easily and rapidly evaluated, since the product of two gaussians on different centers is a third gaussian.¹⁶ However, gaussians are not ideal for representing Slater orbitals, since Slater orbitals have a cusp at the origin; whereas, gaussians do not. To duplicate an entire Slater orbital accurately requires

many gaussians. Hence, as opposed to matching the entire Slater orbital, many basis sets try to duplicate the portion of the orbital deemed most important. For inner shell orbitals, not involved much in bonding, duplication of the cusp is most important. For valence shell orbitals, the outer portions of the atomic orbitals are the most important, since they are involved bonding.

Examples of common basis sets are STO-3G,¹⁷ 3-21G,¹⁸ 6-31G*,¹⁹ DZ,²⁰ and DZP.²¹ STO-3G is a minimal basis set. It replaces each Slater Type Orbital (STO) with 3 gaussians (G). A minimal basis set has no flexibility, since the same gaussians are used to describe all orbitals within a given shell, regardless of the environment surrounding the atom or type of bond that an orbital is used to form. Thus, for example, the 2p orbital in STO-3G gives a much better description of C-C σ bonds than of C-C π bonds.²²

A more flexible basis set is 3-21G. It is a split-valence basis set, where the inner shell orbitals are still represented by 3 gaussians, but the valence shell orbitals are represented by two different and independent groups of gaussians. One group has 2 gaussians, optimized for short distance interactions; the other consists of one gaussian, optimized for longer distance interactions. The weights of the two groups of gaussians on each center in each MO are determined variationally by RHF, UHF, or MCSCF calculations.

The 6-31G* basis set is also a split-valence basis set. Here, however, there are 6 gaussians to represent inner shell orbitals and a split pair of 3 and 1 gaussian functions for the valence orbitals. The asterisk denotes the addition of polarization

functions on all non-hydrogen atoms. This means the addition of d orbitals to first and second row atoms and the addition of f orbitals to atoms below row two. Polarization functions allow π electron density to be shifted away from the center of each atom. This is especially important in small rings and in polar bonds, such as in carbonyl groups,²³ where the electron density is concentrated more at one end of the bond than the other.

DZ and DZP basis sets are similar, respectively, to 3-21G and 6-31G*, but in a double zeta (DZ) basis set, the orbitals in each shell, not just the valence shell, are all represented by two sets of gaussians. The most commonly used DZ and polarized DZ (DZP) basis sets are those of Dunning and Hay.^{20,21} They found that different atoms require different numbers of gaussians; hence, there is no generic specification of the number of gaussians, as there is in the basis sets derived by Pople and coworkers (e.g. STO-3G, 3-21G, and 6-31G*).

Section 1-5 Isodesmic Reactions

Just as chemists balance equations stoichiometrically, computational chemists often balance equations isodesmically.²⁴ By ensuring that there are similar types of bonds and the same spin multiplicity of states on both sides of an equation, the magnitudes of the errors in energies, due to basis set deficiencies and inadequate treatment of electron correlation, can be reduced.

For example, it is much more difficult to calculate the carbon-hydrogen bond strength in ethane or in methane exactly than to calculate the carbon-hydrogen bond

strength in ethane, relative to that in methane. Thus, although the calculated energy changes for (35) and (36) may not be accurate, if the errors in each are identical, then the energy for (37) will be exact, since this isodesmic reaction is simply the difference between the first two.



At the HF/6-31G* level of theory, the calculated bond strength of the C-H bond in ethane is 73.4 kcal/mol and in methane is 76.1 kcal/mol. These values are considerably lower than the experimental values of 100.4 kcal/mol,²⁵ and 104.9 kcal/mol²⁶ respectively. However, since equation (37) is the difference, it predicts that the C-H bond in ethane is 2.7 kcal/mol weaker than in methane, which is reasonably close to the experimental difference of 4.5 kcal/mol.

The way to improve the accuracy of the energy of reaction predicted via ab initio techniques is to increase the size of the basis set or increase the amount of electron correlation. Inclusion of electron correlation through second order Møller-Plesset perturbation theory usually provides a closer match of predicted to experimental results than do calculations at the SCF level. For example, using MP2/6-31G* derived energies, the C-H bond strength in ethane is 90.7 kcal/mol and in methane is 93.4 kcal/mol. Inclusion of electron correlation at the MP2 level

obviously provides better absolute energies of reaction, but leaves the difference between the two reactions the same, 2.7 kcal/mol. MP4SDTQ/6-31G* derived energies give only a small further increase in the bond strengths, to 91.3 kcal/mol for ethane and 94.5 kcal/mol for methane. The energy difference also increases slightly to 3.1 kcal/mol.²⁷

The absolute bond strengths can be further improved through addition of more extensive electron correlation and use of larger basis sets.²⁸ However, isodesmic reactions allow accurate predictions, usually on the same order as the experimental uncertainty, with the use of moderate sized basis sets and low levels of electron correlation. Indeed, in the example discussed above, although addition of electron correlation dramatically improves the calculations for the absolute C-H bond strengths, since the isodesmic reactions allows for cancellation of errors in each of the absolute bond strengths, addition of electron correlation provides no or little improvement in the calculation of the relative C-H bond strengths.

Isodesmic reactions are useful when absolute energies are of less interest than differences between compounds. In those cases where absolute energies are important, they can be calculated via isodesmic reactions, relative to an experimentally known value. Because calculations of absolute values for quantities like bond dissociation energies are computationally demanding, use of isodesmic reactions provides an attractive alternative.

Chapter 1 Notes

1. Hehre, W. J.; Radom, L.; Schleyer, P. v.R.; Pople, J. A. "Ab Initio Molecular Orbital Theory," Wiley, 1986.
2. Born, M.; Oppenheimer, J. R. *Ann. Physik*, **1927**, *84*, 457.
3. This treatment does not take into account zero-point vibrations of the nuclei. Even at absolute zero, these nuclear motions are present. They are a result of the uncertainty principle and wave nature of quantum particles. If an energy minimum is sufficiently shallow, the zero-point vibrational energy of the nuclei may be adequate to overcome the barrier that separates it from surrounding points of lower energy.
4. If a stationary point has more than one negative eigenvector, then it represents a point on the potential surface that is a mountain top. Mountain tops are of little interest, since there are always lower energy pathways between minima than those which pass through such points.
5. Pauli, W. *Zeit. für Phys.*, **1925**, *31*, 765.
6. In actuality, any complete set of functions is capable of giving an exact description of Ψ . Atomic orbitals have the advantage of providing a wave function that is readily interpretable physically.
7. Lennard-Jones, Sir J. E. *Trans. Faraday Soc.*, **1929**, *25*, 668; Lennard-Jones, Sir J. E. *Proc. Roy. Soc. A*, **1937**, *158*, 280; Mulliken, R. S. *J. Chem Phys.*, **1935**, *3*, 375.
8. Roothaan, C. C. J. *Revs. of Mod. Phys.*, **1951**, *23*, 69.
9. Hall, G. G. *Proc. Roy. Soc. A*, **1951**, *203*, 541.
10. Pople, J. A.; Nesbet, R. K. *J. Chem. Phys.*, **1954**, *22*, 571.
11. Brillouin, L.; Les Champs "Self-Consistents" de Hartree et de Fock, *Actualités Scientifiques et Industrielles*, n°71, chapt. 5, Hermann, Paris (1933).
12. Møller, C.; Plesset, M. S. *Phys. Rev.*, **46**, 618, (1934).
13. For more details on deriving these equations, see either reference (1), or (12).
14. Size consistent results scale linearly with the number of orbitals and electrons considered. The energy calculated for two molecules at infinite separation should equal the sum of the energies of each of the molecules calculated separately. For more details, see Chapter 2 of reference (1).

15. The number of mathematical operations required to derive an MP3 energy is about the same as the number required for CI-D calculation. Since the degree of correlation is greater for the MP3 calculation than for the CI-D, perturbative numbers not only require less disk space, but also require less CPU time. The advantage of reduced disk space usage by perturbative means is quickly diminishing as direct CI techniques are developed. This technique reduces the amount of disk space required by the CI calculation, but does not significantly reduce the amount of CPU time required.

16. Boys, S. F.; Cook, G. B. *Revs. of Modern Phys.*, **1960**, 32, 285.

17. Hehre, W. J.; Stewart, R. F.; Pople, J. A., *J. Chem. Phys.*, **1969**, 51, 2659; Collins, J. B.; Schleyer, P. v. R.; Binkley, J. S.; Pople, J. A. *J. Chem. Phys.*, **1976**, 64, 5142.

18. Binkley, J. S.; Pople, J. A.; Hehre, W. J. *J. Amer. Chem. Soc.*, **1980**, 102, 939; Gordon, M. S.; Binkley, J. S.; Pople, J. A.; Pietro, W. J.; Hehre, W. J. *J. Amer. Chem. Soc.*, **1982**, 104, 2797; Pietro, W. J., Francl, M. M.; Hehre, W. J.; Defrees, D. J. Pople, J. A.; Binkley, J. S. *J. Amer. Chem. Soc.*, **1982**, 104, 5039.

19. Harihan, P. C.; Pople, J. A. *Theor. Chim. Acta* **1973**, 28, 212; Francl, M. M.; Pietro, W. J.; Hehre, W. J.; Binkley, J. S.; Gordon, M. S.; Defrees, D. M.; Pople, J. A. *J. Chem Phys.* **1982**, 77, 3654.

20. Dunning, T. H.; Hay, P. J. in "Modern Theoretical Chemistry", Plenum, New York, 1976, pp. 1-28 ch. 1.

21. Dunning, T. H.; Hay, P. J. in "Methods of Electronic Structure", Vol 2, Schaefer, H. F. II, ed. Plenum: New York, 1977.

22. Reference (1), pages 288-291.

23. Feller, D.; Huyser, E. S.; Borden, W. T.; Davidson, E. R. *J. Am. Chem. Soc.* **1983**, 105, 1459.

24. See Chapter 1 of reference 1.

25. Parmar, S. S.; Benson, S. W. *J. Am. Chem. Soc.* **1986**, 111, 57.

26. Pasto, D. J.; Krasnansky, R.; Zercher, C. *J. Org. Chem.*, **1987**, 52, 3062.

27. Using the UHF wave function and Møller-Plesset perturbation theory actually introduces a slight bias in this system. The carbon-hydrogen bond strength for ethane is overestimated relative to methane since the ethyl radical contains a greater degree of spin contamination from the quartet state than does the methyl radical. An alternate technique is to add electron correlation using configuration interaction techniques on a wave function that, for the radicals, is pure doublet. The

CISD/6-31G* derived bond strengths are 92.2 kcal/mol for methane and 88.1 kcal/mol for ethane. These individual BDEs are not in as close agreement with the experimental values as the MP2 derived values, probably because of size consistency problems in the CISD values. However, the predicted difference in bond strength of 4.1 kcal/mol matches the experimental difference more closely than any of using the UHF wave function.

28. Pople, J. A.; Frisch, M. J.; Luke, B. T. *Inter. J. of Quant. Chem. Symp.*, **1983**, *17*, 307.

Chapter 2 Substituent Effects on Carbon-Hydrogen versus Silicon-Hydrogen Bond Strengths

Section 2-1 Experimental Carbon-Hydrogen versus Silicon-Hydrogen Bond Strengths

Carbon-centered radicals have been extensively studied.^{1,2,3} Much less work has been done on silicon-centered radicals.^{3,4,5} Since carbon and silicon are both group IVb elements in the periodic table, bonds to carbon and to silicon might be presumed to be similar. However, this apparently is not the case.

Table 2-1 Experimental data^a for bond dissociation energies (kcal/mol) for the reaction, $R-H_2X-H \rightarrow R-H_2X\cdot + \cdot H$

Compound	X = C	X = Si
H_3X-H	104.8	90.3
$(CH_3)H_2X-H$	100.4	89.6
$CH_3)_2HX-H$	95.9	89.6
$(CH_3)_3X-H$	93.3	90.3
$(CH_3)_3C-H_2X-H$	99.7	
$(CH_3)_3Si-H_2X-H$	99.2	
H_3Si-H_2X-H		86.3
$[(CH_3)_3Si]_3-X-H$		79.0

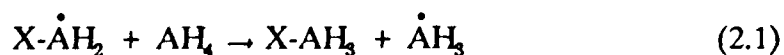
^aData from reference 4, except for the BDE of CH_3CH_2-H , which comes from reference 2, and $[(CH_3)_3Si]_3Si-H$, which comes from reference 5.

Walsh⁴ found experimentally that alkyl substituents have different effects on silicon-hydrogen versus carbon-hydrogen bond strengths (see Table 2-1). Alkyl substituents appear to weaken the carbon-hydrogen bond by roughly 4-5 kcal/mol per substituent group, but they have no obvious effect on silicon-hydrogen bond strengths. However, silyl substituents weaken both silicon-hydrogen and carbon-hydrogen bonds by roughly 4 kcal/mol per silyl substituent.

To understand these differences in substituent effects on silicon-hydrogen and carbon-hydrogen bonds strengths, we decided to investigate the effects of a wide range of substituents by computational means. We examined all first row substituents plus silicon, phosphorous, sulfur, chlorine, from the second row and a limited number of substituent groups containing π bonds. We hoped that this range of substituents would be sufficient to elucidate completely all the different mechanisms by which substituents affect C-H and Si-H bond dissociation energies (BDEs).

Section 2-2 Theoretical Methodology

To calculate substituent effects on carbon-hydrogen and silicon-hydrogen bond strengths, we used equation 2.1. Equation 2.1 is an isodesmic reaction that measures



the effect of substituent group X on the A-H bond strength, relative to that in methane (A=C) or silane (A=Si). As discussed in Chapter 1, use of an isodesmic reaction allows cancellation of most of the errors made in calculation of the individual BDEs.

The radical geometries were optimized with a UHF wave function and the 6-31G* basis set. Initially, the geometries were fully optimized with respect to all degrees of freedom. Later, some radicals were also optimized to a transition state involving a conformational change. Many of these transition states were located by imposing symmetry constraints. Others were optimized with the constraint that the second derivative of the Hessian matrix have exactly one negative eigenvalue. Electron correlation was then added using MP4SDTQ at the UHF optimized geometry. The MP4SDTQ/6-31G* energies for the reaction of equation (2.1) are given in Tables 2-2 through 2-6.

The UHF wave functions for the allylic type radicals proved to be have a large degree of spin contamination. In order to obtain a pure doublet wave function, instead of using MP4SDTQ calculations to include electron correlation, we employed the direct CI-SD⁸ routine in GAUSSIAN 86.⁷ This CI-SD routine calculates the CI wave function energy considering all single and double excitations from the lowest energy configuration. The CI-SD energies for the allylic systems are given in Tables 2-7 through 2-9.

Section 2-3 First Row Substituents

First row substituents can be classified into three distinct types: (1) those with empty p orbitals, (2) those with lone pairs of electrons, and (3) those without either, e.g. methyl. Each of these groups of substituents behave differently and so will be discussed individually.

Section 2-3-1 Substituents with Empty p Orbitals

The early first row substituents, Li, BeH and BH₂, all have at least one empty p orbital available to delocalize the odd electron at a carbon or silicon radical center. The resulting partial π bonds should stabilize the substituted silyl or methyl radicals. Indeed, as shown in Table 2-2, equation 2.1 is calculated to be exothermic in all cases for both carbon and silicon. This indicates that all of these substituents lower the bond dissociation energy (BDE) of the A-H bond.

Testing for the existence of π delocalization in X-AH₂ as the probable source of stabilization is straightforward using the BH₂ substituent. Rotation of the empty p orbital out of conjugation with the singly occupied orbital on the radical center precludes any stabilization through π delocalization. The barrier to rotation about the carbon-boron bond in H₂ $\dot{\text{C}}$ -BH₂ is 9.7 kcal/mol. Since the boron substituent reduces the C-H BDE by 12.4 kcal/mol, most of the reduction in the BDE by BH₂ comes from delocalization of the odd electron on carbon into the empty p orbital on boron.

Table 2-2 Effect of substituents with empty p orbitals on the MP4SDTQ/6-31G* derived BDEs using the reaction^a $[X-AH_2]^\bullet + AH_4 \rightarrow X-AH_3 + \bullet AH_3$

Substituent Group (X)	ΔE (kcal/mol)		X-A bond length in the radical (Å)	
	A=C	A=Si	A=C	A=Si
Li	9.4	12.0	1.943	2.426
BeH	9.0	8.0	1.665	2.166
BH ₂ ^b	12.4	12.2	1.536	1.954
BH ₂ ^c	2.7	0.8	1.555	2.046
BH ₂ ^d	2.7	-4.5	1.555	2.045

^aA positive ΔE implies that the substituent weakens the A-H bond.

^bBoth carbon and silicon are planar.

^cRadical center is rotated out of conjugation with empty p orbital and allowed to pyramidalize. Carbon remains planar, but silicon has an out of plane angle (ϕ) of 51°.

^dRadical center is rotated out of conjugation with empty p orbital and constrained to be planar.

The $H_2B-\dot{Si}H_2$ radical gives similar results. Rotation about the B-Si bond requires 11.4 kcal/mol. Upon rotation however, there is significant change in the geometry at the silicon center. In the conjugated geometry, the silicon center is planar; but upon rotation, the silicon becomes significantly pyramidal. Therefore, the energy change is not due strictly to the breaking of the π bond but also contains the energy lowering that accompanies pyramidalization of the silicon center. Hence, to get a true measure of the silicon-boron π delocalization energy, the silicon center must be held planar when rotated. Optimization of this C_{2v} structure reveals that breaking the π bond requires 16.8 kcal/mol, and pyramidalization regains 5.4

kcal/mol of that energy. The larger magnitude of the π delocalization energy in $\text{H}_2\text{B}-\dot{\text{Si}}\text{H}_2$ than in $\text{H}_2\text{B}-\dot{\text{C}}\text{H}_2$ effect can be understood using either resonance theory or qualitative MO perturbation theory.

In resonance theory, delocalization of the odd electron on A by an empty orbital on X is represented using equation 2.2. The amount of stabilization should



be proportional to the contribution the second resonance structure makes. The second resonance structure should contribute more as the electronegativity of atom A decreases. This explains why, although silicon generally forms weaker π bonds than carbon,⁸ the π bond strength is greater in $\text{H}_2\text{B}-\dot{\text{A}}\text{H}_2$ for A=Si than for A=C.

The second resonance structure should also contribute more as the electronegativity of X increases. Hence, the anticipated order of π bond strengths for substituent groups, X, is: $\text{BH}_2 > \text{BeH} > \text{Li}$. However, this is not the calculated order found in Table 2.2. The actual order has Li lowering the A-H BDE more than BeH for both A=C and A=Si. Apparently, there is a second effect that, unlike the formation of the 1-electron π bond, increases the A-H BDE as the electronegativity of the substituent group, X, increases.

Use of MO perturbation theory gives an identical prediction of the effect of substituent electronegativity on the strength of the 1-electron π bond in $\text{X}-\dot{\text{A}}\text{H}_2$. Since the empty orbital on X and the orbital containing the odd electron on A

overlap, there will be mixing of these two orbitals. Using second-order perturbation theory, the amount of energy lowering that results is roughly proportional to the square of the overlap of these two orbitals, divided by the energy gap between them. The less electronegative A is, the closer the half filled orbital is to the empty orbital in energy, the smaller the energy gap between them, and the larger the energy lowering due to their mixing. Once again, this explains why the π bond to BH_2 is stronger for $\text{A}=\text{Si}$ than $\text{A}=\text{C}$.

The more electronegative the substituent group X is, the closer in energy its empty p orbital is to the half filled orbital, and once again, the larger the energy lowering caused by the formation of the resultant π bond. MO perturbation theory thus also predicts that the anticipated order for the substituent groups in decreasing the A-H BDE is: $\text{X}=\text{BH}_2 > \text{X}=\text{BeH} > \text{X}=\text{Li}$. As indicated in the paragraph above, the data in table 2.2 shows that there is an additional effect, not yet identified, that apparently acts to increase the A-H BDE as the electronegativity of X increases.

Section 2-3-2 Substituents with Lone Pairs

The later first row substituents, $\text{X} = \text{NH}_2$, OH , and F , all contain at least one lone pair of electrons that can interact with the radical center on A. Stabilization of the odd electron on A can occur through formation of a 3-electron π bond. Although one of the three electrons will be in an anti-bonding π orbital, the two electrons that occupy the bonding π orbital should result in net stabilization for the 3-electron system. Since NH_2 has a single lone pair, the strength of the 3-electron

Table 2-3 Effect of substituents with lone pairs on the MP4SDTQ/6-31G* derived BDEs using the reaction^a $[X-AH_2]^\bullet + AH_4 \rightarrow X-AH_3 + \bullet AH_3$

Substituent Group (X)	ΔE (kcal/mol)		X-A bond length in the radical (Å)	
	A=C	A=Si	A=C	A=Si
NH ₂	12.2	0.9	1.402 ^e	1.729 ^d
NH ₂ ^b	3.7	-2.5	1.420 ^e	1.721 ^f
OH	8.6	-0.8	1.359	1.652
OH ^b	4.2	-1.6	1.366	1.652
F	4.4	-3.5	1.331	1.599

^aA positive ΔE implies that the substituent weakens the A-H bond.

^bRadical center is rotated out of conjugation with lone pair orbital.

^cPyramidalization angle at C (ϕ_C) is 34°, $\phi_N = 46^\circ$.

^d $\phi_{Si} = 56^\circ$, $\phi_N = 28^\circ$.

^e $\phi_C = 4.4^\circ$, $\phi_N = 52^\circ$.

^f $\phi_{Si} = 48^\circ$, $\phi_N = 10^\circ$.

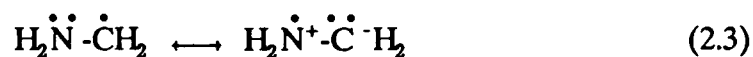
π bond in $H_2N-\dot{A}H_2$ can be measured by rotation of the substituent group out of conjugation with the radical orbital.

Our calculations find that in $H_2N-\dot{C}H_2$, 9.5 kcal/mol is required to rotate the carbon radical out of conjugation with the nitrogen lone pair. Even at the rotated geometry, hyperconjugation of the radical with the N-H bonds of the amino group may provide some stabilization for the radical. Thus, the 9.5 kcal/mol barrier to NH₂ rotation indicates that most, if not all, of the 12.2 kcal/mol reduction in the C-H BDE by NH₂ is due to formation of a π bond in the radical.

Additional evidence of the formation of a partial π bond in $H_2N-\dot{C}H_2$ comes from careful examination of the geometry changes that occur upon rotation of the

H_2N group. The complete geometries are given in Appendix I, but some parameters are listed in Table 2-3. In the equilibrium structure, the N-C bond length is 1.402\AA , which is shorter than the N-C bond length of 1.420\AA in the rotated structure.

At first glance, since neither atomic center is planar in either of these structures, it is not obvious that a π bond that is formed; but the changes in pyramidalization at the two centers are significant. In the equilibrium geometry, the pyramidalization angles are 34° for carbon and 46° for nitrogen; for the rotated structure, they are 4.4° for carbon and 52° for nitrogen. The carbon center is more pyramidal and the nitrogen is less pyramidal in the equilibrium structure because of a transfer in electron density from the nitrogen to the carbon, as depicted in the second resonance structure of equation 2.3. An increase in electron density at the



carbon center would tend to make the carbon center behave more like a carbanion, and carbanions generally prefer pyramidal geometries. The reduction in electron density at the nitrogen would tend to flatten it. Hence, the changes in geometry are consistent with formation of a 3-electron π bond.

Both resonance theory and MO perturbation theory predict that formation of a three-electron π bond requires electron transfer from the substituent group, X, to A. In resonance theory, the transfer is represented in the second resonance structure



in equation 2.4. In MO theory, when the orbitals on X and A mix, some of the electron density in the doubly occupied orbital on X is transferred to the singly occupied orbital on A. Using either of these theories, the greatest stabilization of the radical and hence, the greatest lowering of the BDE is expected when the difference in electronegativity between X and A is smallest. This predicts that carbon, which is more electronegative than silicon, should have a stronger π bond in $\text{X}-\dot{\text{A}}\text{H}_2$ and hence a lower A-H BDE than silicon. Also, the anticipated trend for the π bond strengths of the substituent groups, X, should be $\text{NH}_2 > \text{OH} > \text{F}$. This is exactly what is found in the calculated A-H BDEs that are listed Table 2-3.

However, the Si-H BDE in $\text{X}-\text{AH}_3$ actually increases relative to that in silane for $\text{X} = \text{OH}$, and F , and for $\text{X} = \text{NH}_2$ when the amino lone pair is rotated out of conjugation. Three electron π bonding in the radical obviously cannot explain these increases in BDE. Hence, once again, there is evidence of another effect acting; and once again, this effect appears to increase the Si-H BDEs as the electronegativity of X increases. Thus, while NH_2 , OH and F can stabilize silicon centered radicals

through π electron donation, these substituents increase the Si-H BDE presumably by withdrawing electron density from silicon through the σ bond. There is experimental evidence for the existence of this second effect in both Si-H and C-H BDEs.

Experimentally, it is found that in F_3A-H , the A-H bond is stronger than in AH_4 for both $A=C$ and $A=Si$. The Si-H bond strength in trifluorosilane has been measured at 100.1 kcal/mol⁹ which is 9.8 kcal/mol greater than that in silane. In addition, despite the probable stabilization of $\dot{C}F_3$, The C-H bond strength of 106.0 kcal/mol¹⁰ in trifluoromethane is greater than that in methane by 1.2 kcal/mol.

Additional evidence exists that indicates C-H bond strengths can be increased by a single substituent group that is sufficiently electron withdrawing. Thus, experimentally, 1,1,1-trifluoroethane has a carbon-hydrogen bond strength of 106.2 kcal/mol,¹ presumably because of the presence of the very electron withdrawing CF_3 group attached to the incipient carbon radical center. We find that the C-H BDE in $H_3N^+-CH_3$ exceeds that in CH_4 by 4.0 kcal/mol, again because the H_3N^+ group is very electron withdrawing.

Although both C-H and Si-H BDE are increased by σ electron withdrawal, this effect is masked by π delocalization in $:X-\dot{C}H_2$. Since π delocalization is less important in $:X-\dot{Si}H_2$, the σ withdrawing nature of substituents more electronegative than hydrogen actually results in an increase in calculated BDEs for $:X-SiH_3$, except for $X=NH_2$ when the nitrogen lone pair is allowed to conjugate in the $H_2N-\dot{Si}H_2$ radical.

The σ electronegativity effect also explains why $X=\text{Li}$ reduces both C-H and Si-H BDEs more than $X=\text{BeH}$. Lithium is more electropositive than beryllium; and, hence, although Be is a better π acceptor, Li is a better σ electron donor. It appears that the σ electron donation effect dominates for these two substituents.

For the early first row substituents, BH_2 is actually an aberration. Its electronegativity allows it to be very effective at delocalizing the odd electron on A by forming a strong π bond to both $A = \text{C}$ and Si. This masks the fact that it is a worse σ electron donor than either BeH or Li.

Thus, our calculations on π acceptors and π donor substituents reveal that there are actually two types of substituent effects on A-H BDE. One is electron delocalization by π bonding in the radical, which always lowers the A-H BDE. The other is a σ effect, which appears to lower the A-H BDE when the substituent, X, is less electronegative than hydrogen and raises the BDE when X is more electronegative than hydrogen.

Section 2-3-3 Methyl and Silyl as Substituents

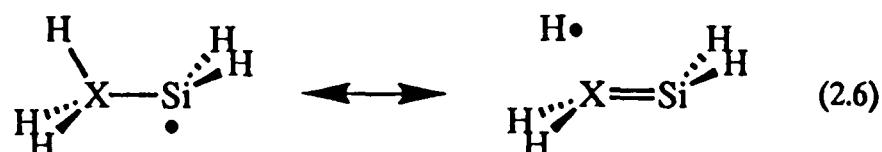
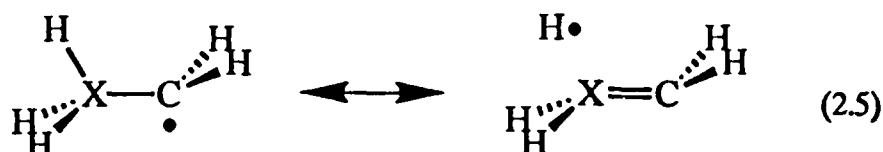
Based on these two effects, we are now prepared to answer the original question: Why do silyl groups weaken both silicon-hydrogen and carbon-hydrogen bonds whereas alkyl groups only weaken carbon-hydrogen bonds?

Granted, π delocalization is less important for substituents like methyl and silyl that do not have a lone pair or an empty p orbital; but hyperconjugation does allow delocalization of the odd electron, as depicted in equations 2.5 and 2.6.

Table 2-4 Effect of methyl and silyl substituents on the MP4SDTQ/6-31G* derived BDEs using the reaction^a $[X-AH_2]^\bullet + AH_4 \rightarrow X-AH_3 + \bullet AH_3$

Substituent Group (X)	ΔE (kcal/mol)		X-A bond length in the radical (Å)	
	A=C	A=Si	A=C	A=Si
CH ₃	3.3	-0.8	1.498	1.894
SiH ₃	4.4	2.9	1.860	2.345

^aA positive ΔE implies that the substituent weakens the A-H bond.



Hyperconjugation should play a larger role in stabilizing carbon-centered than silicon-centered radicals, since, the resultant π bond to carbon is stronger than the π bond to silicon for both $X=\text{CH}_3$ and $X=\text{SiH}_3$. Thus, hyperconjugation is expected to have a larger effect on reducing the C-H BDE than the Si-H BDE.

It is a little harder to predict whether a CH₃ substituent should hyperconjugate better than a SiH₃, because the difference in the strengths of the π bonds formed is

partially compensated for by the difference in the strengths of the bond that is broken.¹¹ However, because SiH_3 , unlike CH_3 , is less electronegative than hydrogen, the σ donating effect of $\text{X} = \text{SiH}_3$ should lower the BDE for both $\text{A} = \text{C}$ and Si .

As expected, the results in Table 2-4 show that both substituents reduce the C-H BDE. Despite the fact that CH_3 hyperconjugation is expected to be slightly more radical stabilizing than SiH_3 hyperconjugation,¹¹ an SiH_3 substituent is calculated to cause a slightly larger reduction in the C-H BDE. Presumably this is due to the fact that SiH_3 is a better σ donor than CH_3 .

Because of the weakness of π bonds to silicon, neither substituent is expected to reduce the Si-H BDE significantly through hyperconjugative radical stabilization. Consequently, since methyl is slightly more σ electron withdrawing than hydrogen, it is perhaps not entirely surprising that a methyl substituent is actually calculated to slightly increase the Si-H BDE. In contrast, the σ donating ability of the SiH_3 substituent, relative to H, results in the lowering of the Si-H BDE in $\text{H}_3\text{Si-SiH}_3$ relative to that in SiH_4 .

Section 2-3-4 Origin of the σ Electronegativity Effect

In addition to the well understood effect of substituent electronegativity on π delocalization in $\text{X-}\dot{\text{A}}\text{H}_2$ radicals, our calculations have revealed that σ electron donor substituents weaken A-H bonds while σ electron withdrawing substituents

strengthen them. This second effect has been little appreciated, but it can be understood on the basis of a rule enunciated by Bent:

*Atomic p character concentrates in orbitals directed toward electronegative substituents.*¹²

Concentration of the p character of atom A in the X-A bond in $X-AH_3$ implies that s character will be concentrated in the A-H bonds. For an electronegative substituent, X, this should strengthen the A-H bonds, since the bond strength increases with increasing s character on A.¹³ Conversely, when X is more electropositive than H s character will be concentrated in the X-A bond. Consequently, p character will be concentrated in the A-H bonds and weaken them.

The σ electronegativity effect is particularly apparent in Si-H BDE when electronegative substituents are present since, as discussed above, π delocalization by donation of substituent lone pairs is not very important for silicon-centered radicals. Similarly, since hyperconjugation provides little stabilization for silicon-centered radicals, the σ electronegativity effect is particularly apparent in the comparison of how alkyl and silyl substituents affect Si-H BDEs.

Section 2-3-5 First-row Substituents Containing π Bonds

Organic chemists have long known that adjacent π bonds stabilize carbon-centered radicals by π electron delocalization¹⁴. From the preceding discussion, adjacent π bonds should stabilize carbon-centered more than silicon-centered radicals, since silicon forms weaker π bonds. To test this hypothesis,

we examined computationally the effect of several different substituent groups that are commonly used to stabilize carbon centered radicals.

Table 2-5 Effect of first row substituents containing π bonds on the MP4SDTQ/6-31G* derived BDEs using the reaction^a $[X-AH_2]\cdot + AH_4 \rightarrow X-AH_3 + \cdot AH_3$

Substituent Group (X)	ΔE (kcal/mol)	
	A = C	A = Si
-CN	5.1	-1.0
-NC	7.4	-1.6
-C ₂ H ₅	13.2	-3.1
-CHO	5.4	0.4
-NO ₂	2.5	-1.2

^aA positive ΔE implies that the substituent weakens the A-H bond.

As expected, all the substituents in Table 2-5 are calculated to lower the C-H BDE. None of these substituents reduced the Si-H BDE from that in SiH₄, since π delocalization is relatively ineffective in stabilizing silyl radicals; and all of these substituents are relatively σ electron withdrawing. The effect of substituents containing π bonds to second-row elements will be discussed in Section 2-5.

Section 2-4 Second Row π Donor Substituents

Second row elements differ from their corresponding first row elements by forming weaker π bonds and by being more electropositive. Since Si-H BDEs are

more affected by the σ electronegativity of substituents than by their bonding abilities, second row substituents should reduce Si-H BDEs more than their first row counterparts.

Table 2-6 Comparison of effects of second and first row substituents on the MP4SDTQ/6-31G* derived BDEs using the reaction^a $[X-AH_2\cdot] + AH_4 \rightarrow X-AH_3 + \cdot AH_3$

Subst. Group (X)	ΔE (kcal/mol)		Subst. Group (X)	ΔE (kcal/mol)	
	A=C	A=Si		A=C	A=Si
PH ₂	5.7	2.6	NH ₂	12.2	0.9
PH ₂ ^b	2.8	0.7	NH ₂ ^b	3.7	-2.5
PH ₃ ^c	10.4		NH ₃ ^c	12.8	
SH	7.9	1.6	OH	8.6	-0.8
SH ^b	3.6	-0.2	OH ^b	4.2	-1.6
Cl	4.9	-0.3	F	4.4	-3.5

^aA positive ΔE implies that the substituent weakens the A-H bond.

^bRadical orbital rotated out of conjugation with lone pair.

^cSubstituent group constrained to be planar.

The expected effect of these substituents on the C-H BDE is more complicated. The lower electronegativity of second rows substituents should make them better π donors than their first row counterparts, but the weaker π bonds that second row substituents form could cause them to provide less stabilization for the radicals than their first row counterparts, hence increasing the C-H BDE. Of course, the lower electronegativity of the second row substituents should again result in the σ effect acting to lower the C-H BDEs, relative to their first row counterparts.

The second row substituents on silicon behave just as expected. Each gives a lower calculated Si-H BDE than its first row counterpart. $X=PH_2$ lowers the Si-H BDE more than $X=NH_2$, despite the fact that the latter substituent provides more π bonding in the $X-SiH_2$ radical. Evidence for a stronger π bond in $X=NH_2$ comes from the finding that it costs 1.9 kcal/mol to rotate the PH_2 group out of conjugation, compared to 3.6 kcal/mol for NH_2 .

For carbon, SH and Cl substituents are calculated to give almost the same reduction in C-H BDE as their first row counterparts. PH_2 however provides much smaller reduction than NH_2 .

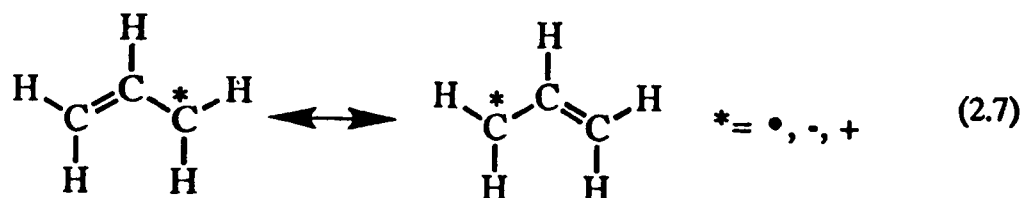
The much smaller barrier to rotating the PH_2 out of conjugation in $X-\dot{C}H_2$ again suggests that π delocalization in the radical is much less stabilizing for PH_2 than NH_2 . This is not surprising since the phosphorous lone pair does not overlap well with the carbon radical orbital, due to the highly pyramidal geometry at phosphorous, which results in a large amount of s character in the phosphorous lone pair. If the phosphorous is constrained to be planar in both H_2P-AH_3 and $H_2P-\dot{A}H_2$, the amount of π stabilization increases. This is evidenced by the fact that a planar PH_2 substituent is calculated to reduce the C-H BDE by 10.4 kcal/mol. The C-H BDE reduction and barrier to rotation for a planar NH_2 substituent are 12.8 and 10.3 kcal/mol.

In contrast to PH_2 , both SH and Cl substituents have lone pairs in pure p orbitals. This accounts for the fact that they reduce the C-H BDE more than a pyramidalized PH_2 group but not as much as a planar PH_2 . The barrier of 4.3

kcal/mol to rotation of the lone pair in the pure p orbital on S-H out of conjugation is also intermediate between the values of 2.9 and 21.2 kcal/mol for rotating, respectively, pyramidalized and planar PH_2 groups in $\text{PH}_2\text{-}\dot{\text{C}}\text{H}_2$.

Section 2-5 Vinylic Substituents Containing Silicon

Organic chemists have long known that vinyl substituted carbon radicals and ions possess additional stability compared to alkyl substituted carbon radicals and ions.¹ This additional stability comes from the ability of the π bond in vinyl to delocalize the radical or charge through allylic resonance, as shown in equation 2.7.



We wanted to know if allylic type resonance would bestow comparable stability and delocalization when silicon replaces one or more of the carbon atoms. Therefore, we performed calculations on the effect of vinyl substituents and their $\text{H}_2\text{C}=\text{SiH}$, $\text{H}_2\text{Si}=\text{CH}$, and $\text{H}_2\text{Si}=\text{SiH}$ analogs on C-H and Si-H BDEs.

Since, as discussed above, substituents alter BDE through both σ and π effects, we separated these effects by the now familiar technique of rotating the vinyl group out of conjugation in the radical.

Section 2-5-1 Computational Methodology Used

A problem with UHF calculations is that they give wave functions for radicals that are not pure doublet states. In $X-\dot{A}H_2$ radicals, the spin contamination becomes serious when X is unsaturated. For example, for allyl radical ($X = H_2C=CH$ and $A = C$) a UHF calculation with the 6-31G* basis set gives a wave function with $S^2 = 0.972$, compared to $S^2 = 0.750$ for a pure doublet.

When electron correlation is provided by Møller-Plesset perturbation theory, spin contamination raises the energy of the resulting wave function, since the contaminant states, quartets and even higher multiplicities, lie above the doublet wave function in energy. Since spin contamination is much more of a problem in $X-\dot{A}H_2$ radicals than in AH_3 , especially when X is unsaturated, the values for the lowering of the A-H BDEs by the unsaturated substituents in Table 2-5 should be regarded as lower bounds on the actual BDEs.

One way of handling spin contamination is to project the largest spin contaminant from a UHF wave function.¹⁵ However, rather than using spin projection, we elected to perform CI-SD calculations, which, being strictly variational, necessarily give pure doublet wave functions. The effects of the vinyl substituents on

the A-H BDEs in Tables 2-7 and the barriers to rotation in Table 2-8 were all calculated from CI-SD energies.

Section 2-5-2 Effects of Vinyl Substituents Containing Silicon on BDEs

Since, as discussed above, π bonding to C is generally more important than π bonding to Si, one would expect that each type of vinyl substituent, X, would have a greater stabilizing effect in $X-\dot{C}H_2$ than in $X-\dot{Si}H_2$. Therefore, one would expect that in all cases, the C-H bond in $X-CH_3$ would be weakened significantly more than the Si-H bond in $X-SiH_3$.

Table 2-7 Effects of vinyl derivatives on the MP4SDTQ/6-31G* derived BDEs using the reaction^a $[X-AH_2]\cdot + AH_4 \rightarrow X-AH_3 + \cdot AH_3$

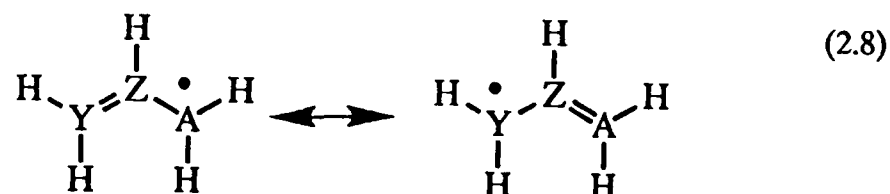
Vinyl Substituent Group (X)	ΔE (kcal/mol)	
	A = C	A = Si
$H_2C=CH$	17.2	-0.7
$H_2Si=CH$	36.3	-0.2
$H_2C=SiH$	13.1	3.3
$H_2Si=SiH$	18.8	8.4

^aA positive ΔE implies that the substituent weakens the A-H bond.

As shown in Table 2-7, this is the case. However, the amount of reduction in BDE reduction depends on the identity of the vinyl group, X, in $X-AH_3$, as well as on the identity of A. Interestingly, $H_2Si=CH$ has by far the greatest effect of all the

substituents on reducing the C-H BDE, but $X = H_2Si=SiH$ has the largest effect on reducing the Si-H BDE.

Since π delocalization in the allylic radicals formed is anticipated to be the dominant effect on C-H BDEs, it should be possible to understand the effects of the various vinyl groups by examining the two allylic resonance structures in equation 2.8.



For $Y=C$, $Z=C$ or Si , and $A=C$, the two structures are identical and, hence, equally important. However, for $Y=Si$ and $Z=C$, the fact that the strength of the C-C π bond is nearly twice that of the Si-C π bond makes the second resonance structure much more important. This accounts for the fact that the $H_2Si=CH$ group has such a large effect on reducing the C-H BDE. Breaking the C-H bond in $H_2Si=CH-CH_3$ allows π delocalization to occur, resulting in the Si-C π bond in the reactant being transformed into an allylic radical in which the π bond is largely C=C in character.

The same allylic radical is formed by breaking the Si-H bond in $\text{H}_2\text{C}=\text{CH}-\text{SiH}_3$, and the expected localization of the double bond in the radical is evidenced by the absence of any appreciable effect of the $\text{H}_2\text{C}=\text{CH}$ substituent on the Si-H BDE and by the bond lengths in the radical, which are nearly the same as those in $\text{H}_2\text{C}=\text{CH}-\text{SiH}_3$. The predicted inability of an adjacent $\text{C}=\text{C}$ π bond to provide appreciable delocalization for an $\dot{\text{SiH}}_2$ center is consistent with the experimental finding that the SiH BDE is unaffected by a phenyl substituent⁴ and that of the EPR spectrum of $\text{Ph}-\text{SiH}_2$ shows the radical to be largely centered at silicon.¹⁶ The EPR spectrum of $[\text{H}_2\text{C}=\text{CH}-\text{SiH}_2]^\bullet$ likewise has the radical center primarily localized at silicon center, although there is some delocalization into the C-C π bond.¹⁷

For $\text{Y} = \text{Z} = \text{Si}$, and $\text{A} = \text{C}$, the second structure in equation 2.8 also makes the dominant contribution because of the greater strength of Si-C compared to Si-Si π bonds.¹¹ However, the difference between Si-C and Si-Si π bond strengths is smaller than that between Si-C and C-C π bonds, thus accounting for the fact that $\text{H}_2\text{Si}=\text{SiH}$ has a smaller effect on reducing the C-H BDE than does $\text{H}_2\text{Si}=\text{CH}$.

The dominance of the $\text{H}_2\text{C}=\text{SiH}-\dot{\text{SiH}}_2$ resonance structure predicts little stabilization of an Si radical center by a $\text{H}_2\text{C}=\text{SiH}$ substituent. However, this group effects a significant reduction in the Si-H BDE, as does a $\text{H}_2\text{Si}=\text{SiH}$ substituent. In order to separate possible σ from π effects of vinylic substituent groups on the A-H BDEs and, particularly, on the Si-H BDEs, once again the effect of rotating the

substituent group, X, out of conjugation in $X-\dot{A}H_2$ was calculated for each substituent group.

Section 2-5-3 Calculation of Allylic Resonance Energies

Resonance energies in radicals containing unsaturated groups, X, are sometimes estimated by the reduction in the A-H BDE caused by the presence of X in $X-AH_2$.¹⁸ However, due to the existence of possible σ effects on the A-H BDEs, the energy required to rotate an unsaturated X group out of conjugation provides a more accurate assessment of the π resonance energies. The allylic resonance energies (AREs) that we computed in this manner are listed in Table 2-8.

Table 2-8 CISD/6-31G* Derived Allylic Resonance Energies (AREs) for Allylic Radicals, $[X-AH_2]^\bullet$.

Substituent Group (X)	ΔE (kcal/mol)	
	A = C	A = Si
$H_2C=CH$	15.3	0.2
$H_2Si=CH$	31.6	0.8
$H_2C=SiH$	8.2	0.3
$H_2Si=SiH$	13.6	5.6
$H_2Si=CH^a$		7.4
$H_2Si=SiH^a$		5.0

^aAll centers are constrained to be planar.

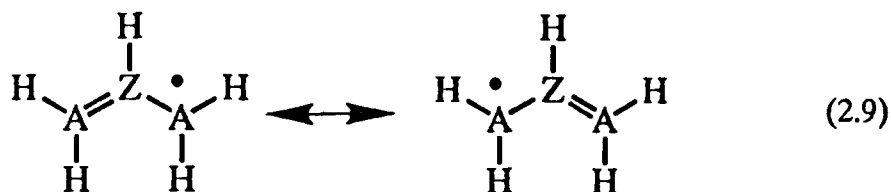
Section 2-5-3-1 Unsymmetrical Allylic Radicals

As expected, because of the greater strength of π bonds to carbon than to silicon, the AREs for each substituent group are larger when the partial π bond in the allylic radical that is broken leaves the unpaired electron on carbon rather than silicon. For example, in $[\text{H}_2\text{SiCHCH}_2]^\bullet$ radical, the results in Table 2-8 predict that it should cost about 32 kcal/mol to rotate about the C-C bond, but rotation about the C-Si bond should be almost without cost. The difference in the energy required to rotate each of the two terminal groups out of conjugation is almost exactly equal to the difference between the energies of the C-C (65 kcal/mol)⁸ and C-Si (35 kcal/mol)⁸ π bonds. Similarly, the difference of 13.3 kcal/mol in the energies required to rotate the SiH_2 and CH_2 groups out of conjugation in $[\text{H}_2\text{SiSiHCH}_2]^\bullet$ is equal to the difference in Si-C (35 kcal/mol) and Si-Si (22 kcal/mol)⁸ π bond energies.

Section 2-5-3-2 Symmetrical Allylic Radicals

When the terminal groups of the allylic radical are identical, rotation of either group out of conjugation must, by symmetry, be equivalent to rotation of the other. Hence, unlike the case with unsymmetrical allylic radicals, comparison of the AREs for symmetrical allylic radicals must be between different radicals.

The allyl analogs -- $[\text{H}_2\text{C-SiH-CH}_2]^\bullet$, $[\text{H}_2\text{Si-CH-SiH}_2]^\bullet$, and $[\text{H}_2\text{Si-SiH-SiH}_2]^\bullet$ -- like the parent allyl radical, $[\text{H}_2\text{C-CH-CH}_2]^\bullet$, each have two equivalent resonance structures. Simple Hückel theory predicts that the ARE in each allylic radicals is



proportional to the strength of the A-Z π bond present in each of the two resonance structures. As a result, the anticipated trend for AREs is expected to be : $[\text{H}_2\text{C}-\text{CH}-\text{CH}_2]^\bullet > [\text{H}_2\text{C}-\text{SiH}-\text{CH}_2]^\bullet \approx [\text{H}_2\text{Si}-\text{CH}-\text{SiH}_2]^\bullet > [\text{H}_2\text{Si}-\text{SiH}-\text{SiH}_2]^\bullet$. More quantitatively, the ratio between the AREs should be approximately 9:5:5:3 based on the relative strengths of the π bonds that are involved.¹¹

Inspection of Table 2-8 reveals that, with one glaring exception, this is the ratio of the calculated AREs. The one exception is a computed ARE of 0.8 kcal/mol for $[\text{H}_2\text{Si}-\text{CH}-\text{SiH}_2]^\bullet$, as opposed to 8.2 kcal/mol computed for $[\text{H}_2\text{C}-\text{SiH}-\text{CH}_2]^\bullet$. As discussed above, one would naively expect both to have the same ARE.

However, inspection of the geometries of the allylic and rotated-allylic structures in Appendix 1 discloses significant pyramidalization of terminal silicon groups in $[\text{H}_2\text{Si}-\text{CH}-\text{SiH}_2]^\bullet$. If the silicon centers are constrained to remain planar, the ARE for $[\text{H}_2\text{Si}-\text{CH}-\text{SiH}_2]^\bullet$ is calculated to be 7.4 kcal/mol, which follows the

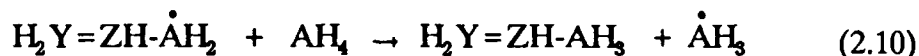
anticipated trend, and is very close to the ARE of 8.2 kcal/mol calculated for $[\text{HC}_2\text{-SiH-CH}_2]^\bullet$. Due to the fact that, unlike silicon centered radicals, those centered on carbon tend to be planar, the terminal atoms in the latter allylic radical are planar even without being constrained to be so.

Inspection of the geometries also reveals that $[\text{H}_2\text{Si-SiH-SiH}_2]^\bullet$ contains three pyramidal silicon centers. However, unlike the case in $[\text{H}_2\text{Si-CH-SiH}_2]^\bullet$, the ARE does not appear to be affected by pyramidalization, since constraining the silicon centers to be planar actually decreases the calculated ARE from 5.4 kcal/mol to 5.0 kcal/mol. This finding is the opposite of the usual result that constraining atomic centers to planarity increases the strength of the π bonds that they form, since planarity allows better overlap of the orbitals involved in π bonding.

Constraining the silicon centers in the $[\text{H}_2\text{Si-SiH-SiH}_2]^\bullet$ system to planarity decreases the calculated ARE slightly, since, when forced to be planar, the preferred geometry at the three silicon centers is artificially altered in the conjugated geometry; whereas, just a single silicon center is affected in the rotated geometry. The energy required to planarize the three silicon centers in the conjugated geometry apparently exceeds slightly the energy required to planarize the non-conjugated SiH_2 center in the rotated geometry.

Section 2-5-4 Effects of Vinyl Substituents at Unconjugated Geometries

As discussed in Section 2-3, A-H BDEs can be influenced by both, σ and π effects. The previous section describes the π effects of vinyl substituents on reducing



the A-H BDEs; the remaining component is σ donation/withdrawal by the vinyl substituents. This effect can be computed from the energy of equation 2.10, with the singly occupied orbital in $\text{X}-\dot{\text{A}}\text{H}_2$ held orthogonal to the π bond in X. The energies, which are reported in Table 2-9, are equal to the difference between the BDEs in Table 2-7 and the AREs in Table 2-8.

Table 2-9 σ Effects vinyl derivatives on the CI-SD/6-31G* derived BDEs using the reaction^a $[\text{X}-\dot{\text{A}}\text{H}_2] + \text{AH}_4 \rightarrow \text{X}-\text{AH}_3 + \cdot\text{AH}_3$

Vinyl Substituent Group (X)	A=C	A=Si
$\text{H}_2\text{C}=\text{CH}$	1.9	-0.9
$\text{H}_2\text{Si}=\text{CH}$	4.7	-1.0
$\text{H}_2\text{C}=\text{SiH}$	4.9	3.0
$\text{H}_2\text{Si}=\text{SiH}$	5.3	2.8

^aThe radical orbital in the reactant is orthogonal to the π bond.

Inspection of the data in Table 2-9 reveals that, as discussed for a CH_3 substituent in Section 2-3-3, the Si-H BDEs are very slightly increased when a carbon is bound to the silicon center; but are reduced when a silicon is the α atom of the substituent group.¹⁹ Not surprisingly, σ electronic effects in altering the Si-H BDE are primarily determined by the substituent atom α to the Si-H bond being broken and are nearly independent of the atom β to it.

The C-H BDEs, as expected, are reduced by all substituents. What is not clear at first, however, is why there is a nearly 3 kcal/mol difference between $\text{H}_2\text{C}=\text{CH}$ and $\text{H}_2\text{Si}=\text{CH}$ substituents on reducing the C-H BDE. If σ electronic effects are primarily determined by the α atom of the substituent group, then these two substituents would be predicted to have similar effects on the C-H BDEs.

As discussed in Section 2-3-3, carbon centered radicals are stabilized by hyperconjugation. The Si-C σ bond in $\text{H}_2\text{Si}=\text{CH}$ is weaker than the C-C σ bond in $\text{H}_2\text{C}=\text{CH}$; and, hence, the former substituent might hyperconjugate better than the latter. However, this explanation cannot be verified directly with these vinyl substituent since rotation of the Si-C σ bond out of conjugation with the radical orbital would result in alignment of the π bond with the radical orbital. Comparison of the calculated BDE for $\text{SiH}_3\text{CH}_2\text{CH}_2\text{-H}$ with that for $\text{CH}_3\text{-CH}_2\text{-H}$ can elucidate if a carbon centered radical can more effectively hyperconjugate with a C-Si σ bond than with C-H. Rotation of the Si-C σ bond out of conjugation with the radical center in $\text{H}_3\text{Si-CH}_2\text{-}\dot{\text{C}}\text{H}_2$ provides another test of the effect of hyperconjugation with an Si-C σ bond on stabilization of a carbon centered radical.

The calculated CI-SD BDE of $\text{H}_3\text{SiCH}_2\text{CH}_2\text{-H}$ is 2.8 kcal/mol less than that of $\text{CH}_3\text{CH}_2\text{-H}$ when the Si-C σ bond is aligned with the orbital containing the unpaired electron in the radical. Rotation about the C-C bond by 90° in the $\text{H}_3\text{SiCH}_2\text{-}\dot{\text{C}}\text{H}_2$ radical requires 2.2 kcal/mol showing that the lowering of the BDE is largely due to Si-C σ bond hyperconjugation. Therefore, the σ effect calculated for

the $\text{H}_2\text{Si}=\text{CH}$ substituent on lowering the C-H BDE probably also actually includes a contribution from delocalization of the carbon radical through hyperconjugation.

Hyperconjugation with a C-Si bond might also be expected to be important in stabilizing $[\text{H}_2\text{C}-\text{SiH}-\text{CH}_2]^\bullet$ when the π bond of the vinyl group is twisted out of conjugation with the singly occupied orbital on carbon. However, since Si-C π bonds are weaker than C-C π bonds, hyperconjugation should be less important in twisted $[\text{H}_2\text{C}-\text{SiH}-\text{CH}_2]^\bullet$. In order to test this prediction, we performed calculations on the BDE of $\text{CH}_3\text{SiH}_2\text{CH}_2\text{-H}$ and the barrier to rotating the Si-C σ bond out of conjugation in the resulting radical.

The calculated CI-SD BDE of $\text{CH}_3\text{SiH}_2\text{CH}_2\text{-H}$ is 1.0 kcal/mol weaker than that of $\text{H}_3\text{SiCH}_2\text{-H}$, and the barrier to twisting the Si-C bond out of conjugation in $\text{CH}_3\text{SiH}_2\dot{\text{C}}\text{H}_2$ is only 0.1 kcal/mol. Clearly, stabilization of this radical by hyperconjugation with the Si-C σ bond is less important than in $\text{SiH}_3\text{CH}_2\dot{\text{C}}\text{H}_2$.

This finding implies that the similar C-H BDEs for non-conjugated $\text{H}_2\text{Si}=\text{CH}$ and $\text{H}_2\text{C}=\text{SiH}$ substituents is due to the fact that, although the σ bond in the former substituent hyperconjugates better, the latter has the more electropositive silicon atom in the α position. Further evidence for the relative unimportance of σ bond hyperconjugation when silicon is in the α position of the substituent group comes from the finding in Table 2-9 that a twisted $\text{H}_2\text{Si}=\text{SiH}$ substituent lowers the C-H BDE only 0.4 kcal/mol more than a twisted $\text{H}_2\text{C}=\text{SiH}$ substituent; whereas with carbon in the α position, twisted $\text{H}_2\text{Si}=\text{CH}$ lowers the C-H BDE by 2.8 kcal/mol more than twisted $\text{H}_2\text{C}=\text{CH}$.

Section 2-6 Conclusions

As noted in section 2-3-4, we found that a substituent affects A-H BDEs in two ways. First, the well understood effect of π delocalization in $X-\dot{A}H_2$ weakens A-H bonds by stabilizing the radicals. Second, σ electron donors weaken A-H bonds, whereas σ electron withdrawing substituents strengthen them.

Both of these effects play an important role in determining the strength of C-H bonds. π stabilization of carbon centered radicals usually can overcome the effects of σ electron withdrawal, except when σ withdrawal is severe, as in F_3CH .

Conversely, the Si-H bond is most strongly influenced by σ electronic effects. Of all the substituents examined, only two -- BH_2 , $H_2Si=SiH$ -- have been shown to provide a significant amount of π delocalization.

Chapter 2 Notes

1. Pasto, D. J.; Krasnansky, R.; Zercher, C. *J. Org. Chem.* **1987**, *52*, 3062 and references cited within.
2. Parmar, S. S.; Benson, S. W. *J. Am. Chem. Soc.*, **1989**, *111*, 57.
3. Coolidge, M. B.; Borden, W. T. *J. Am. Chem. Soc.*, **1988**, *110*, 2298.
4. Walsh, R. *Acc. Chem. Res.* **1981**, *14*, 246.
5. Kanabus-Kaminska, J. M.; Hawari, J. A.; Griller, D.; Chatgililoglu, C. *J. Am. Chem. Soc.* **1987**, *109*, 5267.
6. J. A. Pople, J. S. Binkley, and R. Seeger, *Int. J. Quantum Chem. Symp.*, **10** 1 (1976)
7. Frisch, M. J.; Binkley, J. S.; Schlegel, H. B.; Raghavachari, K.; Melius, C. F.; Martin, R. L.; Stewart, J. J. P.; Bobrowicz, F. W.; Rohlfing, C. M.; Kahn, L. R.; Defrees, D. J.; Seeger, R.; Whiteside, R. A.; Fox, D. J.; Fleuder, E. M.; Pople, J. A. Carnegie-Mellon Quantum Chemistry Publishing Unit, Pittsburgh PA, 1984.
8. Kutzenigg, W. *Angew. Chem., Int. Ed. Engl.* **1984**, *23*, 272. Schmidt M. W.; Truong P. N.; Gordon M. S. *J. Am. Chem. Soc.*, **1987**, *109*, 5217 and references therein.
9. Doncaster, A. M.; Walsh, R. *Int. J. Chem. Kinet.*, **1978**, *10*, 101.
10. Benson, S. W. "Thermochemical Kinetics", 2nd ed., Wiley, New York, 1976
11. Actual numbers for π bond strength come from reference 8 and are summarized as follows: C=C is 65 kcal/mole, C=Si is 35-36 kcal/mol, and Si=Si is 22 ± 2 kcal/mol. The relative strength of the σ bond from 4 shows that a C-H bond is approximately 14 kcal/mol stronger than a Si-H bond. Hyperconjugation requires that the X-H σ bond be broken to form the π bond. It is easier to break a Si-H σ bond, but the resultant π bond that is formed is weaker than the π bond formed using a C center. Therefore, it is difficult to say whether a SiH₃ or a CH₃ substituent group will stabilize a radical center better through hyperconjugation. This is especially true when the radical center is at silicon, since the difference in the energies of the π bonds formed to SiH₃ and CH₃ substituents is almost exactly equal to the difference in the energies of the SiH and CH bonds being broken. For a carbon centered radical, CH₃ should be slightly more stabilizing than SiH₃.
12. Bent, H. A. *Chem. Rev.* **1961**, *61*, 275.

13. The increase in C-H BDE from 100.3 kcal/mol for H_3CCH_3 , to 106 kcal/mol for H_2CCH_2 and to 132 kcal/mol for HCCH demonstrates this fact very well. All values are from: *CRC Handbook of Chemistry and Physics*, 67th ed.; Weast, R. C., Ed.; CRC Press: Boca Raton, FL, 1986; p F-178.
14. For leading references, see Pasto (1).
15. Borden, W. T. "Modern Molecular Orbital Theory for Organic Chemists," Prentice-Hall, Inc., 1975.
16. Sakurai, H.; Umino, H.; Sugiyama, H. *J. Am. Chem. Soc.*, 1980, 102, 6837.
17. Jackson, R. A.; Zarkadis, A. K. *Tetrahedron Letters*, 1988, 29, 3493.
18. See, for example, Doering, W. v. E.; Roth, W. R.; Breuckmann, R.; Figge, L.; Lennartz, H.-W.; Printzbach, H. *Chem. Ber.*, 1988, 121, 1.
19. The values in Table 2-7 are calculated at the CI-SD/6-31G* level of theory. Since the BDE values given in Section 2-3-3 were calculated using the MP4SDTQ/6-31G* level of theory, these values were recomputed at the CI-SD/6-31G* level for direct comparison. The CI-SD values for the difference in C-H BDEs are 4.3 kcal/mol for ethane, 5.6 kcal/mol for silylmethane. The difference in the Si-H BDEs are -0.1 kcal/mol for methylsilane, and 3.5 kcal/mol for silylsilane. The CI-SD values result in approximately 1.0 kcal/mol additional stabilization over MP4SDTQ values for the difference in BDEs of the C-H bond and 0.6 kcal/mol for the Si-H bond. The difference in energy is a direct result of the wave function of the more substituted radical containing a greater amount of spin contamination from the quartet state. Møller-Plesset perturbation theory then spuriously overestimates the BDE of the more highly substituted radical, resulting in a difference of BDEs that is too small.

Chapter 3 Pyramidalization of Phosphorus in Borylphosphines

Section 3-1 Chemical Background

Section 3-1-1 Phosphorus versus Nitrogen

Trivalent phosphorous compounds differ from their nitrogen analogs, not only by having longer bond lengths but also by being highly pyramidal¹ and having much larger barriers to inversion.² Indeed, unlike their nitrogen analogs, optically active phosphines can be prepared and racemize only at elevated temperatures.³

Due to the highly pyramidal geometry and large energies required for planarization of phosphines, the lone pair on phosphorous is much less available for π bonding than the lone pair of amines.^{4,5} For example, phosphines are not planar, even when attached to three formyl groups; and the barrier to rotation about the phosphorus-carbonyl bond is small; whereas amides have planar geometries at nitrogen and considerably larger barriers to rotation about the nitrogen-carbonyl bond.

Section 3-1-2 Competition for Electron Density

The rotational barrier about the nitrogen carbonyl bond in an amide decreases when multiple carbonyls are attached to a central nitrogen. When only one formyl group is attached, the rotational barrier about the C-N bond is 17.8 kcal/mol. However, the barrier goes down to 12.9 kcal/mol with the addition of a second formyl group, and a third formyl reduces the rotational barrier all the way to 7.5

kcal/mol.⁶ Apparently, the formyl groups compete for the electron density in the nitrogen lone pair orbital, which is why π bond strength and, hence, the rotational barrier decreases with increasing number of formyl groups.

The same type of competition has been computationally predicted to exist in aminoboranes, borylamines, hydroxyboranes and borylhydroxides.⁷ Both of these types of compounds have lone pairs of electrons on atoms that compete to donate electron density into an empty boron π orbitals. In both cases, the greatest barrier to rotation occurs when there is just one substituent with a lone pair adjacent to a single boron with its empty orbital. When there is an excess of either boron substituents attached to a center with a lone pair or substituents with lone pairs attached to a boron center, there is reduction in barrier to rotation.⁸

Competition effects are also found in the rotational barriers about C-C bond along the series $(\text{CH}_2)_n\text{CH}_{3-n}$, where $n=1$ is ethene, $n=2$ is allyl, and $n=3$ is trimethylenemethane. The strongest π bond is that in ethene, where rotation, which breaks a full π bond, requires 65 kcal/mol.⁹ In allyl, the barrier to rotation of one methylene is reduced to 15 kcal/mol.¹⁰ Calculations reproduce these two barriers rather well.¹¹ In triplet trimethylenemethane, the barrier height has not been measured; but it has been calculated to be 10 kcal/mol at comparable levels of theory.¹²

Competition effects on the barriers to C-C rotation in the series $(\text{CH}_2)_n\text{CH}_{3-n}$ are predicted qualitatively even by simple Hückel molecular orbital theory. The HMO energies of the bonding MOs are respectively $\alpha + \beta$ for $n=1$, $\alpha + 1.414 \beta$

for $n=2$, and $\alpha + 1.732 \beta$ for $n=3$.¹³ Hence, the energy increase on breaking one π bond in each of these hydrocarbons is 2β , 0.828β , and 0.636β respectively.¹⁴

Given the apparently ubiquitous nature of competitive substituent effects, the discovery of a cooperative substituent effect would be noteworthy. As discussed in Section 3-3, we discovered such an effect in $\text{HP}(\text{BH}_2)_2$ and performed calculations to establish its origin.

Section 3-1-3 Experimental Examples of Electron Delocalization from Phosphorus

Despite the fact that phosphorus has a high barrier to planarity, there is experimental evidence that in boryl phosphines, the empty boron π orbital is effective in delocalizing the phosphorous lone pair. The x-ray structure of a monoboryl phosphine, (diphenylphosphino)dimesitylborane, shows a pyramidalization angle, ϕ (the angle between the extension of the P-B bond and the plane containing phosphorus and the other two groups bound to it) of 43° ¹⁵ compared to pyramidalization angles of about 68° ¹⁶ in the unconjugated phosphine, PPh_3 . In a similarly substituted derivative of diboryl phosphine, the boron-phosphorous bond lengths are shorter¹⁷ and the phosphorous is now planar ($\phi = 0^\circ$).¹⁸

There is also evidence for strong P-B π bonding in the crystal structures of cyclic phosphorous boron compounds. The six-membered ring in (mesityl B-P cyclohexyl)₃ is planar and exhibits equal P-B bond lengths of 1.84\AA .¹⁹ The four membered ring in (2,2,6,6-tetramethylpiperidino B-P 2,4,6-tris-*t*-butylbenzene)₂ is not planar,²⁰ but this is not surprising, since planarity would yield a conjugated cyclic

4-electron π system. Hückel MO theory predicts that this π system would be antiaromatic; hence, delocalization of the phosphorus lone pairs would be less stabilizing than in the molecule containing a six-electron cyclic π system.

In order to examine computationally the effect of boron substituents on the barrier to inversion of phosphorous, we performed calculations on $(\text{BH}_2)_n\text{PH}_{3-n}$, $n=1-3$, and on the cyclic $(\text{HBPH})_n$ compounds with $n=2$ and $n=3$.

Section 3-2 Theoretical Methodology

Calculations were carried out using Gaussian 82²¹ and 86²² with the 6-31G* basis set. All geometries were first optimized using a RHF wave function. Electron correlation was added at these geometries using fourth order Møller Plesset perturbation theory, MP4SDTQ. Some geometries were reoptimized using MP2, to verify that inclusion of electron correlation during optimization did significantly alter the geometry or the MP4SDTQ energy of the RHF optimized molecule. Zero point energy corrections from RHF vibrational analyses were included.

The four geometries optimized for H_2PBH_2 are the same as those chosen by Groper²³ for his RHF calculations. The geometries are pictured in Figure 3-1. They are: 1, the equilibrium C_s geometry with the lone pair and empty orbital in the symmetry plane; 2, the completely planar, C_{2v} , structure; 3, the rotated C_s structure with the boron hydrogens in the symmetry plane and the H-P-H bond angle bisected by the BH_2 group; and 4, the rotated C_{2v} structure with a planar phosphorus. Reoptimization of the C_s equilibrium (1) and the completely planar C_{2v} structure (2)

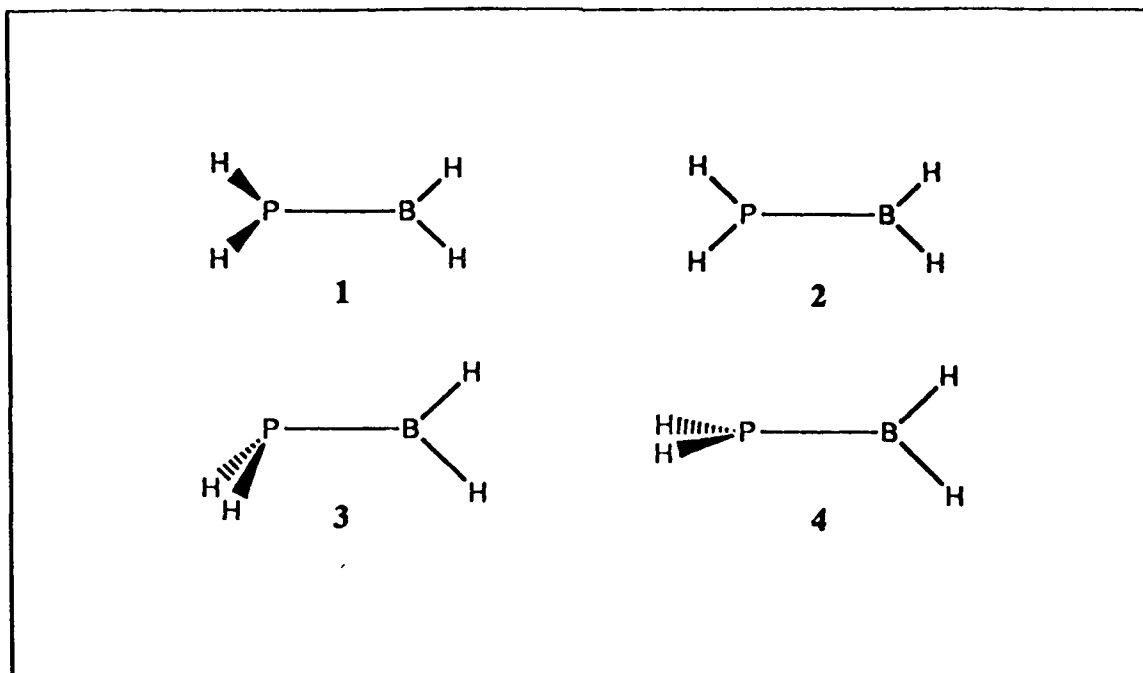


Figure 3-1 H_2PBH_2 geometries.

at the MP2 level resulted in a decrease in the central bond length of 1-2%.²⁴ The change in the MP4SDTQ energies relative to each other amounted to less than 0.5 kcal/mol.²⁵ These differences were not considered large enough to warrant using electron correlation during optimization of any of the other structures.

For $\text{HP}(\text{BH}_2)_2$, we optimized the six structures in Figure 3-2. They are: 5, the equilibrium C_s structure with both empty boron orbitals aligned with the phosphorous lone pair; 6, the completely planar C_{2v} structure; 7, the transition state for rotation of one BH_2 out of conjugation with the phosphorus lone pair; 8, the C_s structure with one BH_2 rotated out of conjugation with the phosphorus lone pair; 9, the dirotated C_s transition state structure; and 10, the dirotated C_{2h} structure with a planar geometry at phosphorous. The equilibrium (5) and the completely planar (6) structures were

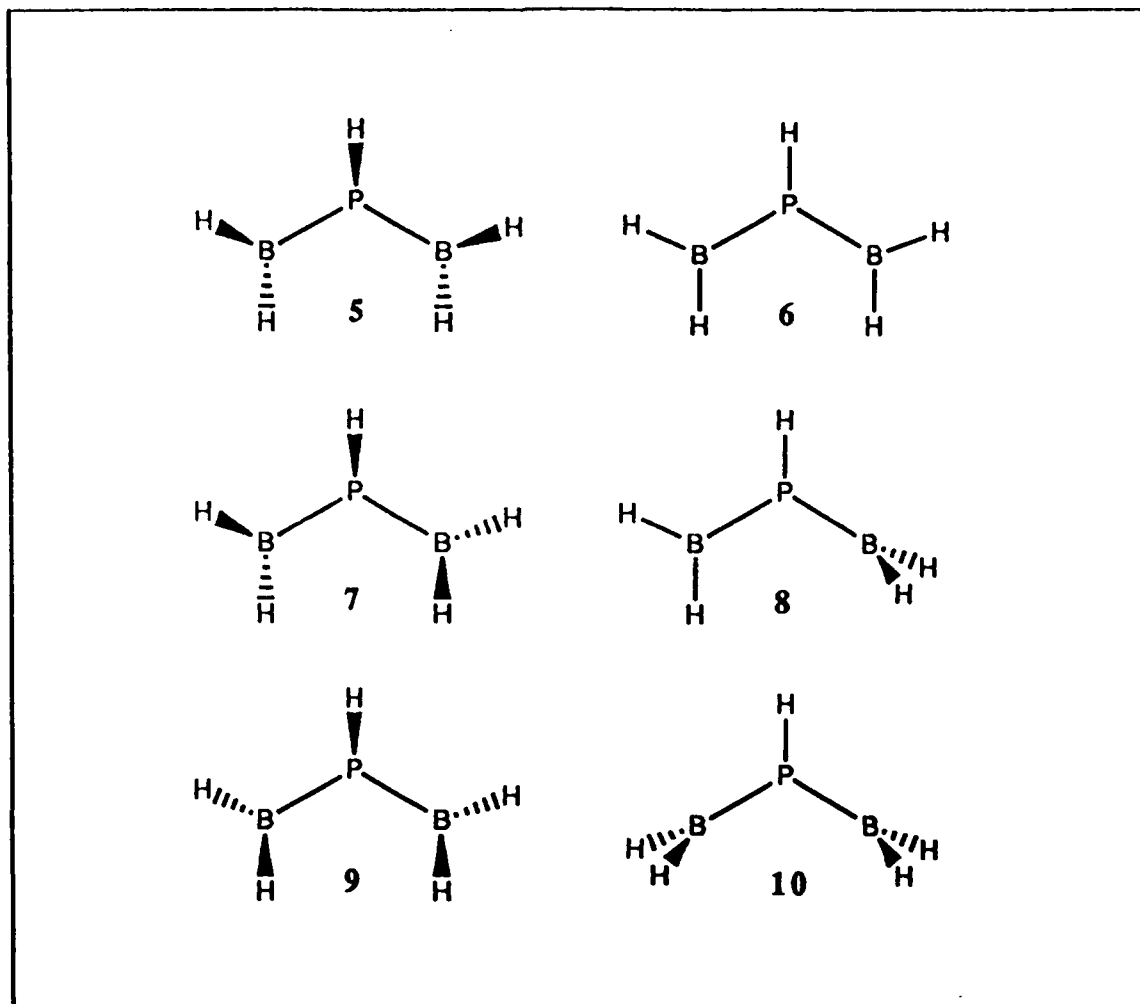


Figure 3-2 $\text{HP}(\text{BH}_2)_2$ geometries.

again reoptimized with inclusion of electron correlation at the MP2 level; and, once again, little change was found in the optimized geometries or MP4SDTQ energies.²⁶

Vibrational analyses were performed at all stationary points. The monorotated geometries, 3 and 7, were found to have exactly one imaginary frequency, corresponding to rotation of the twisted boron back into conjugation, and each was thus demonstrated to be true transition states. In contrast, the dirotated C_s structure (9) was found to have two imaginary frequencies. Hence it is not a true

saddle point but is only a transition state when constrained by symmetry. One vibrational mode with an imaginary frequency does, in fact, correspond to disrotary motion of the two BH_2 groups, which preserves the symmetry plane; but the other corresponds to conrotary motion, which destroys the symmetry plane.

Five geometries of triborylphosphines were studied. These geometries, which are depicted in Figure 3-3, were: **11**, the equilibrium, D_{3h} , planar structure in which the empty p orbitals on each boron is aligned for overlap with the phosphorous lone pair; **12**, the non-planar, monorotated, C_s structure; **13**, the planar, monorotated, C_{2v} structure; **14**, the planar, dirotated, C_{2v} structure; **15**, the planar, trirotated, D_{3h} structure in which the empty boron orbitals cannot conjugate with the phosphorous lone pair. No attempt was made to optimize any of these geometries with the inclusion of electron correlation at the MP2 level.

Three conformations of the four membered ring, $\text{P}_2\text{B}_2\text{H}_4$, were examined. These were the completely planar structure, **16**, a puckered C_{2v} structure, **17**, with the hydrogens at phosphorus pyramidalized cis to each other, and a C_{2h} structure, **18**, with the phosphorous hydrogens pyramidalized trans to each other and the rest of the molecule coplanar. For the 6-membered ring the conformations examined were, the planar D_{3h} benzene-like geometry, and the non-planar, C_{3h} geometry, **20**, which resembles chair cyclohexane with the phosphorus lone pairs taking the place of three axial hydrogens. Since these cyclic systems were rather large and required a significant amount of cpu time to optimize at even the RHF level, we did not try reoptimizing any of them at the MP2 level.

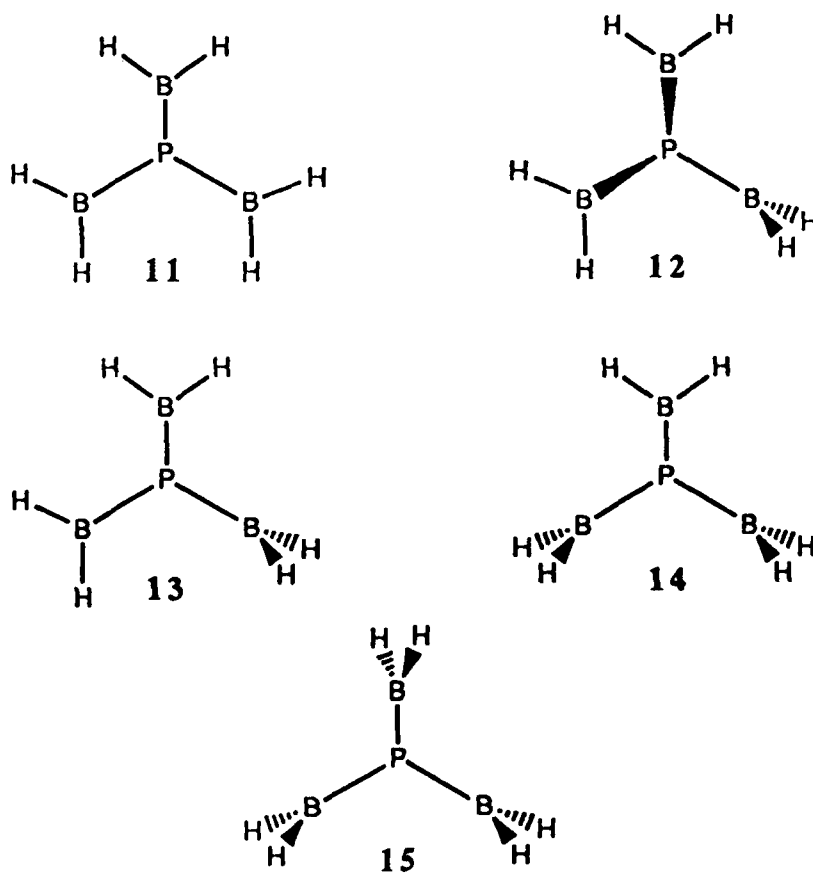


Figure 3-3 $P(BH_2)_3$ geometries

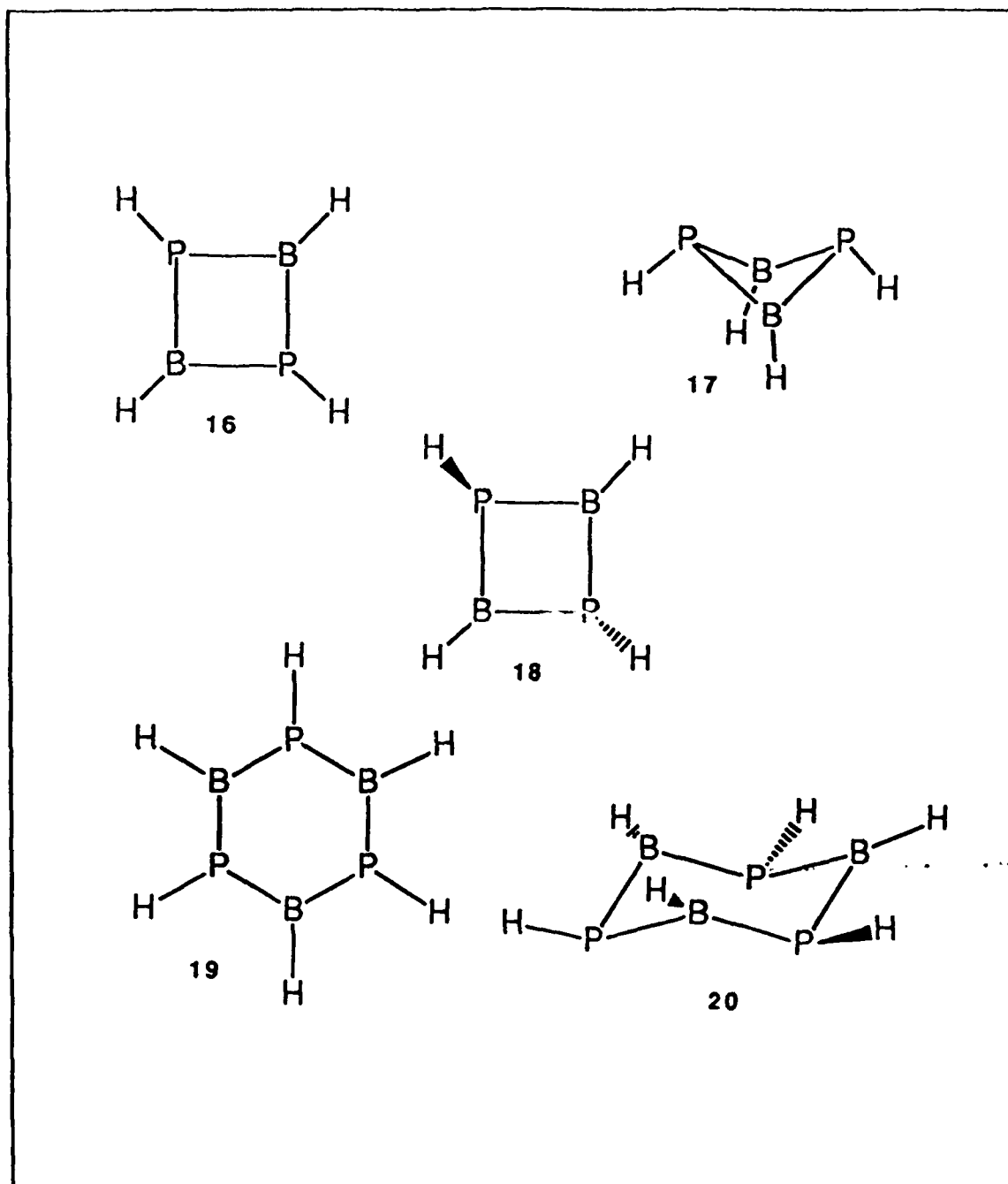


Figure 3-4 $P_2B_2H_4$ and $P_3B_3H_6$ geometries.

Section 3-3 Results

Section 3-3-1 Monoboryl Phosphine

 Table 3-1 Relative Energies (kcal/mol) for H_2PBH_2 Calculated with the 6-31G* Basis Set.

<u>Geometry</u>	<u>Symmetry</u>	<u>RHF</u>	<u>MP4SDTQ</u>
Equilibrium (1)	C_s	0	0
Planar (2)	C_{2v}	8.4	4.2
Rotated (3)	C_s	7.9	9.8
Planar Rotated (4)	C_{2v}	41.9	43.3

A phosphorus with a single BH_2 substituent was calculated to have a pyramidal equilibrium geometry. This finding is in agreement with earlier calculations²³ and the experimental results on a highly substituted derivative.¹⁵ The calculated pyramidalization angle, ϕ , at phosphorus of 71° in H_2PBH_2 is less than that of 86° in PH_3 ;²⁷ and the MP4SDTQ barrier to planarization of 4.2 kcal/mol in H_2PBH_2 is substantially reduced from the 35.8 kcal/mol calculated for PH_3 . At the MP4SDTQ level, it requires about half the energy to planarize the phosphorous as it does to rotate the boron out of conjugation. This last prediction is the opposite of that made by earlier RHF calculations by Gropen.²³ He found that rotation of the boron is easier than inversion of the phosphorous -- 6.6 kcal/mol versus 8.1 kcal/mol. Although, his calculations did not include d polarization functions on the boron, a

larger barrier to inversion than to rotation is also found by our RHF calculations with the polarized 6-31G* basis set.

The inclusion of electron correlation favors π electron delocalization.²⁸ This decreases the barrier to planarization of the phosphorus and increases the barrier to rotation of the boron out of conjugation. Planarization of the phosphorus with the empty boron orbital rotated out of conjugation requires 34.0 kcal/mol at the RHF level and 33.5 kcal/mol at the MP4SDTQ level, which are close to the values of 37.8 kcal/mol and 35.8 kcal/mol for PH_3 at the same levels of theory. Basis set differences apparently account for the difference between our RHF value for planarization of H_2PBH_2 and Gropen's value of 42.0 kcal/mol.

The effect of a single boron group conjugated with the phosphorous lone pair is not enough to planarize the phosphine, but it does make planarization much easier. Indeed, when conjugated with the BH_2 group, the phosphorus resembles an unconjugated amine in its barrier to inversion. The stabilization through π delocalization increases as phosphorus becomes more planar, since at a planar geometry the π overlap between the phosphorus lone pair and the empty orbital on boron is maximized. This accounts for the high barrier to rigid rotation of the BH_2 group when phosphorus is held planar.

Section 3-3-2 Diboryl Phosphine

With two BH_2 groups, the potential energy surface becomes more complicated. In addition, we find that predicting the equilibrium geometry accurately

becomes difficult because the potential surface for planarization at phosphorus is remarkably flat. The MP2 optimized pyramidalization angle at phosphorous is 40° ,²⁹ but the barrier to planarity is only 0.3 kcal/mol at the MP4SDTQ level. Thus, the hydrogen on the phosphorus can be swung through more than 80° of arc³⁰ with hardly any change in energy. Although the minimum on the potential surface occurs at a significantly pyramidalized geometry, the experimental finding that a highly substituted derivative of $\text{HP}(\text{BH}_2)_2$ is planar³¹ is not at all surprising.

Table 3-2 Relative Energies (kcal/mol) for $\text{HP}(\text{BH}_2)_2$ Calculated Using the 6-31G* Basis Set

<u>Geometry</u>	<u>Symmetry</u>	<u>RHF</u>	<u>MP4SDTQ</u>
Equilibrium (5)	C_s	0	0
Planar (6)	C_{2v}	0.4	0.3
Monorotated (7)	C_1	13.1	16.6
Planar Monorotated (8)	C_s	19.9	20.2
Dirotated (9)	C_s	20.4	24.8
Planar Dirotated (10)	C_{2v}	53.5	59.5

One very surprising result of the calculations on the $\text{HP}(\text{BH}_2)_2$ surface is that rotation of the first BH_2 group out of conjugation requires 16.6 kcal/mol whereas rotation of the BH_2 group in H_2PBH_2 required about half that, 9.8 kcal/mol. Rotation of the second BH_2 group out of conjugation in $\text{HP}(\text{BH}_2)_2$ requiring 8.2 kcal/mol is consistent with the value in H_2PBH_2 . Since the first BH_2 group in $\text{HP}(\text{BH}_2)_2$ requires more energy to rotate out of conjugation than the second, it

would appear that the empty orbitals on the two borons do not compete for electron density from the phosphorous lone pair, but instead, somehow act cooperatively.

Never the less, the empty orbitals on each boron can be shown to compete for phosphorus electron density when the phosphorus is constrained to remain planar. With this constraint, rotation of the first BH_2 group out of conjugation requires 19.9 kcal/mol; and rotation of the second requires an additional 39.3 kcal/mol, which is very close to the value of 39.1 kcal/mol for rotation in planar H_2PBH_2 . In planar $\text{HP}(\text{BH}_2)_2$, competition between the two BH_2 groups apparently makes the energy required for rotation of the first BH_2 out of conjugation half of that for the second. Once the first BH_2 group has been rotated out of conjugation, there is virtually no effect of the first BH_2 group on rotation of the second BH_2 group out of conjugation.

Based on the calculated barriers to BH_2 group rotation, two BH_2 groups, both conjugated with the lone pair on a planar phosphorus, compete for electron density; but, when the phosphorus is allowed to pyramidalize, the two BH_2 groups appear to cooperate with one another in delocalizing the phosphorus lone pair. Thus, depending on whether or not phosphorus is constrained to remain planar, our calculations find that the two borons can cooperate with each other. What happens with the addition of a third BH_2 group?

Section 3-3-3 Triboryl Phosphine

According to our calculations, the equilibrium structure about the trivalent phosphorous in $\text{P}(\text{BH}_2)_3$ is planar. This result was confirmed by a frequency analysis

which gave no imaginary frequencies, so the planar geometry is a true minimum. The potential surface for pyramidalization of monorotated $\text{P}(\text{BH}_2)_3$ is as flat as that of fully conjugated $\text{HP}(\text{BH}_2)_2$ surface. The equilibrium geometry occurs at $\phi = 25.5^\circ$, but the barrier to inversion is only 0.3 kcal/mol.

Table 3-3 Relative Energies (kcal/mol) for $\text{P}(\text{BH}_2)_3$ Using the 6-31G* Basis Set

<u>Geometry</u>	<u>Symmetry</u>	<u>RHF</u>	<u>MP4SDTQ</u>
Equilibrium (11)	D_{3h}	0	0
Monorotated (12)	C_1	14.4	12.8
Planar Monorotated (13)	C_{2v}	14.4	13.0
Planar Dirotated (14)	C_{2v}	34.0	32.8
Planar Trirotated (15)	D_{3h}	68.1	72.7

Rotation of a single BH_2 group out of conjugation in $\text{P}(\text{BH}_2)_3$, requires 12.8 kcal/mol, which is less than the 16.6 kcal/mol in $\text{HP}(\text{BH}_2)_2$. Thus, it appears that the three BH_2 groups in $\text{P}(\text{BH}_2)_3$ are competing for electron density, instead of cooperating. The competition is also seen in $\text{P}(\text{BH}_2)_3$ when rotating BH_2 groups out of conjugation while maintaining a planar phosphorus center. The energy required for rotation of the first is 13.0 kcal/mol; the barrier, for rotation of the second BH_2 group is 19.8 kcal/mol; and rotation of the third BH_2 group requires 39.9 kcal/mol. Once again, the latter two values are almost identical to those calculated for rotation about the P-B bond, while maintaining a planar phosphorus in, respectively, $\text{HP}(\text{BH}_2)_2$ and H_2PBH_2 .

Section 3-4 Competition versus Cooperation

Based on competitive substituent effects, the anticipated trend for rotation of one BH_2 group out of conjugation in $\text{H}_{3-n}\text{P}(\text{BH}_2)_n$ would be progressively lower barriers to rotation as the number of BH_2 groups bound to a central phosphorus increases. However, as shown by the data summarized in Table 3-4, H_2PBH_2 has a lower barrier than either $\text{HP}(\text{BH}_2)_2$ or $\text{P}(\text{BH}_2)_3$. This finding suggests the existence of a second substituent effect that is cooperative, rather than competitive. This second effect appears to vanish when the phosphorus is constrained to be planar, since the predicted barriers to rotation are restored to the order anticipated on the basis of pure competition between substituents.

Table 3-4. MP4SDTQ Barrier to Rotation of One BH_2 Group Out of Conjugation in $\text{H}_{3-n}\text{P}(\text{BH}_2)_n$, $n=1-3$, With and Without the Constraint of a Planar Phosphorus.

Compound	ΔE_{rot} (kcal/mol)			
	$\phi_{\text{conj}}^{\text{a}}$	$\phi_{\text{rot}}^{\text{b}}$	Equilibrium Structures	Planar Phosphorus
H_2PBH_2	71.0°	82.4°	9.8	39.1
$\text{HP}(\text{BH}_2)_2$	45.1°	71.9°	16.6	19.9
$\text{P}(\text{BH}_2)_3$	0.0°	25.5°	12.8	13.0

^aPyramidalization angle at phosphorus in conjugated structure.

^bPyramidalization angle at phosphorus in rotated structure.

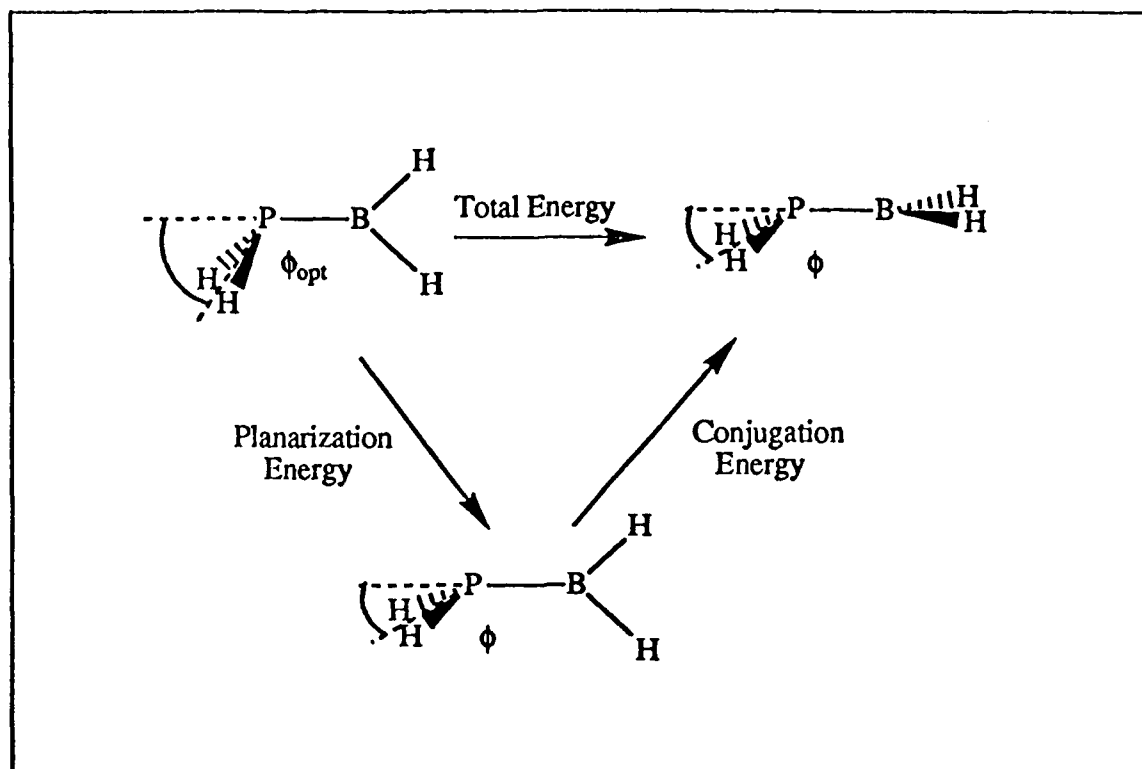


Figure 3-5 Separation of the Total Energy into Planarization Energy and Conjugation Energy.

As summarized in Table 3-4, there are changes in the geometry at the phosphorus center that occur as more BH_2 groups are added, namely, phosphorus becomes more planar (i.e. ϕ gets smaller). There is also a change in geometry at phosphorus that occurs on rotation of a BH_2 group out of conjugation. In order to separate the changes in energy that accompany the changes in geometry at phosphorus from the pure conjugation energy of each BH_2 group, we examined the potential energy surfaces of H_2PBH_2 and $\text{HP}(\text{BH}_2)_2$ in greater detail using the energies of the reactions depicted in Figure 3-5. Since two sets of calculations were performed at each of several values of the pyramidalization angle, ϕ , these

calculations were, for the sake of economy, carried out at the RHF rather than MP4SDTQ level of theory.

Section 3-4-1 The H_2PBH_2 Potential Surface

The equilibrium structure of H_2PBH_2 contains a pyramidal phosphorus and a rather weak π bond between the phosphorus and boron. Since the energy required to rotate the BH_2 group increases substantially when the phosphorus is constrained to be planar, the π bond strength apparently increases as the phosphorus becomes more planar. This is depicted graphically in Figure 3-6.

The RHF conjugation energy -- the negative of the energy required to rotate the BH_2 group out of conjugation with the phosphorus lone pair -- is plotted as a function of ϕ . Also plotted is the RHF planarization energy -- the energy required to flatten the phosphorus with the BH_2 group twisted out of conjugation, relative to the RHF energy of the monorotated equilibrium geometry, which has $\phi = 82.4^\circ$. The sum of these two energies is the RHF total energy -- the RHF energy of the conjugated molecule, relative to the RHF energy of the optimal, monorotated structure. The total energy curve in Figure 3-6 is that which is traversed when the phosphorus center inverts in conjugated H_2PBH_2 .

Since the conjugation energy and planarization energy both have a functional dependence on ϕ that is similar in magnitude but opposite in sign, addition of these two energies gives a total energy curve that is rather flat.³² Therefore, although a conjugated BH_2 group reduces the equilibrium value of ϕ only slightly, from 82° to

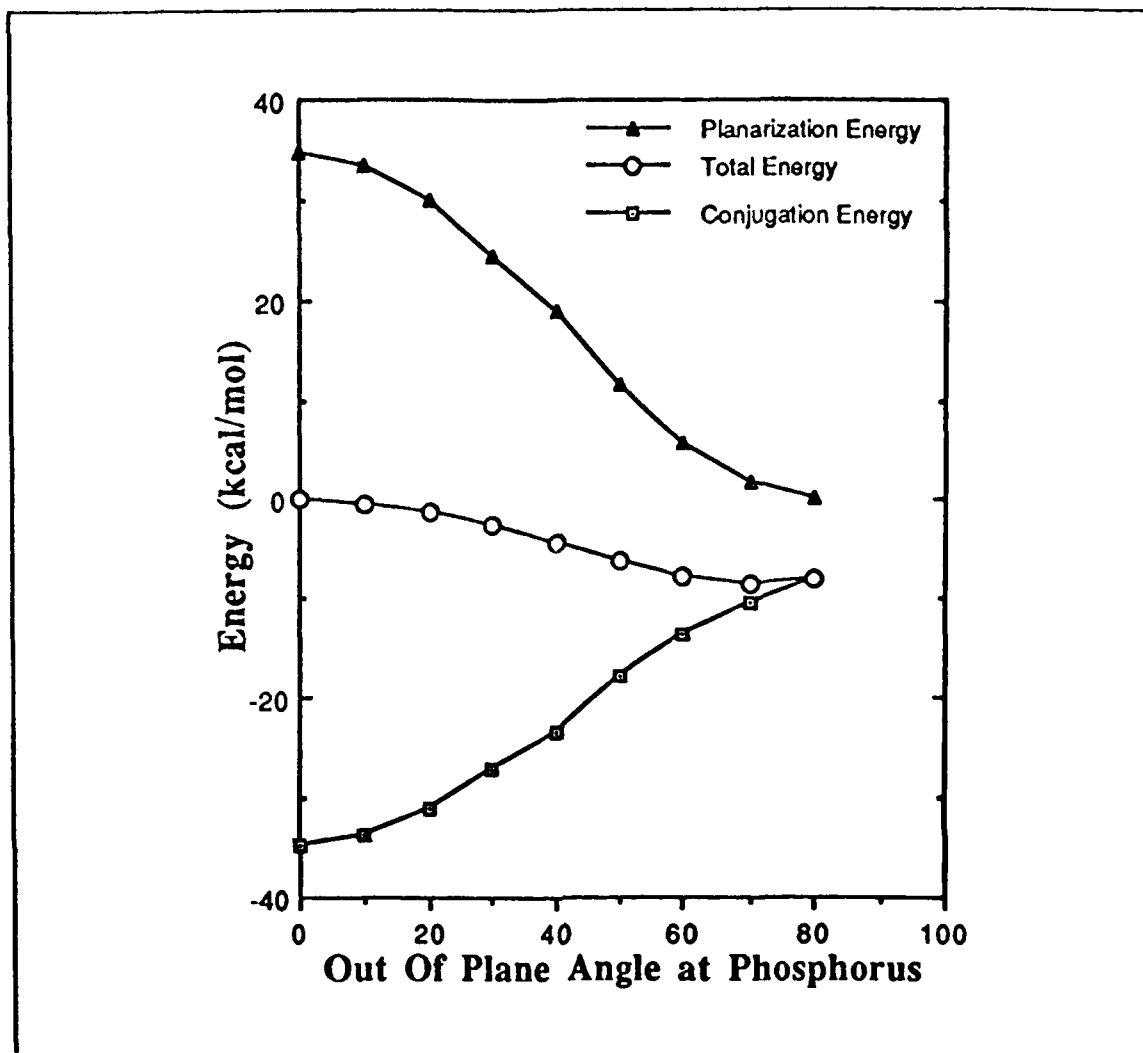


Figure 3-6 One dimensional H_2PBH_2 potential energy surface in ϕ .

71°, conjugation reduces the barrier to planarity substantially, from 34.0 kcal/mol to 8.4 kcal/mol at RHF level and from 33.5 kcal/mol to 4.2 kcal/mol at MP4 level.³³

Section 3-4-2 The $\text{HP}(\text{BH}_2)_2$ Potential Surface

As discussed above, in $\text{HP}(\text{BH}_2)_2$ the barrier to rotation of one BH_2 out of conjugation appears to indicate that the two BH_2 substituents are cooperating, rather than competing. An important clue to the origin of this apparent cooperative effect

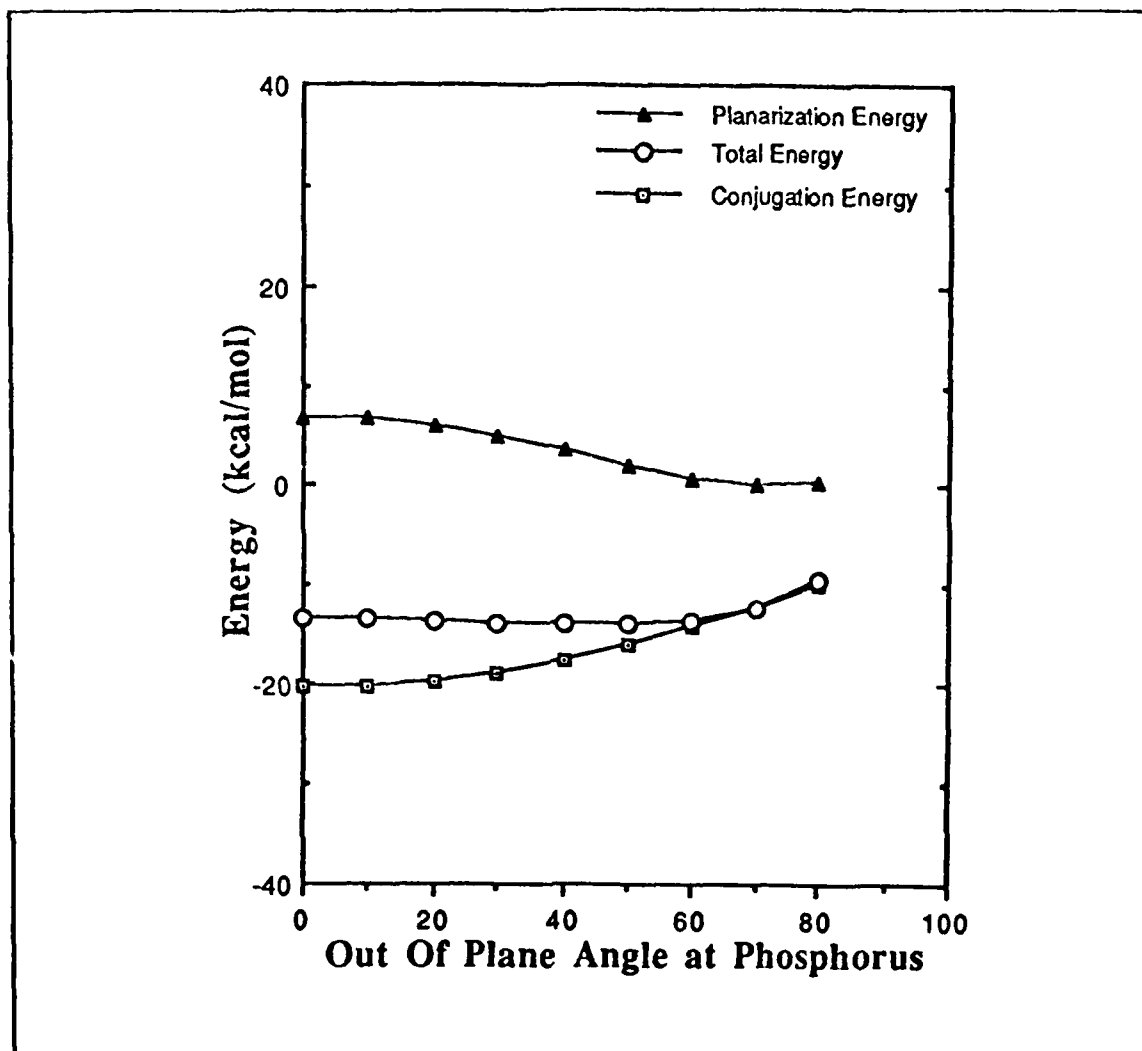


Figure 3-7 One dimensional $\text{HP}(\text{BH}_2)_2$ potential energy surface in ϕ .

is the shape of the curve in Figure 3-7 for the planarization energy. This curve resembles more closely the curve in Figure 3-6 for the total energy of H_2PBH_2 instead of the planarization energy of H_2PBH_2 .

Since the potential curve for planarizing monorotated $\text{HP}(\text{BH}_2)_2$ is relatively flat, ϕ can be decreased, in order to form strong P-B π bonds in the fully conjugated structure, at a fraction of the cost required in rotated H_2PBH_2 . Because the curve for the planarization energy in $\text{HP}(\text{BH}_2)_2$ is quite flat, the total energy curve is flatter

still. Indeed, at the RHF level, only 0.5 kcal/mol is required to go from the equilibrium structure, at $\phi = 45^\circ$, to the planar structure.

Although the softer potential surface for planarization of monorotated $\text{HP}(\text{BH}_2)_2$ results in an apparent cooperative effect between the two BH_2 substituents; comparison of the curves for the conjugation energies in Figure 3-6 and Figure 3-7 reveals the expected competition in $\text{HP}(\text{BH}_2)_2$ between the two BH_2 groups. Hence, at most values of ϕ , the magnitude of the conjugation energy (the energy required to twist a BH_2 group out of conjugation at fixed ϕ) is larger in H_2PBH_2 than $\text{HP}(\text{BH}_2)_2$. For example, as noted earlier, when the phosphorus is constrained to be planar, competition is seen (Table 3-4); and the barrier to rotate a BH_2 group out of conjugation in $\text{H}_{3-n}\text{P}(\text{BH}_2)_n$ decreases as n increases.

However, at large values of ϕ , careful comparison of Figures 5 and 6 shows that two BH_2 groups do cooperate, since the conjugation energy in $\text{HP}(\text{BH}_2)_2$ is slightly larger than that in H_2PBH_2 for $\phi > 60^\circ$. At these highly pyramidalized geometries, the phosphorus lone pair has a large amount of s character and is not close to being parallel to the empty orbitals on boron. Indeed, the bulk of the electron density in the phosphorus lone pair is concentrated away from the boron substituents. In this region, the ability of the BH_2 group to delocalize the phosphorus lone pair is greatly diminished. The mixing of these orbitals is reduced to the point that it can be accurately examined using second order perturbation theory.

Applying second-order perturbation theory, the energy lowering that results from mixing of orbitals is proportional to the overlap of the orbitals squared divided

by the energy difference separating the orbitals. It is easy to show³⁴ that the numerator is twice as large for $\text{HP}(\text{BH}_2)_2$ as for H_2PBH_2 , which reflects the fact that there are two P-B interactions in $\text{HP}(\text{BH}_2)_2$. However, the energy difference in the denominator is not the same in the two molecules, because the in-phase combination of BH_2 p orbitals in $\text{HP}(\text{BH}_2)_2$ is lower in energy than the lone BH_2 p orbital in H_2PBH_2 . This causes the denominator in the second-order perturbation energy expression to be smaller in $\text{HP}(\text{BH}_2)_2$ than in H_2PBH_2 , so that the energy lowering due P-B interactions are larger in $\text{HP}(\text{BH}_2)_2$ than in H_2PBH_2 . Since in second-order perturbation theory interactions are additive, in the region of very weak interactions, where second-order perturbation theory is valid, competitive effects are necessarily absent.

Section 3-4-3 Concluding Remarks on the $\text{H}_{3-n}\text{P}(\text{BH}_2)_n$ Molecules

One BH_2 group appears at first to not have much of an effect on the phosphorus center since the optimized geometry is only slightly less pyramidal than that of PH_3 . However, one BH_2 group actually has quite a large effect on lowering the barrier to planarity of the phosphorus to amine-like values. A second BH_2 group can then form a strong π bond, since the potential for planarizing phosphorus has already been softened by the first. As a result, the first BH_2 group appears to cooperate with the second by making accessible, without large energetic cost, geometries where phosphorus can form strong π bonds to both BH_2 groups. Since the presence of two conjugated BH_2 groups provide only a slightly softer potential

for planarizing phosphorus than does one BH_2 group, addition of a third BH_2 group does not give a cooperative effect. Instead, the competition of the third BH_2 group with the first two for electron density is the dominant effect; and so the energy required to rotate a BH_2 group out of conjugation is smaller in $\text{P}(\text{BH}_2)_3$ than in $\text{HP}(\text{BH}_2)_2$.

These quantitative predictions of the sizes of the rotational barriers, and hence the π bond strength, in $\text{H}_{3-n}\text{P}(\text{BH}_2)_n$ should be experimentally testable provided that non-sterically demanding substituents could be used. Of greater importance is the qualitative definition given by this study, of the conditions under which cooperative, rather than competitive, effects of electronically similar, conjugating substituents are likely to be observed.

Section 3-5 Ring Systems Containing P-B π Bonds

In acyclic systems, we find that the presence of one BH_2 group reduces the barrier to planarity at phosphorus but adding a second BH_2 group nearly eliminates the barrier. These findings raise the question of whether cyclic $(\text{HP-BH})_n$ systems will have planar geometries at phosphorus, since each phosphorous is flanked by two borons, or whether they will have non-planar geometries, since, as the formula implies, there is one boron for each phosphorous. Depending on whether n is odd or even, $(\text{HP-BH})_n$ will have either $4m+2$ or $4m$ π electrons and hence will be, respectively, potentially aromatic or anti-aromatic in nature. This effect should act to make the odd members of the series tend to prefer geometries with planar

phosphorus atoms and the even members tend to prefer geometries with pyramidal phosphorus atoms.

Table 3-5. Boraphosphine ring system, $P_2B_2H_4$ and $P_3B_3H_6$, relative using the 6-31G* basis set.

<u>Geometry</u>	<u>RHF</u>	<u>MP2</u>	<u>MP4SDTQ</u>
$P_2B_2H_4$ Planar (16)	30.7	32.7	33.3
$P_2B_2H_4$ Cis Hydrogens (17)	0	0	0
$P_2B_2H_4$ Trans Hydrogens (18)	6.0	9.5	9.2
$P_3B_3H_6$ Planar (19)	7.4	0.0	1.4
$P_3B_3H_6$ Chair (20)	0	0	0

Indeed, we find for $P_2B_2H_4$ that a C_{2v} geometry, with all hydrogens cis and pyramidalization angles at phosphorous of $\phi = 68.2^\circ$, is preferred to a planar D_{2h} geometry by 33.3 kcal/mol at the MP4SDTQ level. In contrast, $P_3B_3H_6$ is computed to have a smaller pyramidalization angle, $\phi = 59.0^\circ$ at the RHF level, and the barrier to planarization at all three phosphorus atoms ($C_{3v} \rightarrow D_{3h}$) is only 1.4 kcal/mol at the MP4SDTQ level.

The aromatic system has such a low barrier to planarization that even better calculations might find a planar equilibrium geometry. As noted in Section 3-1-3, a planar equilibrium geometry has been found for a highly substituted derivative of $(HIPBH)_3$ by x-ray crystallography.¹⁹ Since our calculations were performed on the parent molecule and refer to the gas-phase, the discrepancy between our

computational result and experiment could, of course, be due to substituent effects or to packing forces in the crystal.

Although calculations predict the C_{2v} structure (17) of $P_2B_2H_4$ to be the ground state, X-ray crystallography of a substituted derivative resembles C_{2h} structure (18), which we calculate to be 9.2 kcal/mol higher in energy at the MP4SDTQ level. Examination of structure 17 reveals that all the substituents would be confined to the same side of the PB ring. Since the substituted derivative contains sterically demanding groups,²⁰ this may account for the fact that the less sterically crowded 18 is found to be preferred for this derivative. However, we expect a derivative with less sterically demanding substituents to adopt a conformation similar to structure 17.

Chapter 3 Notes

1. Magnusson, E. *Aust. J. Chem.*, 1986, 39, 735.
2. For barriers of inversion for amines: Stackhouse, J.; Baechler, R. D.; Mislow, K. *Tetrahedron Letters*, 1971, 37, 3437. For barriers of inversion for phosphines: Dougherty, D. A.; Mislow, K. *Tetrahedron Letters*, 1979, 25, 2321; Lambert, J. B.; Jackson III, G. F.; Mueller, D. C. *J. Am. Chem. Soc.*, 1970, 92, 3093; Baechler, R. D.; Mislow, K. *J. Am. Chem. Soc.*, 1971, 93, 773.
3. Some examples of optically active phosphines: Burdon, J.; Hotchkiss, J. C.; Jennings, W. B. *J. C. S. Perkin II*, 1976, 1052; Lambert, J. B.; Jackson III, G. F.; Mueller, D. C. *J. Am. Chem. Soc.*, 1970, 92, 3093; Baechler, R. D.; Mislow, K. *J. Am. Chem. Soc.*, 1971, 93, 773.
4. Magnusson, E. *Tetrahedron*, 1985, 22, 5235; Gropen, O. *J. of Mol. Struct.* 1977, 36, 111.
5. Dougherty, D. A.; Mislow, K. *Tetrahedron Letters*, 1979, 25, 2321.
6. All three numbers are from: Noe, E. A.; Rapan, M. *J. Am. Chem. Soc.* 1975, 97, 5811. For similar results starting with N, N-Dimethylamide, see: Drakenberg, T.; Dahlqvist, K.-I.; Forsén, S. *J. of Phys. Chem.*, 1972, 76, 2178.
7. Fjeldberg, T.; Gundersen, G.; Jonvik, Torgeir, Seip, H. M.; Sæbø, S. *Acta Chemica Scandinavica A*, 1980, 34, 325.
8. Gundersen, G. *Acta Chemica Scandinavica*, 1981, A 35, 729.
9. Kutzenigg, W. *Angew. Chem., Int. Ed. Engl.* 1984, 23, 272. Schmidt M. W.; Truong P. N.; Gordon M. S. *J. Am. Chem. Soc.*, 1987, 109, 5217 and references therein.
10. Doering, W. v. E.; Roth, W. R.; Breuckmann, R.; Figge, L.; Lennartz, H.-W.; Printzbach, H. *Chem. Ber.* 1988, 121, 1.
11. Ethylene π bond strength is calculated to be 67.8 kcal/mol at the MP2/6-31G* level of theory by Dobbs, K. D.; Hehre, W. J. *Organometallics*, 1986, 5, 2057. The barrier to rotation of one CH_2 end group in allyl is calculated to require 18.2 kcal/mol at the CI-SD/6-31G* level of theory (? of Chapter 2).
12. Hood, D. M.; Pitzer, R. M.; Schaefer, H. F. III *J. Am. Chem. Soc.* 1978, 100, 2227; Feller, D.; Tanaka, K. Davidson, E. R.; Borden, W. T. *J. Am. Chem. Soc.* 1982, 104, 967.

13. The symbols used are standard notation of HMO theory. α refers to the energy of an electron in the orbital while the atom is isolated. β is the overlap or bonding energy resulting from two orbitals interacting. Since both numbers are negative, the most stabilization occurs when the largest positive coefficients precede these numbers.
14. These numbers come from subtracting the energy of the orbital for n from $n-1$. Then, since each orbital has two electrons, multiply the result by 2.
15. Feng, Xudong; Olmsted, M. M.; Power, P. P. *Inorg. Chem.* **1986**, *25*, 4615.
16. Daly, J. J.; Zuerich, S. A. *Kristallogr.* **1963**, *118*, 332.
17. P-B bonds with a strict bond order of unity are about 1.92-1.96Å: Perri, J. A.; La-Placa, S.; Post, B. *Acta Crystallog.* **1958**, *11*, 310; Bartlett, R. A.; Feng, X.; Power, P. P. *J. Am. Chem. Soc.* **1986**, *108*, 6817.
18. P-B bond length of 1.871Å as measured by x-ray crystallography and reported in: Bartlett, R. A.; Dias, R. H. V.; Power, P. P. *Inorganic Chemistry*, **1988**, *27*, 3919.
19. Dias, H. V. R.; Power, P. P. *Angew. Chem. Int. Ed. Eng.* **1987**, *26*, 1270.
20. Arif, A. M.; Boggs, J. E.; Cowley, A. H. *J. Am. Chem. Soc.* **1986**, *108*, 6083. Other examples of similar compounds are: Dias, H. V. R.; Power, P. P. *J. Am. Chem. Soc.* **1989**, *111*, 144; Arif, A. M.; Cowley, A. H.; Pakulski, M.; Power, J. M. *J. Chem. Soc., Chem. Commun.* **1986**, 889.
21. Binkley, J. S.; Frisch, M. J.; Raghavachari, M.; Fluder, E.; Seeger, R.; Pople, J. A. Carnegie-mellon University.
22. Frisch, M. J.; Binkley, J. S.; Schlegel, H. B.; Raghavachari, K.; Melius, C. F.; Martin, R. L.; Stewart, J. J. P.; Bobrowicz, F. W.; Rohlfing, C. M.; Kahn, L. R.; Defrees, D. J.; Seeger, R.; Whiteside, R. A.; Fox, D. J.; Fleuder, E. M.; Pople, J. A. Carnegie-Mellon Quantum Chemistry Publishing Unit, Pittsburgh PA, 1984.
23. Gropen, O. *J. of Mol. Struct.*, **1977**, *36*, 111.
24. The MP2 equilibrium geometry reduces the P-B bond length by 0.042Å to 1.863Å. The P-H bonds and B-H bonds lengthen slightly, on the order of 0.005Å. The largest change is in ϕ at phosphorus. MP2 optimization reduces this value from 71° to 66°. MP2 optimization of the planar structure again reduces the P-B bond length. This time, the reduction is by 0.023Å to 1.785Å. The change in the B-H bond lengths is as before, but the change in the P-H bond length is greater, it lengthens by 0.013Å.

25. Actual differences in MP4SDTQ energies were 0.38 kcal/mole for the ground state geometry and 0.30 kcal/mole for the planar ground state geometry. Both of these have the MP2 optimized geometry energy below the RHF optimized geometry.
26. Actual differences are 0.38 kcal/mole lower MP4SDTQ energies for both the MP2 optimized ground state geometry and planar ground state geometry.
27. Magnusson, E. *Tetrahedron*, **1985**, *22*, 5235.
28. Borden, W. T.; Davidson, E. R. *J. Chem. Phys.*, **1976**, *64*, 663.
29. The minimum on the RHF surface occurs at $\phi = 45^\circ$. The RHF calculated energy does not rise quickly as ϕ increases. Indeed, the relative energy at $\phi = 60^\circ$ is just 0.1 kcal/mol greater than the completely planar structure.
30. The 80° of arc corresponds to the hydrogen going from 40° on one side of the plane of B-P-B to 40° on the other. From the results of RHF calculations with the hydrogen at larger values of ϕ , it would appear that the potential surface is relatively flat all the way to $\phi = 60^\circ$. Therefore, the hydrogen could swing through 120° of arc with less than 0.6 kcal/mol energy change; hence, the value of 80° of arc is actually conservative.
31. Bartlett, R. A.; Dias, H. V. R.; Power, P. P. *Inorganic Chemistry*, **1988**, *27*, 3919.
32. This may explain why the X-ray structure of a sterically shielded derivative¹⁵ has a significantly smaller pyramidalization angle at phosphorus than the one we calculate for H_2PBH_2 . Minimization of steric interactions between substituents attached to phosphorus should favor a more planar geometry.
33. This reduction in the calculated barrier to phosphorus planarity on inclusion of electron correlation is consistent with our previous experience in computing the barriers to planarity at pyramidal radical centers. See : Feller, D.; Davidson, E. R.; Borden, W. T. *J. Am. Chem. Soc.* **1985**, *107*, 2596; Sun, H.; Hrovat, D. A.; Borden, W. T.; *J. Am. Chem. Soc.* **1987**, *109*, 5275; Hrovat, D. A.; Sun, H.; Borden, W. T. *J. Mol. Struct. (Theochem.)* **1988**, *163*, 51; Wang, S. Y.; Borden, W. T. *J. Am. Chem. Soc.* **1989**, *111*, 7282.
34. Coolidge, M. B.; Borden, W. T. *J. Am. Chem. Soc.*, **1990**, In press.

Chapter 4 Study of Oxyallyl and Dimethyl Oxyallyl

Section 4-1 Introduction

Oxyallyl and dimethyloxyallyl are molecules in which two electrons occupy two orbitals that are close in energy. Thus, these are two examples of diradicals.¹ Since no classical Kekulé structures can be written for these diradicals, they are also called non-Kekulé molecules.^{2,3,4}

Hund's rule⁵ predicts that the lowest energy configuration for two electrons occupying two degenerate orbitals will be that which produces the greatest spin multiplicity. This rule was first applied to atoms, but it is also valid for many molecules.¹ However, as discussed by Borden¹ and Du,³ diradicals in which the unpaired electrons are localized to different regions in space can have a singlet ground-state wave function, even though Hund's rule predicts that the triplet should be the ground state. The reason why such diradicals might be expected to violate Hund's rule is that the Coulomb repulsion energy of the two antiparallel spin electrons is significantly reduced if they are each confined to a different region of space. Electron correlation between these two electrons and the rest of the electrons then becomes the determining factor in whether the singlet or triplet wave function is lower in energy; and the singlet is usually favored.

As a result, in calculations of singlet-triplet energy separations in diradicals, electron correlation is very important. Additionally, since singlet diradicals cannot be adequately described by a single Slater determinant, Møller-Plesset perturbation

theory will not provide accurate results. Consequently, MCSCF or CI calculations are required.

Section 4-1-2 Prior Work on Oxyallyl

Oxyallyl (2) is formed as an intermediate in the reaction that takes allene oxides to cyclopropanones⁶ and in the isomerization and cycloaddition reactions of cyclopropanone⁷. Since oxyallyl is isoelectronic with trimethylenemethane (TMM) (1), both might be expected to have a ground state of the same spin multiplicity. Experiments have found that TMM and derivatives have a triplet ground state,^{8,9} which agrees with theoretical predictions.¹ However, we are unaware of any experimental evidence of a triplet ground-state for oxyallyl or derivatives.

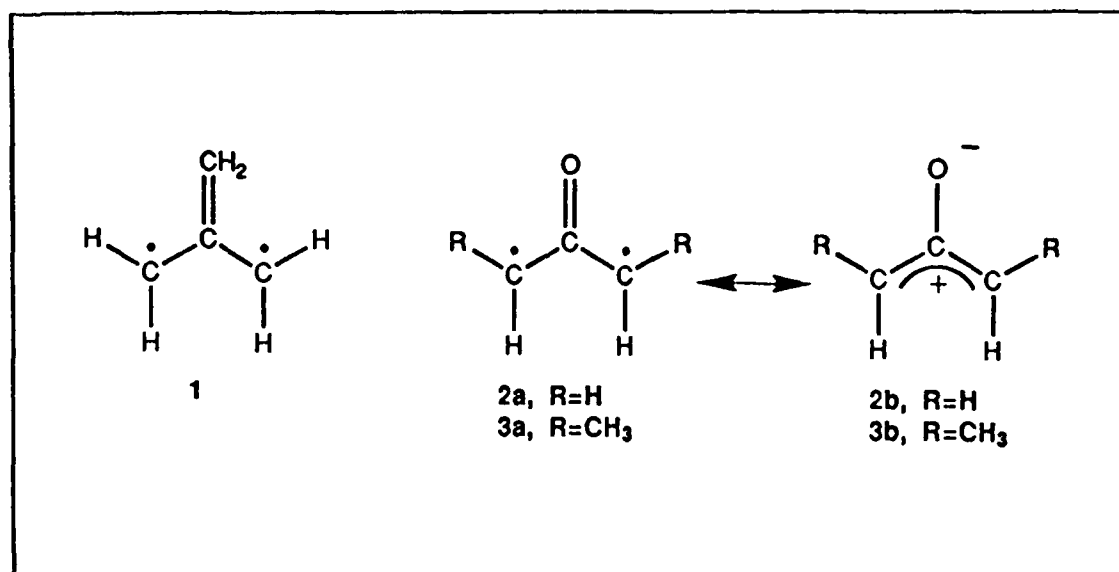


Figure 4-1 Structure of TMM, Oxyallyl and Dimethyloxyallyl.

Several ab initio studies have predicted that oxyallyl has a triplet ground state.^{10,11} MCSCF calculations found that the singlet-triplet gap to be 12.3 kcal/mol with a 3-21G basis set and 5.6 kcal/mol¹⁰ when polarization functions were added. The large change in the energy gap upon adding polarization functions suggested to the authors that, had polarization functions been present during geometry optimization, the singlet might have been stabilized even more, relative to the triplet; but the authors did not explore this possibility computationally. Apparently, the 1A_1 state has a strong, polar carbonyl bond that requires polarization function for an adequate description.¹²

Recent theoretical work on 2,4-dimethylenecyclobutane-1,3 diyl and the mono- and dioxo derivatives¹³ suggests that as in **1**, substitution of O for CH₂ selectively stabilizes the singlet. In fact, the dioxo derivative was predicted to have a singlet ground state. This study found that in all three diradicals, correlation of the σ with the π electrons selectively stabilizes the singlet state.

*The addition of σ - π electron correlation and inclusion of polarization functions during geometry optimization should reduce the theoretically predicted singlet-triplet gap in oxyallyl, possibly leading to the finding that oxyallyl has a ground state singlet. We therefore attempted to recalculate the ground state of oxyallyl, using a better basis set and including more extensive electron correlation. Dimethyloxyallyl was also chosen for study since the 1A_1 state of oxyallyl appears to have a contribution from a zwitterionic resonance structure, **2b**. If this is true, then*

addition of methyl groups to the terminal carbons should selectively stabilize the singlet, relative to the triplet.

Section 4-2 Computational Methodology

Calculations were carried out using the Dunning double zeta basis set¹⁴ with polarization functions on all non-hydrogen atoms.¹⁵ Complete Active Space (CAS) MCSCF calculations, using all the spin adapted configurations (12 for 1A_1 and 9 for 3B_2) that arise from 4 π electron occupying the lowest 4 π orbitals, were performed to optimize the geometry of oxyallyl. The MCSCF calculations were performed at the Institute for Molecular Science in Okazaki, Japan using the MOLPRO package of ab initio programs.¹⁶ Contracted CI-SD calculations¹⁷ were also performed with MOLPRO. Strictly variational CI calculations were carried out using the same DZP basis set for carbon and oxygen and an improved triple zeta basis set for hydrogen.¹⁸ These CI calculations were performed at the University of Washington using the MELD package of ab initio programs.¹⁹

The C-H bond lengths and bond angles were fixed at the values optimized in the earlier MCSCF study.¹⁰ The C-O and C-C bond lengths were optimized by a quadratic 2-dimensional fit of the CAS-MCSCF energies, using 6 points for each state.²⁰

For dimethyl oxyallyl, starting from the MCSCF optimized oxyallyl geometry, the hydrogen cis to the oxygen was replaced with methyl groups at a fixed H_3C-C bond length of 1.499Å. The other geometric parameters for the methyl groups were

MCSCF Optimized geometry of Oxyallyl.
 1A_1 State and 3B_2 State

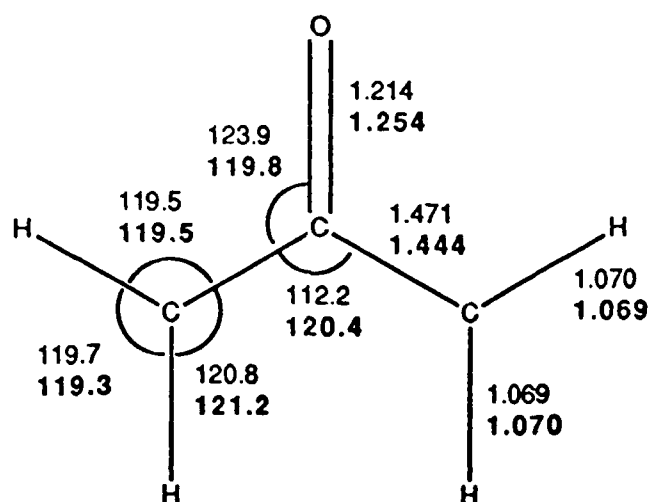


Figure 4-2 Geometric data for Oxyallyl

taken from the results of an UHF/6-31G* calculations on the ethyl radical.²¹ The methyl group conformation was such that the hydrogen in the molecular plane pointed toward the oxygen. A ROHF triplet calculation showed this conformation was lower in energy by 0.0004 hartree (0.25 kcal/mol) than one with in which the hydrogen pointed away from the oxygen.

Section 4-2-1 CI Configuration Selection

The CI calculations on both oxyallyl and dimethyloxyallyl started with molecular orbitals derived from a RHF wave function for the triplet and a TCSCF wave function for the singlet. The virtual orbitals were then transformed into K orbitals,²² in order to generate virtual orbitals that would provide the maximum amount of correlation with the fewest numbers of orbitals. All 1s orbitals on carbon

Table 4-1. Number of spin adapted configurations considered in CI calculations on oxyallyl and dimethyloxyallyl.

CI Level	Number of Spin Adapted Configurations			
	Oxyallyl		Dimethyloxyallyl	
	¹ A ₁	³ B ₂	¹ A ₁	³ B ₂
TCSCF/RHF	2	1	2	1
π -CAS ^a	12	9	900	1192
Full π	6708	9024		
π -CAS + π -SD	1234	1580	350472	592325
π -CAS + σ -S ^b	8679	12645	345176	600942
π -CAS + σ -S, π -SD	9901	14271		

^aCAS for Oxyallyl is all configurations of the 4 π electrons in the 4 lowest π orbitals. For Dimethyloxyallyl, all configurations of the 8 π electrons in the 8 lowest π orbitals.

^bFor Dimethyloxyallyl, σ excitations into the σ virtual orbitals have been limited to only the lowest 13 unoccupied K orbitals.

and oxygen were cored. Several different types of CI calculations were then performed, starting with a complete active π space (π -CAS) CI calculation for 4 π electrons in 4 π orbitals for oxyallyl and 8 π electrons in 8 π orbitals for dimethyloxyallyl.²³ The number of configurations for each CI calculation appears in Table 4-1 and the absolute energies of the 1A_1 states are reported in Table 4-2.

Table 4-2. Energies of 1A_1 states of oxyallyl and dimethyl oxyallyl computed at various levels of theory expressed in hartrees.

CI Level	Oxyallyl	Dimethyloxyallyl
TCSCF/RHF	-190.7464	-268.8156
π -CAS ^a	-190.7684	-268.8775
Full π	-190.7886	
π -CAS + π -SD	-190.7886	-268.9067
π -CAS + σ -S ^b	-190.8677	-268.9721
π -CAS + σ -S, π -SD	-190.8798	

^aCAS for Oxyallyl is all configurations of the 4 π electrons in the 4 lowest π orbitals. For Dimethyloxyallyl, all configurations of the 8 π electrons in the 8 lowest π orbitals.

^bFor Dimethyloxyallyl, σ excitations into the σ virtual orbitals have been limited to only the lowest 13 unoccupied K orbitals.

Additional π correlation was added to the π -CAS CI wave function by inclusion of all single and double excitations in the π space from all the reference π -CAS configurations (π -CAS + π -SD). To verify the π -CAS + π -SD calculation recovered nearly all of the possible correlation energy in the π space, FULL- π CI was performed on oxyallyl. Next, correlation between the σ and π electrons was

added by including single σ excitations from all π -CAS configurations (π -CAS + σ -S). Because of the size of dimethyloxyallyl, the σ -S CI calculation had to be limited to only excitations into the lowest 13 σ virtual K orbitals. To get a measure of the interaction between π and σ - π correlation, an additional CI was performed on oxyallyl that allowed either single excitation within the σ space or single and double excitations within the π space from all π -CAS configurations (π -CAS + σ -S, π -SD).

For oxyallyl, it was also possible to perform SD-CI, using the MCSCF molecular orbitals and allowing all possible σ and π single and double excitations from the π -CAS reference space. The energies of these CI wave functions were calculated with the internally contracted CI method of Werner and Knowles,¹⁶ which assumes certain relationships between the coefficients of sets of configurations and thus reduces the size of the CI calculation that is actually performed. The MCSCF and contracted CI energies are reported in Table 4-3. However, it should be noted that, because the relative weights of the configurations in some groups are assumed, the contracted CI calculations are not strictly variational.

Section 4-3 Results

Section 4-3-1 Oxyallyl

The MCSCF geometries provided by reoptimizing the C-O and C-C bond lengths with using the DZP basis set resulted in a significantly shorter C-O bond length than when the 3-21G basis set was employed. The C-O bond in the 3B_2 state shortened by nearly 0.059 Å with an accompanying increase in each of the C-C bonds

by half this amount, 0.029 Å. For the 1A_1 state, only the C-O bond length changed; it shortened by 0.020 Å. The C-O bond shortening is not surprising, since adding polarization functions should describe the carbonyl bond better.

Using the original 3-21G optimized geometries, the CAS- π MCSCF energy difference of 2.8 kcal/mol between the singlet and the triplet with the Dunning DZP basis set is only half of the 5.6 kcal/mol computed with the 3-21G* basis set.¹⁰ Since geometry reoptimization affects the 3B_2 geometry more than the 1A_1 , the MCSCF value of ΔE_{S-T} increases to 4.4 kcal/mol upon geometry reoptimization.

Table 4-3. Results of MCSCF and contracted CI calculations on oxyallyl.

Calculation ^a	Number of spin adapted configurations		Energy of 1A_1 in hartrees	ΔE_{S-T} in kcal/mol
	1A_1	3B_2		
MCSCF	12	9	-190.7580	4.4
CI-SD	812362	1480927	-190.2072	2.4
CI-SDQ ^b			-190.2703	1.6

^aAll calculations were carried out using a CAS- π MCSCF wave function as the reference space. All single and double excitations were added using the contracted CI method of Werner and Knowles.

^bQuadruple excitations were added using the Davidson method.

The MCSCF value of 4.4 kcal/mol for ΔE_{S-T} is slightly larger than the 2.3 kcal/mol obtained from the CAS- π CI calculations.²⁴ The CAS- π CI calculations, which used the same set of configurations as the MCSCF, do not fully regain as much correlation energy since the virtual orbitals have not been optimized variationally to

provide the largest amount of π electron correlation. Since the triplet wave function is more delocalized than the singlet,²⁵ as expected,¹³ improvements in correlation of the π electrons selectively stabilize the triplet, relative to the singlet. In fact, since the RHF/TCSCF calculation provides correlation for only the two non-bonding π electrons, it actually predicts a singlet ground state. As shown in Table 4-3 and Table 4-4 respectively, addition of π correlation of the non-bonding and π bonding electrons at either the CAS- π MCSCF or π -CAS + π -SD CI level selectively stabilizes the triplet by 9.5 kcal/mol as compared to the RHF/TCSCF energy.

Table 4-4. Predicted ΔE_{S-T} for oxyallyl and dimethyloxyallyl at various levels of CI theory.

CI Level	ΔE_{S-T} (kcal/mol)	
	Oxyallyl	Dimethyloxyallyl
TCSCF/RHF	-5.1	-9.8
π -CAS ^a	2.3	-2.8
Full π	4.4	
π -CAS + π -SD	4.4	-1.3
π -CAS + σ -S ^b	-0.3	-5.3
π -CAS + σ -S, π -SD	0.8	

^aCAS for Oxyallyl is all configurations of the 4 π electrons in the 4 lowest π orbitals. For Dimethyloxyallyl, all configurations of the 8 π electrons in the 8 lowest π orbitals.

^bFor Dimethyloxyallyl, σ excitations into the σ virtual orbitals have been limited to only the lowest 13 unoccupied K orbitals.

Also as expected,¹³ the more ionic π wave function for the singlet state is selectively stabilized through the inclusion of σ - π correlation. Inclusion of σ -S in either the π -CAS CI or the π -CAS + π -SD CI calculations predicts ΔE_{S-T} to be near zero. The π -CAS + π -SD, σ -S value of 0.8 kcal/mol is in good agreement with the value in Table 4-3 of 1.6 kcal/mol for the π -CAS + SD-CI calculation obtained with contracted CI methodology. The exact value of ΔE_{S-T} in oxyallyl is less important than the fact that it is almost an order of magnitude smaller than ΔE_{S-T} in the isoelectric TMM (1).¹

An inspection of the π population analyses²⁶ for **2** in Table 4-5 supports the assertion that the 1A_1 has more charge separation than 3B_2 . Contributions from the zwitterionic structure **2b**, could be responsible for the reduction in ΔE_{S-T} in **2**, compared to **1**. However, although the greater electron density on oxygen in 1A_1 , compared to the 3B_2 supports this explanation, the shorter C-O and longer C-C bond lengths in 1A_1 do not. If structure **2b** was very important in 1A_1 , one would expect the C-O bond length to be longer and the C-C bond lengths to be shorter than in the 3B_2 .

Earlier work suggested the major difference between **1** and **2**,¹⁰ is the greater strength of a C-O π bond, relative to a C-C π bond. On going from **1** to **2**, the 1A_1 state is stabilized relative to the other low lying singlet states,²⁷ 1B_1 and 1B_2 , because the 1A_1 wave function is the only one that allows a C-O π bond to form. Since the 3B_2 wave function could be thought of as a mixture of all three possible covalent

resonance structures, only one of which has a full C-O π bond, it is stabilized less than 1A_1 state by the substitution of O for CH_2 .

Table 4-5. π atomic orbital total and (unpaired) electron populations^{a,b} in the 1A_1 and 3B_2 states of oxyallyl at various levels of theory.

Calculation	State	O	C ₁ (C ₃)	C2
TCSCF	1A_1	1.42	0.93	0.68
RHF	3B_2	1.33 (0.22)	0.94 (0.87)	0.77 (0.03)
CAS- π + π -SD	1A_1	1.39	0.91	0.77
CAS- π + π -SD	3B_2	1.21 (0.48)	0.96 (0.85)	0.86 (-0.18)
CAS- π + σ -S, π -SD	1A_1	1.38	0.89	0.82
CAS- π + σ -S, π -SD	3B_2	1.20 (0.45)	0.96 (0.83)	0.87 (-0.13)

^aSee reference 27.

^bBecause there is some electron density in d- π orbitals, the p- π total populations do not sum to 4.0; nor do the unpaired electron populations in the 3B_2 state sum exactly to 2.0.

Another difference between **1** and **2** is that symmetry mandates that all three resonance structures contribute equally to the triplet state in **1**, but not in **2**. Indeed, as shown in Table 4-5, the ratio of unpaired spin density on carbon to that on oxygen ranges from 1.77 with π -CAS + π -SD to 1.84 with π -CAS + σ -S, π -SD CI. This ratio differs significantly from the ratio of 1.00 demanded by symmetry in **1**. From the ratio in **2**, it can be calculated that **2a** contributes about 2.6 times more than either of the two resonance structures that containing a C-C π bond.

One way to understand the near degeneracy between the 3B_2 and 1A_1 states of oxyallyl begins with the fact that structure **2a** represents the bulk of the bonding

in both states. The triplet does have two other covalent structures that are minor contributors, and the more delocalized wave function for the triplet account for the differences in optimized bond length between the two states. However, 1A_1 has a contribution from **2b**, which is not a contributor to the triplet; and this accounts for the differences in the π electron densities between the two states.

The triplet is selectively stabilized by a more delocalized π wave function. The singlet is selectively stabilized oxygen's ability to accept excess electron density. These two effects are apparently of about the same magnitude, which results in near degeneracy of the energies of the 3B_2 and 1A_1 in oxyallyl.

Section 4-3-2 Dimethyloxyallyl

Because singlet oxyallyl is selectively stabilized through the contribution of **2b**, addition of methyls might result in a singlet ground state. This is confirmed by CI calculations on dimethyloxyallyl (**3**), the results of which are reported in Table 4-4. At all levels of CI theory, ΔE_{S-T} for **3** is smaller than for **2**. The negative sign for every value of ΔE_{S-T} in **3** indicates that, at all levels of theory, a singlet ground state is predicted.

Comparison of the ΔE_{S-T} values at the same levels of theory for **2** and **3** show a 5 to 6 kcal/mol stabilization of 1A_1 , relative to 3B_2 , in **3**. This finding suggests that if a π -CAS + σ -S, π -SD or SDQ CI calculation were performed on **3**, the ΔE_{S-T} for **3** would be around -4 to -5 kcal/mol. Indeed, comparisons of CI calculations with partial and complete σ single excitations from a smaller set of reference

configurations indicate that had all σ virtual orbitals been used for correlation in the π -CAS + σ -S CI calculation, the singlet would have been selectively stabilized by another 1 to 2 kcal/mol. Therefore, the 5 kcal/mol appears to be a conservative estimate of the magnitude by which 1A_1 lies below 3B_2 in 3.

Section 4-4 Conclusion

Although our calculations on oxyallyl predict a small preference for the triplet, the calculations on dimethyloxyallyl unequivocally predict a singlet ground state. This result is consistent with predictions of Lahti and coworkers²⁸ on cyclic derivatives of oxyallyl. Our results indicate that the constraints on the C-C-C bond angle at the carbonyl group, imposed by incorporation of oxyallyl in a four- or five member ring, are not required to obtain a singlet ground state for dialkyl derivatives of oxyallyl.²⁹

Chapter 4 Notes

1. Review: Borden, W. T. in "Diradicals", Borden, W. T., Ed.; John Wiley & Sons: New York. 1982.
2. Longuet-Higgins, H. C. *J. Chem. Phys.*, **18**, 265, (1950).
3. Du, P., PhD thesis, University of Washington, 1988.
4. Du, P.; Borden, W. T. *J. Am. Chem. Soc.* **1987**, *109*, 930. Du, P.; Hrovat, D. A.; Borden, W. T. *J. Am. Chem. Soc.* **1986**, *108*, 8086.
5. Hund, F. *Physik* **1925**, *33*, 345.
6. Crandall, J. K.; Marchleder, W. H. *J. Am. Chem. Soc.* **1968**, *90*, 7347; Camp, R. L.; Greene, F. D.; *J. Am. Chem. Soc.* **1968**, *90*, 7349; Chan, T. H.; Ong, B. S. *J. Org. Chem.* **1978**, *43*, 2994; Chan, T. H.; Ong, B. S. *Tetrahedron* **1980**, *36*, 2269.
7. Liberles, A.; Kang, S.; Greenberg, A. *J. Org. Chem.* **1973**, *38*, 1922. Liberles, A.; Greenberg, A.; Lesk, A. *J. Am. Chem. Soc.* **1972**, *94*, 8685.
8. Review: Berson, J. A. in "Diradicals", Borden, W. T., ed., Wiley-Interscience: New York, 1982, pp. 151-194.
9. Baseman, R. J.; Pratt, D. W.; Chow, M.; Dowd, P. *J. Am. Chem. Soc.* **1976**, *98*, 5726.
10. Osamura, Y.; Borden, W. T.; Morokuma, K. *J. Am. Chem. Soc.* **1984**, *106*, 5112.
11. Of the three ab initio studies, two were performed at SCF level [Liberles, A.; Greenberg, A.; Lesk, A. *J. Am. Chem. Soc.* **1972**, *94*, 8685; Schaad, L. J.; Hess, B. A.; Zahradnik, R. *J. Org. Chem.* **1981**, *46*, 1909] and the third added Møller-Plesset perturbation theory [Ortiz, J. V. *J. Org. Chem.* **1983**, *48*, 4744]. Another did CI in conjunction with a semiempirical INDO/S calculation [Lathi, P. M.; Rossi, A. R.; Berson, J. A. *J. Am. Chem. Soc.* **1985**, *107*, 2273]. Additionally, MCSCF studies have been performed on thioxyallyl. For leading reference to experimental and theoretical work on the thio derivative of oxyallyl, see Ando, W.; Furuhashi, T. *Tetrahedron* **1986**, *27*, 4035.
12. Feller, D.; Huyser, E. S.; Borden, W. T.; Davidson, E. R. *J. Am. Chem. Soc.* **1983**, *105*, 1459.
13. Du, P.; Hrovat, D. A.; Borden, W. T. *J. Am. Chem. Soc.* **1989**, *111*, 3773.

14. Dunning, T. H.; Hay, P. J. in "Methods of Electronic Structure Theory", Vol 2, Schaefer, H. F. III, Ed. Plenum: New York, 1977.
15. The polarization coefficients were set to ($\zeta = 0.75$) on carbon and ($\zeta = 0.85$) on oxygen.
16. Knowles, P. J.; Werner, H.-J.; Elbert, S. T., 1988. We thank Dr. Knowles for providing us with a version of MOLPRO that incorporates internally contracted CI, as well as MCSCF methodology. The MCSCF methodology is described in Werner, H.-J.; Knowles, P. J. *J. Chem. Phys.* **1985**, *82*, 5053; Knowles, P. J.; Werner, H.-J. *Chem. Phys. Lett.* **1985**, *115*, 259. The contracted CI methodology is described in the following reference.
17. Werner, H.-J.; Knowles, P. J. *J. Chem. Phys.*, **1988**, *89*, 5803.
18. Stenkamp, L., PhD thesis, University of Washington, 1975.
19. Developed at the University of Washington by McMurchie, L; Elbert, S.; Langhoff, S.; Davidson, E. R. and modified by Feller, D. and Rawlings, D..
20. The MCSCF calculation used the 4π electrons in 4π orbitals as the Complete Active Space, CAS. Using this CAS one considers 12 configurations for the singlet wave function and 9 configurations for the triplet. These CAS MCSCF calculations were carried out by Borden at the Institute for Molecular Science with the MOLPRO package of ab initio programs, see reference (16).
21. Whiteside, R. A.; Frisch, M. J.; Pople, J. A. Carnegie-Mellon Quantum Chemistry Archive, 3rd edn., 1983, Carnegie-Mellon University.
22. Feller, D.; Davidson, E. R. *J. Chem Phys.* **1981**, *74*, 3977.
23. Preliminary π CI calculations proved that using the same size π -CAS for dimethyloxyallyl as that employed for oxyallyl was inadequate, hence, the larger π -CAS was chosen.
24. MCSCF calculations optimize the coefficients of the virtual orbitals so that they provide the greatest amount of electron correlation. Additional CI calculations using these orbitals include electron correlation not only into the zeroth order wave function, but also into the configurations that contribute the most to lowering the overall energy. CI calculations using RHF/TCSCF orbitals do not have virtual orbitals that provide the most electron correlation using the least number of configurations. As a result, more configurations are necessary to provide the same amount of energy lowering, if starting from RHF/TCSCF orbitals versus MCSCF orbitals, in order to construct virtual orbitals that provide the greatest amount of correlation.

25. Wave functions for singlet diradicals are more localized than those of triplet.¹ In order to reduce electron-electron repulsion in the singlet diradical wave function, non-bonding electrons are confined to different regions of space because anti-parallel spin electrons are not correlated by the Pauli exclusion principle.
26. Population analysis was obtained by projecting the wave function onto a minimal basis set of AOs using the method of Davidson, E. R. *J. Chem. Phys* **1967**, *46*, 3319.
27. With TMM and early work on oxyallyl found three low lying, nearly degenerate singlet states, 1A_1 , 1B_1 , and 1B_2 .
28. Lathi, P. M. *J. Am. Chem. Soc.* **1990**, In press.
29. Coolidge, M. B.; Borden, W. T. *J. Am. Chem. Soc.*, **1990**, In press.

BIBLIOGRAPHY

Ando, W.; Hanyu, Y.; Kumamoto, Y.; Takata, T. *Tetrahedron* **1986**, *42*, 1989.

Arif, A. M.; Cowley, A. H.; Pakulski, M.; Power, J. M. *J. Chem. Soc., Chem. Commun.* **1986**, 889.

Arif, A. M.; Boggs, J. E.; Cowley, A. H. *J. Am. Chem. Soc.* **1986**, *108*, 6083.

Baechler, R. D.; Mislow, K. *J. Am. Chem. Soc.*, **1971**, *93*, 773.

Baird, N. C.; Gupta, R. R.; Taylor, K. F. *J. Am. Chem. Soc.*, **1979**, *101*, 4531.

Bartlett, R. A.; Dias, R. H. V.; Power, P. P. *Inorganic Chemistry*, **1988**, *27*, 3919.

Bartlett, R. A.; Feng, X.; Power, P. P. *J. Am. Chem. Soc.* **1986**, *108*, 6817.

Bartlett, R. J.; Shavitt, I. *International J. of Quantum Chemistry: Quantum Chemistry Symposium*, **1977**, *11*, 165.

Baseman, R. J.; Pratt, D. W.; Chow, M.; Dowd, P. *J. Am. Chem. Soc.* **1976**, *98*, 5726.

Benson, S. W. "Thermochemical Kinetics", 2nd ed., Wiley, New York, 1976.

Bent, H. A. *Chem. Rev.* **1961**, *61*, 275.

Berson, J. A. in "Diradicals", Borden, W. T., ed., Wiley-Interscience: New York, 1982, pp. 151-194.

Berthier, G. *Studies in Physical and Theoretical Chemistry* **1988**, 62, 91.

Binkley, J. S.; Frisch, M. J.; Raghavachari, M.; Fluder, E.; Seeger, R.; Pople, J. A.
Carnegie-mellon University. Gaussian82.

Binkley, J. S.; Pople, J. A.; Hehre, W. J. *J. Amer. Chem. Soc.*, **1980**, 102, 939.

Borden, W. T. In "Diradicals"; Borden, W. T., Ed.; John Wiley & Sons: New York, 1982.

Borden, W. T. "Modern Molecular Orbital Theory for Organic Chemists," Prentice-Hall, Inc., 1975.

Borden, W. T.; Davidson, E. R. *J. Chem. Phys.*, **1976**, 64, 663.

Borden, W. T.; Davidson, E. R. *Tetrahedron*, **1982**, 38, 737.

Born, M.; Oppenheimer, J. R. *Ann. Physik*, **1927**, 84, 457.

Boys, S. F.; Cook, G. B. *Revs. of Modern Phys.*, **1960**, 32, 285.

Boys, S. F. *Revs. of Modern Phys.*, **1960**, 32, 296.

Boys, S. F.; Foster, J. M. *Revs. of Modern Phys.*, **1960**, 32, 300.

Boys, S. F.; Foster, J. M. *Revs. of Modern Phys.*, **1960**, 32, 302.

Boys, S. F.; Foster, J. M. *Revs. of Modern Phys.*, **1960**, 32, 305.

Budzalaar, P. H. M.; Kos, A. J.; Clark, T.; Schleyer, P. v. R. *Organometallics*, **1986**, *4*, 429.

Burdon, J.; Hotchkiss, J. C.; Jennings, W. B. *J. C. S. Perkin II*, **1976**, 1052.

Camp, R. L.; Greene, F. D.; *J. Am. Chem. Soc.* **1968**, *90*, 7349.

Chan, T. H.; Ong, B. S. *J. Org. Chem.* **1978**, *43*, 2994.

Chan, T. H.; Ong, B. S. *Tetrahedron* **1980**, *36*, 2269.

Choi, Y.; Jordan, K. D.; Paik, Y. H.; Chang, W.; Dowd, P. *J. Am. Chem. Soc.*, **1988**, *110*, 7575.

Cohen-Tannoudji, C.; Dui, B.; Franck Laloè "Quantum Mechanics" Translated from French by Hemley, S. R.; Ostrowsky, N.; Ostrowsky, D. Volumes 1 and 2. John Wiley & Sons, 1977.

Collins, J. B.; Schleyer, P. v. R.; Binkley, J. S.; Pople, J. A. *J. Chem. Phys.*, **1976**, *64*, 5142.

Cook, D. B. *J. Chem. Soc., Faraday Trans. 2*, **1986**, *82*, 187.

Coolidge, M. B.; Borden, W. T. *J. Am. Chem. Soc.*, **1988**, *110*, 2298.

Coolidge, M. B.; Borden, W. T. *J. Am. Chem. Soc.*, **1990**, In press.

Coolidge, M. B.; Borden, W. T. *J. Am. Chem. Soc.*, **1990**, In press.

Crandall, J. K.; Marchleder, W. H. *J. Am. Chem. Soc.* **1968**, *90*, 7347.

Daly, J. J.; Zuerich, S. A. *Kristallogr.* **1963**, *118*, 332.

Davidson, E. R. *J. Chem. Phys.* **1967**, *46*, 3319.

Davidson, E. R.; Feller, D. *Chem. Rev.*, **1986**, *86*, 681.

Dias, H. V. R.; Power, P. P. *Angew. Chem. Int. Ed. Eng.* **1987**, *26*, 1270.

Dias, H. V. R.; Power, P. P. *J. Am. Chem. Soc.* **1989**, *111*, 144.

Dobbs, K. D.; Hehre, W. J. *Organometallics*, **1986**, *5*, 2057.

Doering, W. v. E.; Roth, W. R.; Breuckmann, R.; Figge, L.; Lennartz, H.-W.;
Printzbach, H. *Chem. Ber.* **1988**, *121*, 1.

Doncaster, A. M.; Walsh, R. *Int. J. Chem. Kinet.*, **1978**, *10*, 101.

Dougherty, D. A.; Mislow, K. *Tetrahedron Letters*, **1979**, *25*, 2321.

Drakenberg, T.; Dahlqvist, K.-I.; Forsén, S. *J. of Phys. Chem.*, **1972**, *76*, 2178.

Du, P., PHD. thesis, University of Washington, 1988.

Du, P.; Hrovat, D. A.; Borden, W. T.; Lahti, P. M.; Rossi, A. R.; Berson, J. A. *J. Am. Chem. Soc.* **1986**, *108*, 5027.

Du, P.; Hrovat, D. A.; Borden, W. T. *J. Am. Chem. Soc.* **1986**, *108*, 8086.

- Du, P.; Borden, W. T. *J. Am. Chem. Soc.* **1987**, *109*, 930.
- Du, P.; Hrovat, D. A.; Borden, W. T. *J. Am. Chem. Soc.* **1988**, *110*, 3405.
- Du, P.; Hrovat, D. A.; Borden, W. T. *J. Am. Chem. Soc.* **1989**, *111*, 3773.
- Dunning, T. H.; Hay, P. J. in "Methods of Electronic Structure Theory", Vol 2, Schaefer, H. F. III, Ed. Plenum: New York, 1977.
- Dunning, T. H.; Hay, P. J. in "Modern Theoretical Chemistry", Plenum, New York, 1976, pp. 1-28 ch. 1.
- Feller, D.; Davidson, E. R. *J. Chem Phys.* **1981**, *74*, 3977.
- Feller, D.; Davidson, E. R.; Borden, W. T. *J. Am. Chem. Soc.* **1985**, *107*, 2596.
- Feller, D.; Davidson, E. R.; Borden, W. T. *J. Am. Chem. Soc.* **1984**, *106*, 2513.
- Feller, D.; Huyser, E. S.; Borden, W. T.; Davidson, E. R. *J. Am. Chem. Soc.* **1983**, *105*, 1459.
- Feller, D.; Tanaka, K. Davidson, E. R.; Borden, W. T. *J. Am. Chem. Soc.* **1982**, *104*, 967.
- Feng, X.; Olmsted, M. M.; Power, P. P. *Inorg. Chem.* **1986**, *25*, 4615.
- Fjeldberg, T.; Gundersen, G.; Torgeir, T.; Seip, H. M.; Sæbø, S. *Acta Chemica Scandinavica A*, **1980**, *34*, 325.

Franci, M. M.; Pietro, W. J.; Hehre, W. J.; Binkley, J. S.; Gordon, M. S.; Defrees, D. M.; Pople, J. A. *J. Chem Phys.* **1982**, *77*, 3654.

Frisch, M. J.; Binkley, J. S.; Schlegel, H. B.; Raghavachari, K.; Melius, C. F.; Martin, R. L.; Stewart, J. J. P.; Bobrowicz, F. W.; Rohlfing, C. M.; Kahn, L. R.; Defrees, D. J.; Seeger, R.; Whiteside, R. A.; Fox, D. J.; Fleuder, E. M.; Pople, J. A. Carnegie-Mellon Quantum Chemistry Publishing Unit, Pittsburgh PA. 1984.

Furuhata, T.; Ando, W. *Tetrahedron* **1986**, *42*, 5301.

Furuhata, T.; Ando, W. *Tetrahedron Letters* **1986**, *27*, 4035.

Galasso, V. *J. Chem. Phys.* **1984**, *80*, 365.

Gordon, M. S.; Binkley, J. S.; Pople, J. A.; Pietro, W. J.; Hehre, W. J. *J. Amer. Chem. Soc.*, **1982**, *104*, 2797.

Greenberg, M. M.; Blackstock, S. C.; Stone, K. J.; Berson, J. A. *J. Am. Chem. Soc.*, **1989**, *111*, 3671.

Gropen, O.; Seip, H. M. *Chem. Phys. Lett.*, **1974**, *25*, 206.

Gropen, O. *J. of Mol. Struct.* **1977**, *36*, 111.

Gundersen, G. *Acta Chemica Scandinavica*, **1981**, *A 35*, 729.

Ha, T.-K.; Baumann, H.; Oth, J. F. M. *J. Chem. Phys.*, **1986**, *85*, 1438.

- Haddon, R. C. *Pure & Appl. Chem.* **1982**, *5*, 1129.
- Häfelinger, G.; Regelman, C. U. *J. of Comp. Chem.*, **1989**, *10*, 329.
- Hall, G. G. *Proc. Roy. Soc. A*, **1951**, *203*, 541.
- Harihan, P. C.; Pople, J. A. *Theor. Chim. Acta* **1973**, *28*, 212.
- Hehre, W. J.; Radom, L.; Schleyer, P. v.R.; Pople, J. A. "Ab Initio Molecular Orbital Theory," Wiley, 1986.
- Hehre, W. J.; Stewart, R. F.; Pople, J. A., *J. Chem. Phys.*, **1969**, *51*, 2659.
- Hobson, R. F.; Reeves, L. W.; Shaddick, R. C. *Org. Mag. Res.*, **1974**, *6*, 129.
- Hood, D. M.; Pitzer, R. M.; Schaefer, H. F. III *J. Am. Chem. Soc.* **1978**, *100*, 2227.
- Hrovat, D. A.; Sun, H.; Borden, W. T. *J. Mol. Struct. (Theochem.)* **1988**, *163*, 51.
- Jackson, R. A.; Zarkadis, A. K. *Tetrahedron Letters*, **1988**, *29*, 3493.
- Jug, K. *J. Org. Chem.* **1983**, *48*, 1344.
- Kanabus-Kaminska, J. M.; Hawari, J. A.; Griller, D.; Chatgililoglu, C. *J. Am. Chem. Soc.* **1987**, *109*, 5267.
- Knowles, P. J.; Werner, H.-J. *Chem. Phys. Lett.* **1985**, *115*, 259.
- Knowles, P. J.; Werner, H.-J.; Elbert, S. T., 1988. MOLPRO.

Kölle, P.; Linti, G.; Nöth, H.; Wood, G., L.; Narula, C., K.; Paine, R. T. *Chem. Ber.*, **1988**, *121*, 871.

Kutzenigg, W. *Angew. Chem., Int. Ed. Engl.* **1984**, *23*, 272.

Lambert, J. B.; Jackson III, G. F.; Mueller, D. C. *J. Am. Chem. Soc.*, **1970**, *92*, 3093.

Lathi, P. M.; Rossi, A. R.; Berson, J. A. *J. Am. Chem. Soc.* **1985**, *107*, 2273.

Liberles, A.; Greenberg, A.; Lesk, A. *J. Am. Chem. Soc.* **1972**, *94*, 8685.

Liberles, A.; Kang, S.; Greenberg, A. *J. Org. Chem.* **1973**, *38*, 1922.

Longuet-Higgins, H. C. *J. Chem. Phys.*, **18**, 265, (1950).

Luke, B. T.; Pople, J. A.; Krogh-Jespersen, M.-B. Apeloig, Y.; Chandrasekhar, J.; Schleyer, P. v. R. *J. Am. Chem. Soc.* **1986**, *108*, 260.

Magnusson, E. *Tetrahedron*, **1985**, *41*, 5235.

Magnusson, E. *Aust. J. Chem.*, **1986**, *39*, 735.

Malykhanov, Y. B. *Zhurnal Strukturnoi Khimii*, **1985**, *26*, 22.

Maoche, B.; Gayoso, J. *International J. of Quantum Chemistry*, **1983**, *23*, 891.

Matsen, F. A. *J. of Chem. Ed.*, **1985**, *62*, 365.

McDowell, R. S.; Streitwieser, A. Jr. *J. Am. Chem. Soc.*, **1985**, *107*, 5849.

McMurchie, L; Elbert, S.; Langhoff, S.; Davidson, E. R. and modified by Feller, D. and Rawlings, D.. MELD.

Michalska, D.; Schaad, L. J.; Čársky, P.; Hess, B. A. Jr.; Ewig, C. S. *J. of Comp. Chem.*, **1988**, *9*, 495.

Møller, C.; Plesset, M. S. *Phys. Rev.*, **46**, 618, (1934).

Mulliken, R. S. *J. Chem Phys.*, **1935**, *3*, 375.

Murdoch, J. R. *J. Am. Chem. Soc.*, **1982**, *104*, 588.

Neckel, A.; Polesak, H.; Perkins, P. G. *Inorg. Chim. Acta*, **1983**, *70*, 225.

Noe, E. A.; Rapan, M. *J. Am. Chem Soc.* **1975**, *97*, 5811.

Ohno, K. *International J. of Quantum Chemistry Supplement 1*. **1977**, *12*, 119.

Ortiz, J. V. *J. Org. Chem.* **1983**, *48*, 4744.

Osamura, Y.; Borden, W. T.; Morokuma, K. *J. Am. Chem. Soc.* **1984**, *106*, 5112.

Parmar, S. S.; Benson, S. W. *J. Am. Chem. Soc.*, **1989**, *111*, 57.

Pasto, D. J.; Krasnansky, R.; Zercher, C. *J. Org. Chem.*, **1987**, *52*, 3062.

Pasto, D. J. *J. Am. Chem. Soc.*, **1988**, *110*, 8164.

Perri, J. A.; La-Placa, S.; Post, B. *Acta Crystallog.* **1958**, *11*, 310.

Pietro, W. J., Francel, M. M.; Hehre, W. J.; Defrees, D. J. Pople, J. A.; Binkley, J. S.
J. Amer. Chem. Soc., **1982**, *104*, 5039.

Pople, J. A. *Accts. Chem. Res.* **1979**, *3*, 217.

Pople, J. A.; Frisch, M. J.; Luke, B. T. *Inter. J. of Quant. Chem. Symp.*, **1983**, *17*, 307.

Pople, J. A.; Seeger, R.; Krishnan, R. *Int. J. Quantum Chem. Symp.*, **11**, 149, (1977).

Pople, J. A.; Binkley, J. S.; Seeger, R. *Int. J. Quantum Chem. Symp.*, **10**, 1, (1976).

Pople, J. A.; Nesbet, R. K. *J. Chem. Phys.*, **1954**, *22*, 571.

Roothaan, C. C. J. *Revs. of Mod. Phys.*, **1951**, *23*, 69.

Sakuria, H.; Umino, H.; Sugiyama, H. *J. Am. Chem. Soc.*, **1980**, *102*, 6837.

Schaad, L. J.; Hess, B. A.; Zahradnik, R. *J. Org. Chem.* **1981**, *46*, 1909.

Schleyer, P. v. R. *J. Am. Chem. Soc.*, **1985**, *107*, 4793.

Schmidt M. W.; Truong P. N.; Gordon M. S. *J. Am. Chem. Soc.*, **1987**, *109*, 5217.

Seeger, D. E.; Lahti, P. M.; Rossi, A. R.; Berson, J. A. *J. Am. Chem. Soc.*, **1986**, *108*,
1251.

Seip, H. M.; Jensen, H. H. *Chem. Phys. Lett.*, **1974**, *25*, 209.

Sevin, A.; Fazilleau, E.; Chaquin, P. *Tetrahedron*, **1981**, *37*, 3831.

Shankar, R. "Principles of Quantum Mechanics" Plenum Press, 1980.

Sherrod, M. J.; Menger, F. M. *J. Am. Chem. Soc.*, **1989**, *111*, 2611.

Shim, I.; Dahl, J. D. *Theoretica Chimica Acta*, **1978**, *48*, 165.

Skoncke, A.; Schaad, L. J.; Hess, B. A. Jr. *J. Am. Chem. Soc.*, **1988**, *110*, 5315.

Snyder, G. J.; Dougherty, D. A. *J. Am. Chem. Soc.*, **1989**, *111*, 3927.

Snyder, G. J.; Dougherty, D. A. *J. Am. Chem. Soc.*, **1989**, *111*, 3942.

Stackhouse, J.; Baechler, R. D.; Mislow, K. *Tetrahedron Letters*, **1971**, *37*, 3437.

Staley, S. W.; Norden, T. D.; Taylor, W. H.; Harmony, M. D. *J. Am. Chem. Soc.*, **1987**, *109*, 7641.

Stenkamp, L., PHD. thesis, University of Washington, 1975.

Streitwieser, A. Jr.; Heathcock, C. H. "Organic Chemistry" Macmillan Publishing Co. 1976.

Sun, H.; Hrovat, D. A.; Borden, W. T.; *J. Am. Chem. Soc.* **1987**, *109*, 5275.

Walsh, R. *Acc. Chem. Res.* **1981**, *14*, 246.

Wang, S. Y.; Borden, W. T. *J. Am. Chem. Soc.* **1989**, *111*, 7282.

Werner, H.-J.; Knowles, P. J. *J. Chem. Phys.*, **1988**, *89*, 5803.

Wetzel D. M.; Salomon, K. E.; Berger, S.; Brauman, J. I. *J. Am. Chem. Soc.*, 1989, **111**, 3835.

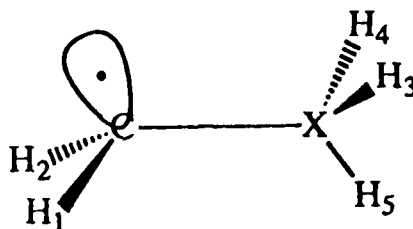
Wheast, R. C., *CRC Handbook of Chemistry and Physics*, 67th ed.; Weast, R. C., Ed.; CRC Press: Boca Raton, FL, 1986; p F-178.

Whiteside, R. A.; Frisch, M. J.; Pople, J. A. Carnegie-Mellon Quantum Chemistry Archive, 3rd edn., 1983, Carnegie-Mellon University.

Wiberg, K. B.; Murcko, M. A. *J. of Comp. Chem.*, 1988, **9**, 488.

APPENDIX 1. Geometries and Energies of Carbon Centered Radicals.

Bond Lengths in Å, Angles in Degrees, Energies in Hartrees.



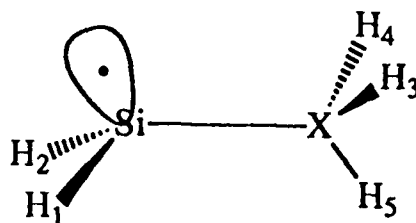
Substituent, X	C-H1	C-H2	C-X	X-H3	X-H4	H3-X-H4
<u>E(UHF/6-31G*)</u>	<u>X-C-H1</u>	<u>X-C-H2</u>	<u>H-C-H</u>	<u>C-X-H3</u>	<u>C-X-H4</u>	<u>H3-X-H5</u>
Li	1.092	1.092	1.943			
-46.39468	126.6	126.6	106.8			
BeH	1.082	1.082	1.665	1.336		
-54.19425	124.6	124.6	110.8	180.0		
BH ₂ rot	1.079	1.079	1.555	1.193	1.193	117.2
-64.80976	122.5	122.5	115.0	121.4	121.4	
BH ₂	1.078	1.078	1.536	1.190	1.190	119.0
-64.82416	123.0	123.0	114.0	120.5	120.5	
CH ₃	1.075	1.075	1.498	1.086	1.086	108.0
-78.59715	120.4	120.4	117.3	111.4	111.4	107.1

Substituent, X	C-H1	C-H2	C-X	X-H3	X-H4	H3-X-H4
<u>E(UHF/6-31G*)</u>	<u>X-C-H1</u>	<u>X-C-H2</u>	<u>H-C-H</u>	<u>C-X-H3</u>	<u>C-X-H4</u>	<u>H3-X-H5</u>
NH ₂ rot	1.079	1.074	1.420	1.002	1.003	107.1
-94.55750	120.3	120.3	119.2	111.4	111.4	
NH ₂	1.076	1.076	1.402	0.999	0.999	109.5
-94.58673	115.7	115.7	116.9	113.5	113.5	
NH ₃ +	1.070	1.070	1.470	1.013	1.013	107.2
	115.7	115.7	124.3	107.2	107.2	105.8
OH rot	1.076	1.076	1.366	0.948		
-114.40433	116.1	116.1	119.2	110.5		
OH	1.078	1.073	1.359	0.946		60.2
-114.40876	112.8	117.6	118.6	110.2		
NC	1.071	1.071	1.347	1.167		
-131.27045	118.7	118.7	112.7	180.0		
CN	1.072	1.072	1.391	1.159		
-131.30689	119.9	119.9	120.2	180.0		
F	1.073	1.073	1.331			
-138.40211	113.9	113.9	121.3			
CHO	1.072	1.074	1.414	1.237	1.086	119.3
-152.30039	119.5	121.2	119.9	122.2	120.0	

Substituent, X	C-H1	C-H2	C-X	X-H3	X-H4	H3-X-H4
<u>E(UHF/6-31G*)</u>	<u>X-C-H1</u>	<u>X-C-H2</u>	<u>H-C-H</u>	<u>C-X-H3</u>	<u>C-X-H4</u>	<u>H3-X-H5</u>
NO ₂	1.068	1.068	1.418	1.198	1.198	125.8
-243.02982	116.5	116.5	126.9	117.1	117.1	
SiH ₃	1.078	1.078	1.860	1.477	1.477	109.5
-329.64374	122.6	122.6	114.7	110.2	110.2	107.9
PH ₂ rot	1.075	1.075	1.821	1.405	1.405	95.3
-380.85599	121.5	121.5	117.0	98.8	98.8	
PH ₂	1.076	1.076	1.807	1.403	1.403	96.2
-380.85710	119.9	119.9	116.7	99.4	99.4	
SH rot	1.086	1.086	1.715	1.373		
-436.95463	109.6	109.6	110.3	117.2		
SH	1.073	1.072	1.749	1.326		
-437.07234	116.0	120.1	119.4			
Cl	1.070	1.070	1.718			
-498.46108	116.5	116.5	122.3			

Appendix 2. Geometries and Energies of Silicon Centered Radicals.

Bond Lengths in Å, Angles in Degrees, Energies in Hartrees.



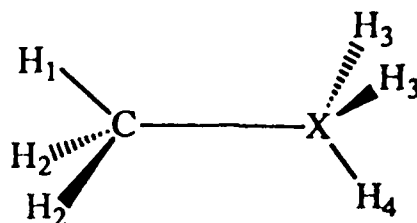
Substituent, X	SiH1	SiH2	SiX	X-H3	X-H4	H3-X-H4
<u>E(UHF/6-31G*)</u>	<u>XSiH1</u>	<u>XSiH2</u>	<u>HSiH</u>	<u>SiXH3</u>	<u>SiXH4</u>	<u>H3-X-H5</u>
Li	1.495	1.495	2.426			
-297.47969	128.1	128.1	102.9			
BeH	1.497	1.497	2.166	1.334		
-305.23926	120.2	120.2	108.8	180.0		
BH ₂ rot	1.469	1.469	2.045	1.188	1.188	117.5
-315.83391	121.8	121.8	116.4	121.3	121.3	
BH ₂ rot A pyr	1.482	1.482	2.046	1.189	1.191	117.3
-315.84524	111.5	111.5	108.7	122.5	120.2	
BH ₂	1.471	1.471	1.954	1.188	1.188	119.6
-315.85687	124.0	124.0	112.0	120.2	120.2	
CH ₃	1.480	1.480	1.894	1.085	1.085	107.8
-329.65181	111.6	111.6	109.2	110.9	110.9	107.9

Substituent, X	SiH1	SiH2	SiX	X-H3	X-H4	H3-X-H4
<u>E(UHF/6-31G*)</u>	<u>XSiH1</u>	<u>XSiH2</u>	<u>HSiH</u>	<u>SiXH3</u>	<u>SiXH4</u>	<u>H3-X-H5</u>
NH ₂ rot	1.480	1.482	1.721	0.995	0.998	112.5
-345.66023	113.3	113.3	107.7	123.2	123.2	
NH ₂	1.480	1.480	1.729	0.998	0.998	110.9
-345.66304	108.5	108.5	110.2	120.2	120.2	
NH ₃ +	1.461	1.461	1.928	1.012	1.012	106.7
-346.01412	101.9	101.9	116.5	112.2	112.2	106.6
OH rot	1.476	1.476	1.652	0.945		
-365.50603	110.4	110.4	109.3	118.7		
OH	1.483	1.473	1.652	0.946		59.8
-365.50694	111.9	106.9	109.9	118.2		
NC	1.470	1.470	1.740	1.163		
-382.35293	108.3	108.3	112.1	180.0		
CN	1.468	1.468	1.853	1.142		
-382.35497	108.6	108.6	113.4	180.0		
F	1.475	1.475	1.599			
-389.52283	108.8	108.8	110.5			
CHO	1.462	1.464	1.863	1.215	1.093	119.5
-403.31552	120.5	119.2	120.3	122.4	118.1	

Substituent, X	SiH1	SiH2	SiX	X-H3	X-H4	H3-X-H4
<u>E(UHF/6-31G*)</u>	<u>XSiH1</u>	<u>XSiH2</u>	<u>HSiH</u>	<u>SiXH3</u>	<u>SiXH4</u>	<u>H3-X-H5</u>
NO ₂	1.464	1.464	1.873	1.197	1.197	125.1
-494.08775	106.0	106.0	114.9	117.5	117.5	
SiH ₃	1.479	1.479	2.345	1.477	1.477	108.8
-580.69070	113.6	113.6	109.4	109.4	109.4	108.5
PH ₂ rot	1.478	1.475	2.271	1.404	1.403	94.5
-631.91699	112.4	112.4	109.5	97.3	97.3	
PH ₂	1.478	1.478	2.264	1.403	1.403	95.8
-631.91914	109.2	109.2	109.2	98.0	98.0	
SH rot	1.474	1.474	2.156	1.328		
-688.15082	110.8	110.8	109.6	97.9		
SH	1.477	1.473	2.149	1.328		
-688.15287	112.0	105.6	110.6	97.9		
Cl	1.472	1.472	2.070			
-749.56312	108.7	108.7	111.2			

APPENDIX 3. Geometries and Energies of Selected Closed-Shell Carbon Molecules.*

Bond Lengths in Å, Angles in Degrees, Energies in Hartrees.

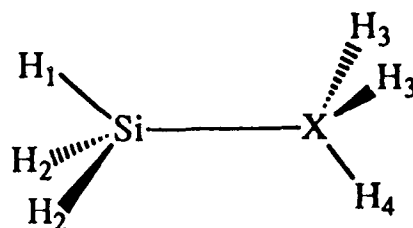


Substituent, X	C-H1	C-H2	C-X	X-H3	X-H4	H3-X-H4
<u>E(RHF/6-31G*)</u>	<u>X-C-H1</u>	<u>X-C-H2</u>	<u>H-C-H</u>	<u>C-X-H3</u>	<u>C-X-H4</u>	<u>H3-X-H5</u>
CN	1.082	1.082	1.468	1.135		
-141.92753	109.8	109.8	109.3	180.0		
NC	1.081	1.081	1.421	1.153		
-131.89436	109.6	109.6	109.2	180.0		
NO ₂	1.080	1.076	1.478	1.191	1.191	125.1
-243.66199	106.5	108.0	112.9	108.0	108.0	
[†] NH ₃	1.078	1.078	1.507	1.012	1.012	107.3
-95.90188	108.1	108.1	110.8	116.6	116.6	107.3

*Numbers not listed appear in the Carnegie-Mellon Quantum Chemistry Archive or in Luke, B. T.; Pople, J. A.; Krogh-Jespersen, M.-B. Apeloig, Y.; Chandrasekhar, J.; Schleyer, P. v. R. *J. Am. Chem. Soc.* 1986, 108, 260.

APPENDIX 4. Geometries and Energies of Selected Closed-Shell Silicon Molecules.^a

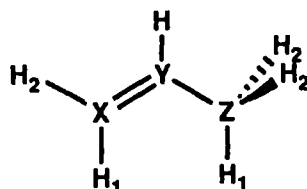
Bond Lengths in Å, Angles in Degrees, Energies in Hartrees.



Substituent, X	C-H1	C-H2	C-X	X-H3	X-H4	H3-X-H4
<u>F(RHF/6-31G*)</u>	<u>X-C-H1</u>	<u>X-C-H2</u>	<u>H-C-H</u>	<u>C-X-H3</u>	<u>C-X-H4</u>	<u>H3-X-H5</u>
CN	1.467	1.467	1.866	1.138		
-382.97440	107.5	107.5	111.3	180.0		
NC	1.467	1.467	1.742	1.162		
-382.97508	108.1	108.1	110.8	180.0		
NO ₂	1.463	1.461	1.870	1.197	1.197	127.0
-494.70911	103.7	106.1	112.6	117.5	117.5	
CHO	1.469	1.475	1.927	1.193	1.100	118.4
-403.93843	109.5	108.2	108.9	122.7	118.9	

^aNumbers not listed appear in the Carnegie-Mellon Quantum Chemistry Archive or in Luke, B. T.; Pople, J. A.; Krogh-Jespersen, M.-B. Apeloig, Y.; Chandrasekhar, J.; Schleyer, P. v. R. *J. Am. Chem. Soc.* 1986, 108, 260.

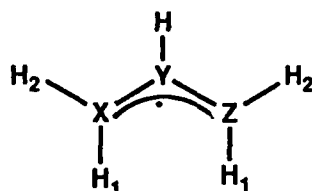
Appendix 5. Geometries and Energies of Saturated Allylic Systems



Bond Lengths are in angstroms and angles in degrees.

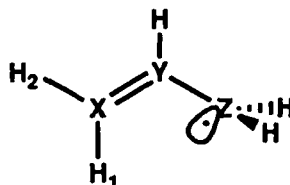
X	Y	Z	XY	YZ	H1X	H2X	HY	H1Z	H2Z
			XYZ		H1XYH2XY	HXH	HYX	H1ZY	H2ZY
E(RHF/6-31G*)							HYZ	H1ZH2	H2ZH2
C	C	C	1.319	1.503	1.077	1.076	1.079	1.084	1.087
			125.3		121.9	121.7	118.9	111.4	110.9
-117.071471					116.5		115.8	108.2	107.0
C	C	Si	1.325	1.873	1.077	1.078	1.081	1.477	1.478
			123.7		122.3	122.3	117.7	109.2	110.9
-368.112508					115.5		118.6	109.1	107.6
C	Si	C	1.693	1.879	1.077	1.076	1.471	1.085	1.086
			125.4		123.2	121.9	120.6	110.6	111.0
-368.085435					114.9		114.0	108.2	107.6
Si	C	C	1.700	1.508	1.468	1.467	1.080	1.085	1.088
			128.2		123.0	121.9	116.9	112.3	111.0
-368.071536					115.1		114.8	107.7	107.0
Si	Si	C	2.127	1.887	1.469	1.468	1.471	1.084	1.085
			125.6		122.6	121.9	119.6	110.7	110.8
-619.122356					115.5		114.9	108.2	108.0
Si	C	Si	1.696	1.855	1.466	1.468	1.080	1.479	1.480
			125.6		123.0	123.7	117.3	109.6	111.9
-619.127295					113.3		117.2	108.2	106.9
C	Si	Si	1.702	2.339	1.076	1.077	1.473	1.475	1.477
			123.0		122.6	122.7	119.5	108.9	110.5
-619.121299					114.7		117.5	109.4	108.3
Si	Si	Si	2.133	2.336	1.469	1.469	1.472	1.476	1.476
			122.7		122.1	123.8	118.3	108.2	110.8
-870.165074					114.2		119.1	109.3	108.3

Appendix 6. Geometries and Energies of Allylic Radicals



X	Y	Z	XY	YZ	H1X	H2X	HY	H1Z	H2Z
			XYZ		H1XYH2XY		HYX	H1ZY	H2ZY
					HXH		HYZ		HZH
E(RHF/6-31G*0)									
C	C	C	1.391	1.391	1.076	1.074	1.078	1.076	1.074
			124.5		121.2	121.5	117.7	121.2	121.5
-116.468100					117.4		117.7	117.4	
C	Si	C	1.778	1.778	1.077	1.076	1.466	1.077	1.076
			122.7		122.2	122.5	118.7	122.2	122.5
-367.477722					115.2		118.7	115.2	
Si	C	C	1.849	1.353	1.477	1.476	1.080	1.077	1.077
			124.6		112.2	112.6	117.8	122.0	122.0
-367.496986					111.4		117.4	116.0	
Si	Si	C	2.281	1.796	1.477	1.477	1.475	1.077	1.077
			119.6		113.6	113.8	116.5	122.2	122.3
-618.523178					110.2		114.0	114.8	
Si	C	Si	1.813	1.813	1.473	1.473	1.082	1.473	1.473
			127.2		114.6	115.3	115.4	114.6	115.3
-618.519739					112.5		115.4	112.5	
Si	Si	Si	2.287	2.287	1.477	1.477	1.479	1.477	1.477
			119.1		114.5	114.2	112.0	114.5	114.2
-869.571405					110.1		112.0	110.1	

Appendix 7. Geometries and Energies of Twisted Allylic Systems



X Y Z	XY	YZ	H1X	H2X	HY	HZ
E(RHF/6-31G*)	XYZ		H1XYH2XY		HYX	HZY
$\overline{\text{C}} \quad \overline{\text{C}} \quad \overline{\text{C}}$	$\overline{\text{---}}$	$\overline{\text{---}}$	$\overline{\text{---}}$	$\overline{\text{---}}$	$\overline{\text{---}}$	$\overline{\text{---}}$
-116.438510	1.326	1.479	1.076	1.075	1.081	1.076
	124.8		121.8	121.4	115.5	120.5
			116.8		119.7	117.4
Si C C	1.700	1.477	1.467	1.467	1.083	1.076
-367.440769	127.4		123.7	121.4	116.4	120.6
			114.9		116.2	117.0
C Si C	1.693	1.851	1.076	1.076	1.469	1.077
-367.455668	125.2		123.3	121.6	120.4	122.6
			115.1		114.4	114.9
Si Si C	2.126	1.854	1.468	1.468	1.470	1.076
-618.493100	125.1		123.2	121.3	119.3	122.3
			115.5		115.6	115.3
C C Si	1.325	1.878	1.076	1.077	1.081	1.479
-367.491447	124.1		122.3	122.1	117.7	111.7
			115.6		118.2	108.7
Si C Si	1.695	1.858	1.466	1.468	1.081	1.480
-618.506179	125.7		122.9	122.7	117.2	112.8
			114.4		117.1	108.0
C Si Si	1.701	2.329	1.076	1.076	1.473	1.477
-618.506562	122.2		122.7	122.5	119.3	113.2
			114.8		118.6	109.3
Si Si Si	2.132	2.324	1.468	1.468	1.473	1.476
-869.550101	121.7		122.2	123.6	118.1	113.5
			114.2		120.2	109.4

Appendix 8. Geometry information for H_2PBH_2 .

All lengths are in Å and angles are in degrees.

Geometry name	PB —	PH <u>PH'</u>	BH <u>BH'</u>	HPB <u>H'PB</u>	PBH <u>PBH'</u>	HPBH <u>H'PBH</u>
Ground State	1.905	1.399	1.187	102.2	120.0	38.8
RHF Optimized		1.399	1.187	102.2	120.0	141.2
Ground State	1.863	1.406	1.191	104.7	119.7	36.8
MP2 Optimized		1.406	1.191	104.7	119.7	143.2
Planar Phosph	1.808	1.380	1.184	124.9	118.4	0.0
RHF Optimized	1.380	1.184	124.9	118.4	180.0	
Planar Phosph	1.785	1.393	1.189	125.4	118.1	0.0
MP2 Optimized		1.393	1.189	125.4	118.1	180.0
Rotated Boron	1.973	1.409	1.188	95.2	120.3	47.2
RHF Optimize		1.409	1.187	95.2	120.8	-47.2
Rotated Planar	1.961	1.378	1.185	122.5	120.3	90.0
RHF Optimized		1.378	1.185	122.5	120.3	-90.0

Appendix 9. Geometry information for $\text{HP}(\text{BH}_2)_2$.

All lengths are in Å and angles are in degrees.

Geometry Name	PH	PB	BH	HPB	BPB	PBH	HPBH
			<u>BH'</u>			<u>PBH'</u>	<u>HPBH'</u>
Ground State	1.391	1.869	1.186	111.9	116.2	120.4	-19.7
RHF Optimized			1.186			118.3	164.5
Ground State	1.401	1.837	1.190	114.8	118.6	120.8	-14.4
MP2 Optimized			1.190			117.2	169.0
Planar Phosp	1.385	1.849	1.185	117.3	125.5	120.2	0.0
RHF Optimized			1.185			118.0	180.0
Planar Phosp	1.399	1.829	1.189	117.7	124.6	120.6	0.0
MP2 Optimized			1.190			117.2	180.0
Monorotated	1.404	1.900	1.189	102.1	105.5	120.4	-35.9
			1.187			119.8	151.1
(The rotated Boron)		1.969	1.187			119.5	115.5
			1.187			121.8	-63.8
Planar Monorot	1.387	1.811	1.185	120.2	128.1	118.7	0.0
			1.186			118.8	180.0
(The rotated Boron)		1.955	1.185	111.7		120.2	90.0
			1.185			120.2	-90.0
Dirotated	1.419	1.969	1.188	91.4	103.1	120.0	124.6
			1.188			121.1	-54.9
Planar Dirot	1.384	1.961	1.186	116.2	127.6	120.6	90.0
			1.186			120.6	-90.0

Appendix 10. Geometry information for $P(BH_2)_3$.

All lengths are in Å and angles are in degrees. (Note, B' is the rotated boron.)

Geometry Name	PB	PB'	BH <u>B'H</u>	BPB	BPB'	PBH <u>PB'H</u>	BPBH <u>BPB'H</u>
Ground state	1.873	1.873	1.186	120.0	120.0	119.4	0.0
Mono-rot planar	1.853	1.940	1.186	120.5	119.7	117.9	0.0
			1.186			120.3	90.0
Mono-rot pyramid	1.859	1.951	1.185	117.7	117.9	120.9	11.3
			1.186			120.2	104.6

VITA

Michael B. Coolidge [REDACTED]

[REDACTED]. He graduated from Lowndes High School in Valdosta, Georgia in 1978. In 1981, he received his BA in chemistry from the University of New Hampshire and entered the Air Force. His first assignment was five years at the Air Force Rocket Propulsion Laboratory studying explosives. In 1986, he came to the University of Washington. Although, original plans were to attain an MS in chemistry, the Air Force later decided to allow him to complete the requirements for a Doctor of Philosophy under Professor Weston T. Borden in the field of theoretical chemistry in 1990.